

**DESIGN OF METAL ARCHITECTURES:
SYNTHESIS AND STUDY OF THEIR PHOTOPHYSICAL
AND BIOMOLECULAR RECOGNITION PROPERTIES**

**Thesis submitted to
Cochin University of Science and Technology
in Partial Fulfillment of the Requirements for the Degree of**

**DOCTOR OF PHILOSOPHY
in Chemistry under the Faculty of Science**

By

AKHIL K. NAIR

**Under the Supervision of
Dr. D. RAMAIAH**



**Photosciences and Photonics
Chemical Sciences and Technology Division
CSIR-National Institute for Interdisciplinary Science and
Technology (CSIR-NIIST), Trivandrum 695 019, Kerala**

OCTOBER 2013

STATEMENT

I hereby declare that the matter embodied in the thesis entitled: **“Design of Metal Architectures: Synthesis and Study of their Photophysical and Biomolecular Recognition Properties”** is the result of investigations carried out by me at the Photosciences and Photonics, Chemical Sciences and Technology Division of the CSIR-National Institute for Interdisciplinary Science and Technology (CSIR-NIIST), Trivandrum, under the supervision of Dr. D. Ramaiah and the same has not been submitted elsewhere for a degree.

In keeping with the general practice of reporting scientific observations, due acknowledgement has been made wherever the work described is based on the findings of other investigators.



(Akhil K. Nair)



राष्ट्रीय अंतर्विषयी विज्ञान तथा प्रौद्योगिकी संस्थान
रसायनविज्ञान तथा प्रौद्योगिकी प्रभाग (सी एस टी डी)
वैज्ञानिक तथा औद्योगिक अनुसंधान परिषद्
इंडस्ट्रियल इस्टेट पी.ओ., तिरुवनंतपुरम, भारत 695 019

NATIONAL INSTITUTE FOR INTERDISCIPLINARY SCIENCE & TECHNOLOGY
CHEMICAL SCIENCE AND TECHNOLOGY DIVISION (CSTD)

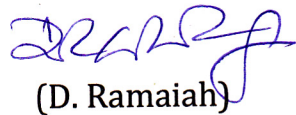
Council of Scientific and Industrial Research
Industrial Estate P.O., Thiruvananthapuram, INDIA 695 019

डॉ. डी. रामाय्या, एफ ए एससी
मुख्य वैज्ञानिक एवं प्रधान, सी एस टी डी
Dr. D. Ramaiah, FASc
Chief Scientist & Head, CSTD

October 03, 2013

CERTIFICATE

This is to certify that the work embodied in the thesis entitled:
**“Design of Metal Architectures: Synthesis and Study of their
Photophysical and Biomolecular Recognition Properties”** has been
carried out by **Mr. Akhil K. Nair** under my supervision at the Photosciences
and Photonics, Chemical Sciences and Technology Division of the CSIR-
National Institute for Interdisciplinary Science and Technology (CSIR-
NIIST), Trivandrum, and the same has not been submitted elsewhere for a
degree. All the relevant corrections and modifications suggested by the
audience and recommended by the doctoral committee of the candidate
during pre-synopsis have been incorporated in the thesis.


(D. Ramaiah)

Thesis Supervisor

डॉ. डी. रामाय्या
Dr. D. RAMAIAH
वैज्ञानिक / Scientist



रसायन विज्ञान तथा प्रौद्योगिकी प्रभाग
Chemical Sciences & Technology Division
राष्ट्रीय अंतर्विषयी विज्ञान तथा प्रौद्योगिकी संस्थान
National Institute for Interdisciplinary
Science & Technology (NIIST), CSIR
तिरुवनन्तपुरम / Thiruvananthapuram-695 019

ACKNOWLEDGEMENTS

I am extremely grateful to Dr. D. Ramaiah, my thesis supervisor, for suggesting the research problem and for his valuable guidance, support and encouragement, leading to the successful completion of this work.

I would like to express my sincere thanks to Prof. M. V. George for his constant support and inspiration during the tenure of this work.

I wish to thank Dr. Suresh Das, Prof. T. K. Chandrashekar and Dr. B. C. Pai, present and former Directors of the CSIR-National Institute for Interdisciplinary Science and Technology for providing me the necessary facilities for carrying out the work.

I sincerely thank Dr. A. Ajayaghosh, Dr. K. R. Gopidas, Dr. K. George Thomas, Dr. Joshy Joseph, Dr. K. Yoosuf and Dr. V. Karunakaran, scientists of the Photosciences and Photonics, Chemical Sciences and Technology Division, for all the help and support extended to me.

I thank all the members of the Photosciences and Photonics and in particular, Dr. Mahesh, Dr. Elizabeth, Dr. Jyothish, Dr. Prakash, Dr. Jisha, Dr. Rekha, Mr. Suneesh, Mr. Nandajan, Mr. Sanju, Ms. Dhanya, Mr. Adarsh, Ms. Betsy, Mr. Albish, Mr. Harishankar, Mr. Shanmugasundaram, Ms. Viji, Mr. Shameel, Dr. Nidhi, Dr. Lavanya and members of other Divisions of CSIR-NIIST for their help and support. I would like to thank Mr. Robert Philip and Mrs. Sarada Nair for their help and support and also Mrs. Saumini and Mrs. S. Viji for NMR and mass spectral analyses.

I owe a lot to my parents, who encouraged and helped me at every stage of my personal and academic life, and longed to see this achievement come true. I am very much indebted to my wife Jaimy, who supported me in every possible way to see the completion of this work.

I sincerely thank the Department of Science and Technology (DST), Government of India and CSIR, for the financial support.

Above all, I owe it all to Almighty God for granting me the wisdom, health and strength to undertake this research task and enabling me to its completion.

Akhil K. Nair

CONTENTS

	Page
Statement	i
Certificate	ii
Acknowledgements	iii
Preface	viii
Chapter 1 Metallo-supramolecular Systems in Biomolecular Recognition: An Overview	
1.1. Introduction	1
1.2. Metallo-supramolecular Architectures	6
1.2.1. Supramolecular Squares	7
1.2.2. Supramolecular Triangles	12
1.2.3. Trigonal and Tetragonal Cages	13
1.2.4. Supramolecular Helicates	17
1.3. Molecular Recognition by Metallo-cyclic Supramolecular Systems	21
1.4. Metallo-cyclophanes for Recognition of Nucleosides and Nucleotides	34
1.5. Objectives of the Present Investigation	38
1.6. References	40
Chapter 2 Synthesis and Study of Photophysical Properties of Metallo-cyclophanes	
2.1. Abstract	47
2.2. Introduction	49

2.3	Results	52
2.3.1.	Synthesis of the Ligands 1, 2 and 3	50
2.3.2.	Photophysical Properties of the Ligands 1-3	54
2.3.3.	Study of Interactions with Metal Ions	56
2.3.4.	Isolation and Characterization of the Metal Complexes	63
2.4.	Discussion	67
2.5.	Conclusions	70
2.6.	Experimental Section	71
2.7.	References	78

Chapter 3 Study of Interactions of Metallocyclophanes with Nucleosides and Nucleotides

3.1.	Abstract	85
3.2.	Introduction	87
3.3.	Results	91
3.3.1.	Interaction of Metallocyclophanes with Nucleosides and Nucleotides	91
3.3.2.	Characterization of Complexation between [1.CuCl₂]₂ and Guanosine-5'-Monophosphate (5'-GMP)	96
3.3.3	Selectivity of 5'-GMP Recognition	101
3.4.	Discussion	104
3.5.	Conclusions	109
3.6.	Experimental Section	110
3.7.	References	113

Chapter 4

Synthesis and Study of Interaction of Pd(II)-NHC Complexes with Nucleosides and Nucleotides

4.1.	Abstract	119
4.2.	Introduction	121
4.3.	Results	124
4.3.1.	Synthesis and Photophysical Properties of Ligands	124
4.3.2.	Interactions of Ligands with Mono and Divalent Metal Ions	128
4.3.3.	Interaction of Pd(II)-NHC Complexes with Nucleosides and Nucleotides	135
4.3.4.	FID Assay: Selectivity of G-Based Nucleosides and Nucleotides Recognition	139
4.4.	Discussion	145
4.5.	Conclusions	148
4.6.	Experimental Section	149
4.7.	References	155
	List of Publications	161

Preface

Design and study of molecular receptors capable of mimicking natural processes has found applications in basic research as well as in the development of potentially useful technologies. Of the various receptors reported, the cyclophanes are known to encapsulate guest molecules in their cavity utilizing various non-covalent interactions resulting in significant changes in their optical properties. This unique property of the cyclophanes has been widely exploited for the development of selective and sensitive probes for a variety of guest molecules including complex biomolecules. Further, the incorporation of metal centres into these systems added new possibilities for designing receptors such as the metallocyclophanes and transition metal complexes, which can target a large variety of Lewis basic functional groups that act as selective synthetic receptors.

The ligands that form complexes with the metal ions, and are capable of further binding to Lewis-basic substrates through open coordination sites present in various biomolecules are particularly important as biomolecular receptors. In this context, we synthesized a few anthracene and acridine based metal complexes and novel metallocyclophanes and have investigated their photophysical and biomolecular recognition properties. The thesis has been divided into

four chapters, and of which the first chapter describes a brief summary about the molecular recognition with a particular emphasis on the metallo-supramolecular systems. Also, the objectives of the present thesis were briefly described in this chapter.

The second chapter of the thesis deals with the synthesis and study of photophysical properties of the anthracene-imidazole based ligands **1** and **3** and their metal complexes [**1**.CuCl₂]₂, [**1**.Hg(ClO₄)₂] and [(**3**)₂.CuCl₂]. These systems were synthesized in good yields and have been characterized on the basis of analytical and spectral evidence. The formation of the metal complexes was confirmed by optical spectroscopic techniques. For example, with increasing concentration of the Cu²⁺ ions, the absorption spectrum of **1** showed *ca.* 28% hypochromicity along with a bathochromic shift of 2 nm, whereas the fluorescence spectra showed *ca.* 50% quenching in the intensity at 421 nm. Similar experiments were carried out with Hg(ClO₄)₂, which showed *ca.* 22% hypochromicity along with a bathochromic shift of 2 nm as well as *ca.* 40% quenching in fluorescence intensity. In addition to this, the ligand **3** having only one imidazole moiety showed *ca.* 44% quenching in fluorescence intensity by increasing concentration of the Cu²⁺ ions.

To understand the nature of the interactions between the ligand **1** and CuCl₂ or Hg(ClO₄)₂, we analyzed the absorption and emission

changes using Job's plot, which indicated a 1:1 stoichiometry for these complexes. The Benesi-Hildebrand analysis of the fluorescence data gave association constants of $K_{\text{ass}} = 1.75 \pm 0.1 \times 10^5$ and $1.37 \pm 0.1 \times 10^5$ M⁻¹ and change in free energy of $\Delta G = -12.1$ and -11.8 kJ mol⁻¹, respectively, for the complexation of the ligand **1** with CuCl₂ and Hg(ClO₄)₂.

The metal complexation was further confirmed by MALDI-TOF mass spectral analysis, which showed a molecular mass of 944.67. This value was in agreement with the calculated molecular mass corresponding to 2:2 stoichiometry for the complex [**1**.CuCl₂]₂. However, in the case of the complex formed between the ligand **1** and Hg(ClO₄)₂, we observed a peak at 737.42, which corresponds to 1:1 stoichiometry. In the ¹H NMR spectrum, we observed regular broadening and complete disappearance of the peaks corresponding to the imidazole protons of the ligand **1** with the addition of *ca.* 11 μM of CuCl₂, whereas the peaks corresponding to the anthracene and methylene protons remained unaffected. Based on the MALDI-TOF MS and NMR evidence as well as the literature reports, we assign a symmetric cyclic structure such as a metallocyclophane for [**1**.CuCl₂]₂. This unique arrangement of the metal ions as bridging motifs between the two ligand molecules creates a highly rigid cavity in [**1**.CuCl₂]₂

making it an ideal choice as a host for biomolecules under physiological conditions.

Investigation of interactions of the metal complexes [**1**.CuCl₂]₂, [**1**.Hg(ClO₄)₂] and [(**3**)₂.CuCl₂] with various nucleosides and nucleotides forms the subject matter of the third Chapter of the thesis. The addition of guanosine 5'-monophosphate (5'-GMP) to an aqueous solution of the complex [**1**.CuCl₂]₂, resulted in significant changes in absorption and emission properties. In contrast, negligible changes were observed with the addition of other nucleotides such as guanosine 5'-diphosphate (5'-GDP), guanosine 5'-triphosphate (5'-GTP), adenosine 5'-triphosphate (5'-ATP), adenosine 5'-diphosphate (5'-ADP), adenosine 5'-monophosphate (5'-AMP), adenosine, guanosine and phosphate ions, indicating thereby that the complex [**1**.CuCl₂]₂ undergoes selective interactions with 5'-GMP. The complexation between [**1**.CuCl₂]₂ and 5'-GMP was further evidenced through fluorescence titration experiments. We obtained an association constant of $K_{\text{ass}} = 1.2 \pm 0.1 \times 10^4 \text{ M}^{-1}$ through the Benesi-Hildebrand analysis with a change in free energy (ΔG) of -9.4 kJ mol^{-1} . Furthermore, this supramolecular complex was isolated and characterized through MALDI-TOF MS analysis, which showed a peak at 1352.44, corresponding to 1:1 stoichiometric supramolecular assembly between [**1**.CuCl₂]₂ and 5'-GMP.

The selective recognition of 5'-GMP by the complex $[\mathbf{1}\cdot\text{CuCl}_2]_2$ when compared to other nucleotides was furthermore confirmed through calorimetric, electrochemical, ^1H and ^{31}P NMR techniques. We observed a significant shift in reduction potential of differential pulse voltammogram (DPV) of the complex $[\mathbf{1}\cdot\text{CuCl}_2]_2$ by the addition of 5'-GMP, whereas a regular endothermic response was observed in the isothermal titration calorimetric (ITC) measurements. In the ^1H NMR spectrum, with the successive addition of the complex $[\mathbf{1}\cdot\text{CuCl}_2]_2$, we observed a decrease in the intensity along with a significant broadening of the peak corresponding to the H_8 proton of 5'-GMP. Similarly, the ^{31}P NMR spectrum of 5'-GMP exhibited a gradual broadening of peak at δ 3.7 ppm, corresponding to the phosphate group of 5'-GMP by the addition of the complex $[\mathbf{1}\cdot\text{CuCl}_2]_2$. In contrast, other complexes $[\mathbf{1}\cdot\text{Hg}(\text{ClO}_4)_2]$ and $[(\mathbf{3})_2\cdot\text{CuCl}_2]$ showed negligible interactions with 5'-GMP and also with other nucleosides and nucleotides, thereby indicating the importance of the cavity size in the biomolecular recognition event. The unusual selectivity of the complex $[\mathbf{1}\cdot\text{CuCl}_2]_2$ for 5'-GMP over other nucleotides could be attributed to the synergy of various interactions. These include, i) the electrostatic interactions between Cu^{2+} ions of $[\mathbf{1}\cdot\text{CuCl}_2]_2$ and the suitably placed phosphate group of 5'-GMP, ii) the coordinative interactions between Cu^{2+} ions and N_7 of the guanine base,

and iii) the π -stacking interactions between the anthracene moieties and the aromatic unit of 5'-GMP.

Synthesis and investigation of interactions of Pd-complexes of the acridine-imidazole conjugates (Pd-NHC) with nucleosides and nucleotides through photophysical, calorimetric and NMR techniques have been included in the fourth Chapter of the thesis. The synthesis of the acridine-imidazole based ligands **9** and **10** and their corresponding Pd-complexes **4** and **5** were achieved in moderate yields and which were characterized on the basis of spectroscopic and photophysical analysis. The ^1H NMR analysis of the complexes **4** and **5** revealed the disappearance of the peaks corresponding to the H_8 proton of the carbene carbon. Similarly, we observed a significant downfield shift of the peak corresponding to the carbene carbon in the ^{13}C NMR spectrum. The MALDI-TOF MS analysis showed characteristic peaks at 1088.87 and 763.18 for the complexes **4** and **5**, which correspond to 2:1 complexes formed between $\text{Pd}(\text{OAc})_2$ and ligands **9** and **10**, respectively.

To explore the potential of the Pd-NHC complexes **4** and **5** as probes, we have investigated their interactions with various nucleosides and nucleotides in the aqueous medium. The addition of 5'-GMP to a solution of the complex **4** resulted in enhancement in its fluorescence intensity at 500 nm, with an association constant of $K_{\text{ass}} = 3.63 \pm 0.12 \times$

10^4 M^{-1} . Similar observations were made with 5'-GDP and 5'-GTP, having association constant values of $K_{ass} = 5.13 \pm 0.12 \times 10^4 \text{ M}^{-1}$ and $K_{ass} = 7.38 \pm 0.12 \times 10^4 \text{ M}^{-1}$, respectively. In contrast, we observed negligible changes in both absorption and fluorescence spectra of **4** by the addition of 5'-AMP, 5'-ADP, 5'ATP, adenosine and phosphate ions. The complex **5**, on the other hand, showed negligible selectivity towards nucleosides and nucleotides, when compared to the complex **4**. The selectivity of the complex **4** for G-based nucleotides was confirmed by isothermal titration calorimetry, which gave an endothermic response and association constants in the order of 10^4 M^{-1} for these nucleotides.

To improve the sensitivity of the probe for G-based nucleotides, we developed a fluorescent indicator displacement assay (FID) by making use of the beneficial properties of the complex **4** and a fluorescence indicator, 8-hydroxy-1,3,6-pyrene trisulfonate (HPTS). With increasing in concentration of the complex **4**, we observed *ca.* 23% hypochromicity in the absorption spectrum of HPTS along with *ca.* 93% quenching in fluorescence intensity at 512 nm with an association constant of $4.66 \pm 0.2 \times 10^4 \text{ M}^{-1}$. The successive additions of the G-based nucleotides (5'-GMP, 5'-GDP, 5'-GTP) to a solution of the non-fluorescent complex resulted in a regular enhancement in the fluorescence intensity corresponding to HPTS at 512 nm, which led to the visual detection

through “turn on” fluorescence intensity. In contrast, the addition of other non-interacting nucleosides and nucleotides such as adenosine, 5'-AMP, 5'-ADP, 5'-ATP and phosphate ions showed negligible changes in the fluorescence intensity of the complex [4·HPTS]. The selectivity of the complex 4 towards the G-based nucleotides has been attributed to the presence of better π -electron cloud to facilitate effective electronic and π -stacking interactions and strong coordinative interactions with N7 nitrogen of the guanine base and the metal centre. These results demonstrate the importance of the presence of Lewis acidic center as well as the aromatic surface in the molecular recognition ability of the complex 4 as a probe for the detection of the G-based nucleotides.

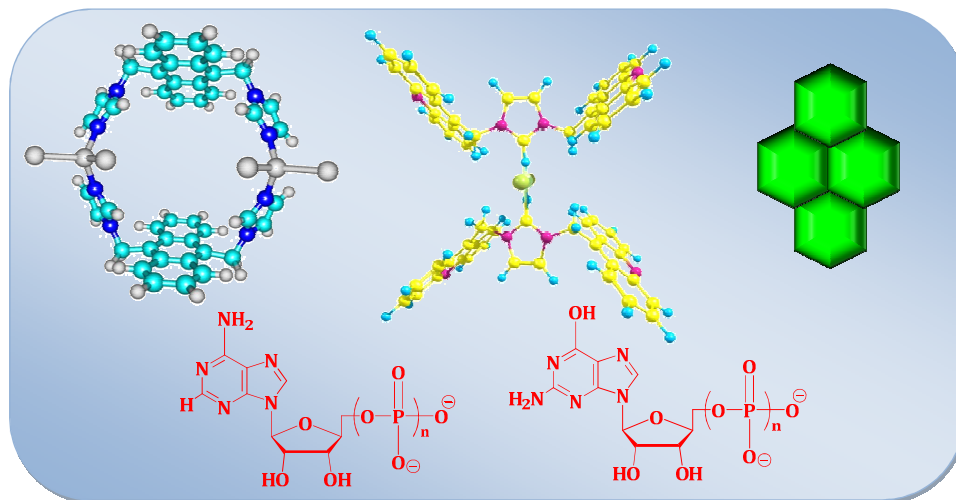
In summary, we have synthesized a few novel anthracene/acridine imidazole conjugates and their corresponding $\text{Cu}^{2+}/\text{Hg}^{2+}$ and Pd^{2+} complexes, and have evaluated their biomolecular recognition properties. These systems were found to exhibit solubility in the aqueous medium and favorable photophysical properties. The study of their interactions with various nucleosides and nucleotides indicate that these systems, depending on the cavity size, bridging unit and aromatic surface, exhibit selective interactions with the G-based nucleotides and signal the event through visual changes in the fluorescence intensity. Of these systems, the metallocyclophane

[**1**.CuCl₂]₂ as well as the Pd-NHC complex **4** showed selectivity for 5'-GMP and G-based nucleotides, respectively, when compared to other nucleosides and nucleotides, thereby demonstrating their potential as fluorescent molecular probes for biological applications.

Note: *The numbers of various compounds given here correspond to those given under the respective chapters.*

CHAPTER 1

METALLO-SUPRAMOLECULAR SYSTEMS IN BIOMOLECULAR RECOGNITION: AN OVERVIEW



1.1. INTRODUCTION

Supramolecular chemistry is one of the active areas of research in recent years, which mainly focuses on weak non-covalent interactions of molecules. The major non-covalent interactions confront in supramolecular chemistry are electrostatic, van der Waals, hydrogen bonding, charge transfer, π -stacking and coordinative interactions.^{1,2} The non-covalent interactions exist between the molecular assemblies are weak and can easily dismantle the complex, when equated to the covalently linked compounds. However, the nature creatively utilizes these weak non-covalent interactions in the construction of large and

ordered complex supramolecular biomolecules.³ For example, tobacco mosaic virus (TMV) is formed through the self-assembly of approximately 2130 identical units to a helical sheath structure having 300 nm in length and 18 nm in diameter around a single stranded RNA containing 6390 base pairs (Figure 1.1).⁴

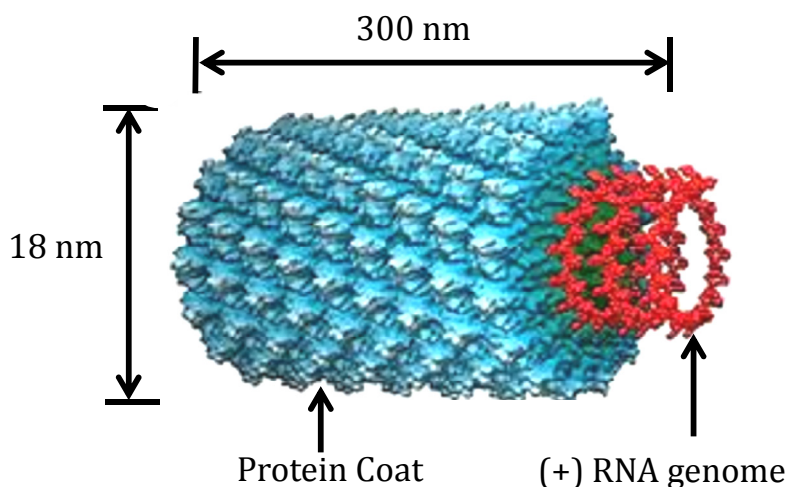


Figure 1.1. Schematic representation of the tobacco mosaic virus (TMV).

By the proper manipulation of the non-covalent interactions, the nature became successful in the construction of highly complicated supramolecular tobacco mosaic virus particle through host-guest interactions or self-assembly based on the two fundamental concepts such as principles of preorganization and complementarity.⁵ Keeping in mind the preorganization and complementarity, the most outstanding examples of the host-guest complexation are lock and key concept and induced fit concept in enzyme substrate binding. In 1902, Emil Fisher

proposed lock and key model for the highly specific enzyme-substrate interactions. According to this model, the formation of stable enzyme-substrate complex is possible, when the interacting surface of the enzyme and substrate are complementary to each other like a key fit to its lock. Since the lock and key model could not explain some of the complex enzyme substrate interactions taking place in living systems, Khosland, in 1958, proposed induced fit model for the enzyme substrate interactions.⁶ According to this model, the preorganization of the enzyme interacting surface has been introduced for the formation of the stable enzyme substrate complex. Motivated from the nature, researchers have been successful in synthesizing host systems, based on the complementarity and preorganization, for the selective recognition of the guest molecules. In 1960s, Pederson and co-workers have synthesized a series of crown ethers such as dibenzo-18-crown-6, and further showed that these compounds form strong complexes with alkali metal ions (Figure 1.2). Pederson's flat crown further provided the concrete platform for the groups of Lehn and Cram to develop increasingly complex systems that selectively recognize a group of substrates. Moreover, Lehn and co-workers were successful in creating 3D crown ethers such as cryptands from a multiple layers of atoms

having interconnected chains, which contained an internal cavity that could encapsulate the guest molecules (Figure 1.2). Similarly, Cram and co-workers were successful in designing a series of progressively complex prototype molecules.

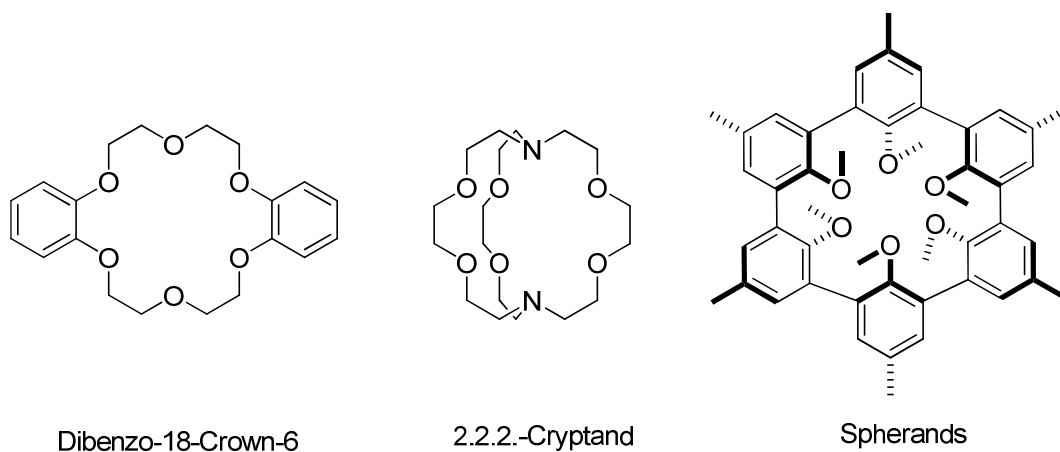


Figure 1.2. Structure of crown ether, cryptand and spherands.

For these magnificent results, Lehn, Pedersen and Cram were honoured with the Nobel Prize in chemistry in 1987 and since then the supramolecular chemistry and the host-guest chemistry has become an active area of research.⁷ Several receptor molecules have been reported, which include crown ethers, cryptands, cyclodextrins, calixarenes, pillararenes, cucurbiturils, porphyrins, metallocrowns, zeolites, cryptophanes, carcerands, foldamers and functional cyclophanes.⁸ Among these wonderful receptor molecules, the functional cyclophanes are one of the successful classes of host systems used for the recognition of guest molecules with the aid of various non-covalent interactions

(Figure 1.3). This chapter provides an overview of the metallo-supramolecular architectures, obtained by the supplementary modification of the functional cyclophanes, and their host-guest complexation properties.

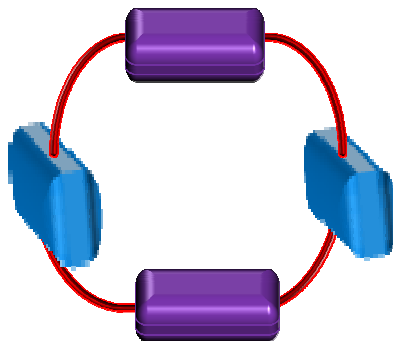


Figure 1.3. Schematic representation of a functionalized cyclophane system.

A number of functional cyclophanes have been designed and developed over the years by various research groups with an aim to selectively recognise different types of the guest molecules.⁹ The introduction of coordination core onto the cyclophanes opened up new promises for designing receptors as in the metallocyclophanes and which enable improved binding through coordinative interactions. In this context, the design of the host systems, which can target a large variety of Lewis basic functional groups of the guest molecule and can stabilize the host-guest complexation through employing the auxiliary

binding interactions such as the coordinative interactions or the cation/anion π -interactions are of particular interest.

The synthetic compounds with large, rigid and molecular-sized cavities combined with an understanding of the coordination chemistry of the metal ions and their structural role in the spatial arrangement lead to the new type of chemistry called supramolecular inorganic chemistry or metallo-supramolecular chemistry.¹⁰ This chapter describes a brief summary on metallo-supramolecular systems with a particular emphasis on molecular recognition properties especially on recognition of nucleosides and nucleotides. Also, the objectives of the present investigations were briefly described in this chapter.

1.2. Metallo-Supramolecular Architectures

The metallo-supramolecular architectures were synthesized by the coordination directed self-assembly of transition metal ions and multitopic ligands. In these cases, the metals act as a type of 'glue' to hold together assemblies of organic molecules, a term coined by Constable in 1994.¹¹ By employing donor groups in organic molecules (ligands) that bridge more than one metal centre, it is possible to construct one, two or three dimensional architectures such as molecular triangles, squares, rectangles, pentagons, hexagons, macrocycles, polyhedrons and cages.¹² Besides, a major advantage of the

metallocyclophanes over the organic cyclophanes is that it is possible to modulate and fine-tune their dimensions, topology, electronic properties and binding selectivity. Furthermore, the synthetic strategy is comparatively easy to introduce the functional units such as chiral, catalytic, luminescent or redox-active centres into the frameworks of the metallocyclophanes.¹³ The cavity size, shape and properties can be altered by using different ligands and metal ions with different oxidation states.¹⁴ An increase in awareness of the coordination chemistry of the specific metal ions together with the knowledge of various organic ligands, led to the design of various metallocyclophanes of interest having exact geometry. Thus the metal-directed self-assembly has led to the development of an array of highly refined architectures including boxes, triangles, helicates and grids and a few examples of such structures are discussed in the following sections.

1.2.1. Supramolecular Squares

The chemistry of the metal architectures evoked in 1990 when Fujita and co-workers demonstrated the spontaneous formation of a Pd based metal complex **1** (Chart 1.1) having square geometry from (ethylenediamine)palladium(II) nitrate and 4,4'-bipyridine.¹⁵ These

ligands were predefined to be complimentary in the formation of the square architecture by the appropriate use of the spacer groups. The authors have carefully chosen the correct number of spatially oriented ligands as well as the metal ions preferring square planar coordination geometry to access 90° and 180° angles for the formation of the square architectures. The leaving nitrate group of (ethylenediamine)-palladium(II) nitrate are *cis* to each other which restrict the possibility of co-ordination of Pd^{2+} ions only through 90° angle resulting in the formation of the square geometry for **1**. Fujita and co-workers have further showed that when the reaction was repeated with a flexibly linked bis(4-pyridine) derivative, a binuclear macrocyclic complex **2** was formed in the presence of Pd^{2+} salt (Chart 1.1).¹⁶

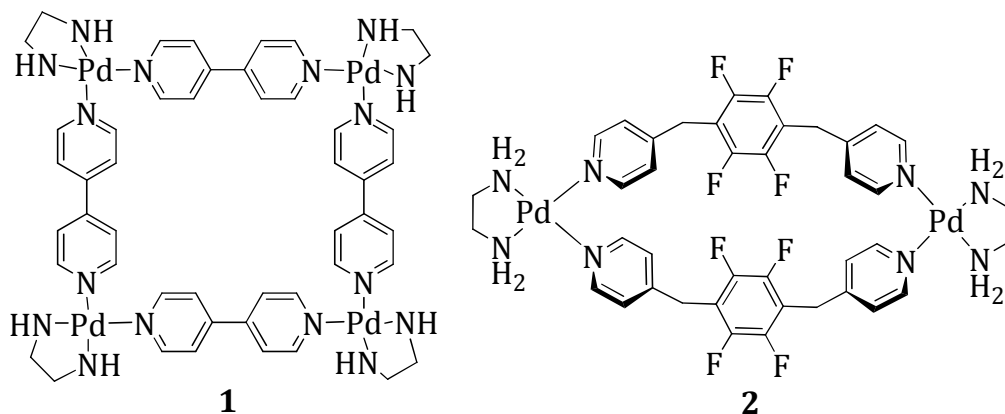


Chart 1.1

A number of other methods have also been used to synthesise the supramolecular squares. Chart 1.2 shows the porphyrin based square geometry **3** reported by Lehn and co-workers in which the Pd^{2+} ions

were blocked in a trans fashion and coordinated to right-angled pyridyl porphyrin ligands. The ligands in this square geometry present at the corner of the square and metal ions were present at the centre of the square sides.¹⁷ Similarly, Constable et al., have reported a dinuclear octacationic box by the reaction of a dicationic bis(2,2':6',2''-terpyridine) with Fe²⁺ ions resulting in the formation of square **4** shown in Chart 1.3.¹⁸

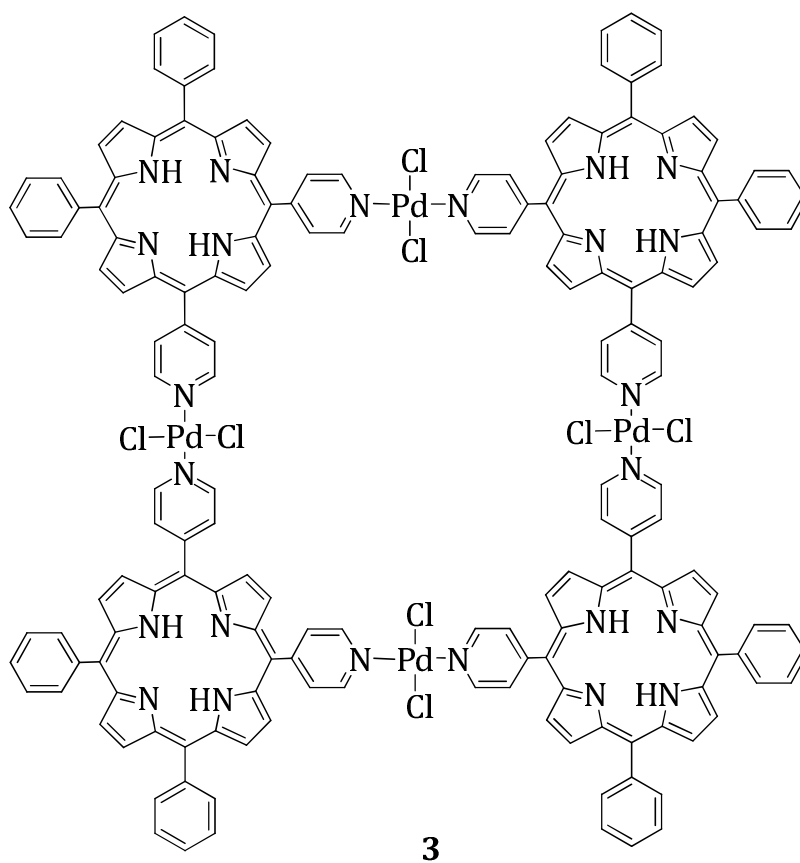


Chart 1.2

Hanoon and co-workers have reported a novel metallo-supramolecular cage having different metal ions. For example, Chart 1.3 shows the structure of metallic square **5** formed by Cu^{2+} ions. The cage structure furnishes each metal ion with only three donor atoms i.e. one from the pyridyl unit of one ligand and two from the bipyridyl unit.¹⁹ Stang and co-workers have designed Pt^{2+} based molecular square **6** having Lewis base receptor sites, which showed a variety of metal-binding capability (Chart 1.4).²⁰

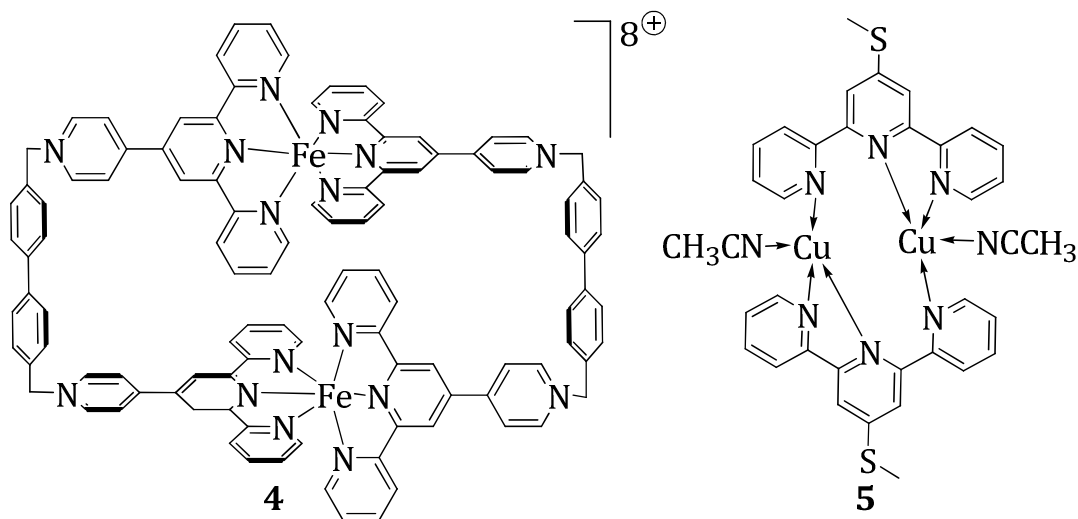


Chart 1.3

Interestingly, the acetylene moieties in the backbone of the molecular square **6** interact with 2 equivalent of silver triflate to give a host-guest complex with considerable stability in solution. The complex **6** was characterized by MALDI TOF MS and ESI-FTICR mass spectrometric techniques. The silver atoms in the complex were located

in a trans arrangement with respect to the Pt–Pt²⁺–Pt plane, resulting in a Ci-symmetric relationship. Che and co-workers have reported a platinum metallocycle **7** complex with a dicarbene and cyanide ligands as chelating agents, which showed hexagonal cavity as shown in Chart 1.4.²¹

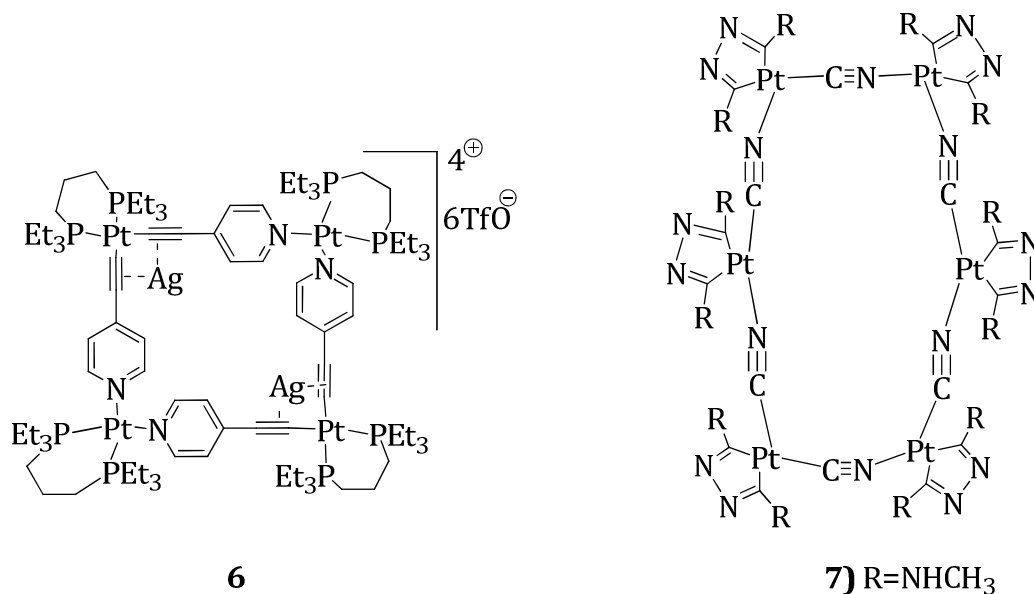


Chart 1.4

This complex exhibited luminescence maximum at 514 nm, when excited in the near-UV region (MLCT). More recently, Maverick and co-workers have synthesized a few supramolecular squares **8** and **9** by the reaction of bis(β -diketone) ligands with Cu²⁺ ions. Addition of Cu²⁺ ions resulted in the formation of a 2:2 complex in which the two metal

centres were held rigidly separated from each other by the aromatic spacer. As in the case of the metallo square reported by Lehn, the organic ligands form the corners of the square and the metal ions were located at the centre of the sides (Chart 1.5).²² These two square planar Cu^{2+} complexes form the walls of a cavity which can bind to substrates via metal ligand coordination.

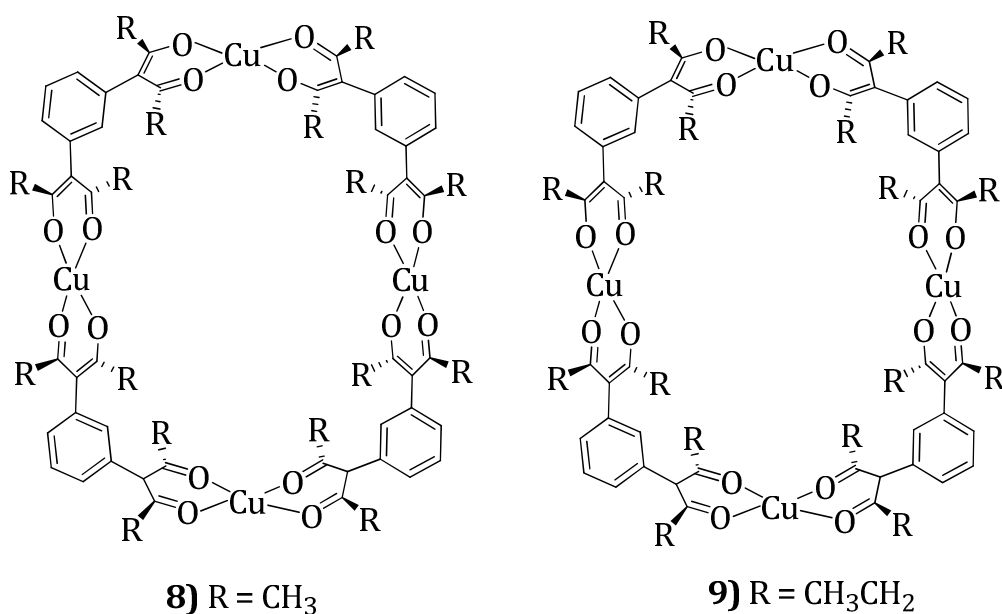


Chart 1.5

1.2.2. Supramolecular Triangles

It was proposed that the use of more flexible ligands during the formation of the metal squares had allowed the synthesis of a molecular triangle, which was in equilibrium with the more stable square architectures. For example, Lippert and co-workers have reported the synthesis of a supramolecular triangle from $[(\text{en})\text{Pd}(2,2'\text{-bpz-N}^1, \text{N}^1)]^{2+}$

and *trans*-(NH₃)₂Pt(II). The Pd²⁺ ions in these cases, form the three vertices of the triangles and the Pt²⁺ ions were located in the sides of the metallo triangle **10** (Chart 1.6).²³ Similarly, Mukherjee and co-workers have recently reported the self-assembly of a heterometallic triangle **11** from the reaction of 1,1'-bis(diphenylphosphino)ferrocene-palladium(II) ditriflate with sodium nicotinate (Chart 1.6).²⁴ The bowing of the ligands along the sides of the triangle allowed the O-Pd-N angles to approach close to the preferred 90°, minimising the angle strain at the metal centre.

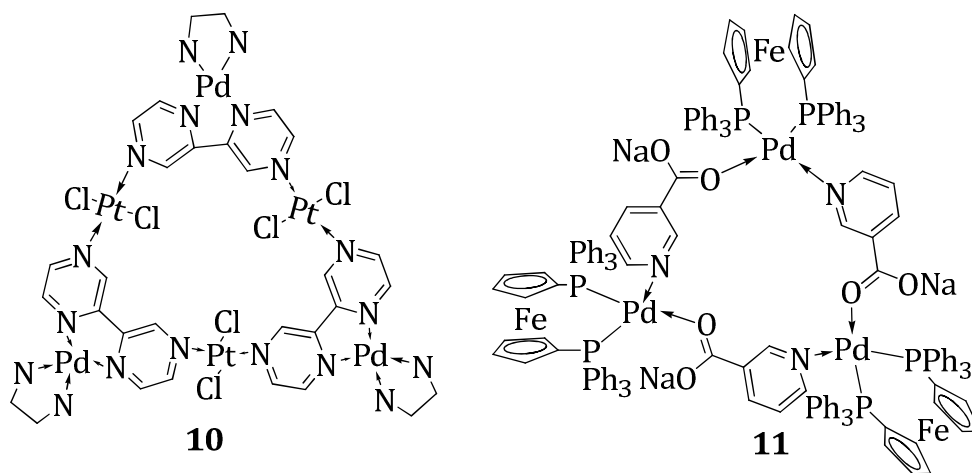


Chart 1.6

1.2.3. Trigonal and Tetragonal Cages

The metallo-supramolecular chemistry facilitated the formation of complex functional architectures that otherwise would have been

achieved using classical organic chemistry. Of the various ions, Ag^+ ions were known to display a flexible coordination geometry varying from 2-6. Su and co-workers have reported the synthesis of a trigonal prismatic cage **12** shown in Chart 1.7. The X-ray crystal structure showed that the two Ag^+ centres occupied a trigonal planar geometry having coordination with the three imino nitrogen atoms. Such a coordination resulted in a trigonal prismatic cage structure in which the central cavity of the cage was occupied by a distorted triflate anion.²⁵ In 2005, Du and co-workers have reported a trigonal cage **13** through the reaction of tetrahedral copper(I) ions with 2,5-di(pyridin-3-yl)-1,3,4-oxadiazole ligands (Chart 1.7).²⁶ In this case one of the metal coordination sites was occupied by the solvent acetonitrile and the other three were coordinated by the nitrogenous ligands. The X-ray crystal structure revealed that each prismatic cage hosts a water molecule inside the central cavity. Atwood and co-workers have further reported a M_2L_4 cage compound **14**, which was achieved by employing four bidentate ligands bound to two octahedral Cu^{2+} ions (Chart 1.7).²⁷ This was one of the example of a tetragonal prismatic cage in which the axial positions were blocked by the use of water molecules. Similar examples incorporating Co^{2+} and Zn^{2+} ions have also been reported in the literature.²⁸

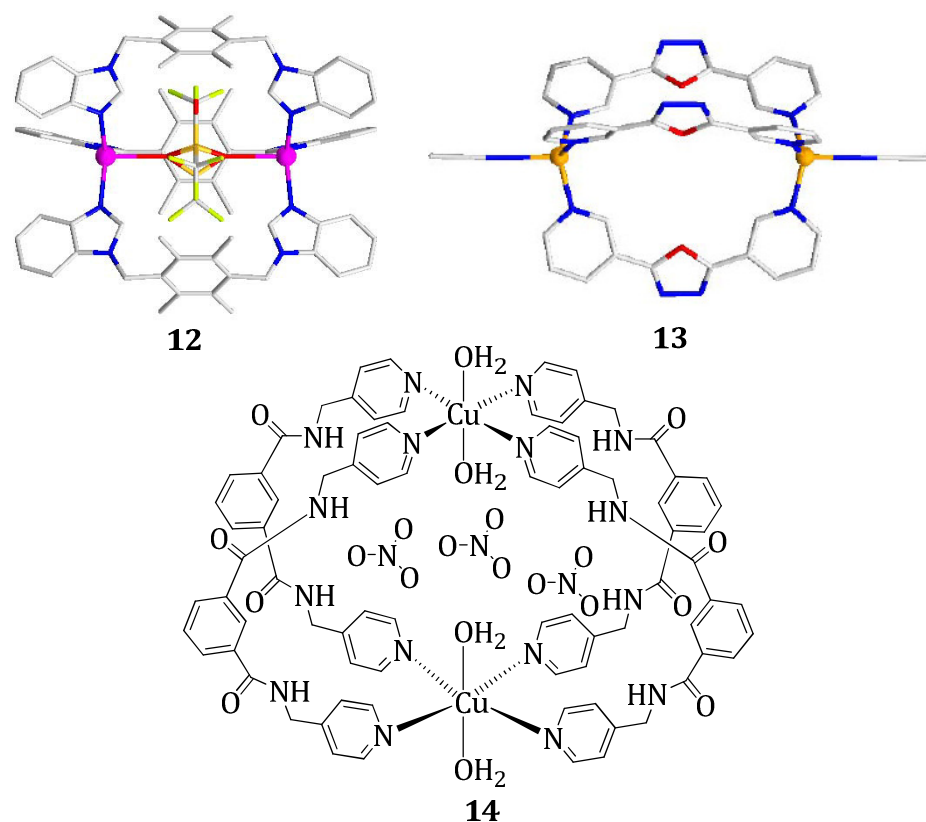


Chart 1.7

More recently, Su and co-workers have presented the formation of tetragonal cage **15** using a bis-monodentate ligand and the Cu^{2+} ions instead of the Cu^+ ions.²⁹ The six-coordinate metal centres bound four different pyridyl nitrogen atoms in the equatorial positions enabling the prismatic structure to be formed as shown in Chart 1.8 and the axial positions were occupied by the anions. Fujita and co-workers have prepared a rigid bis-pyridyl ligand which upon reaction with Pd^{2+} ions in

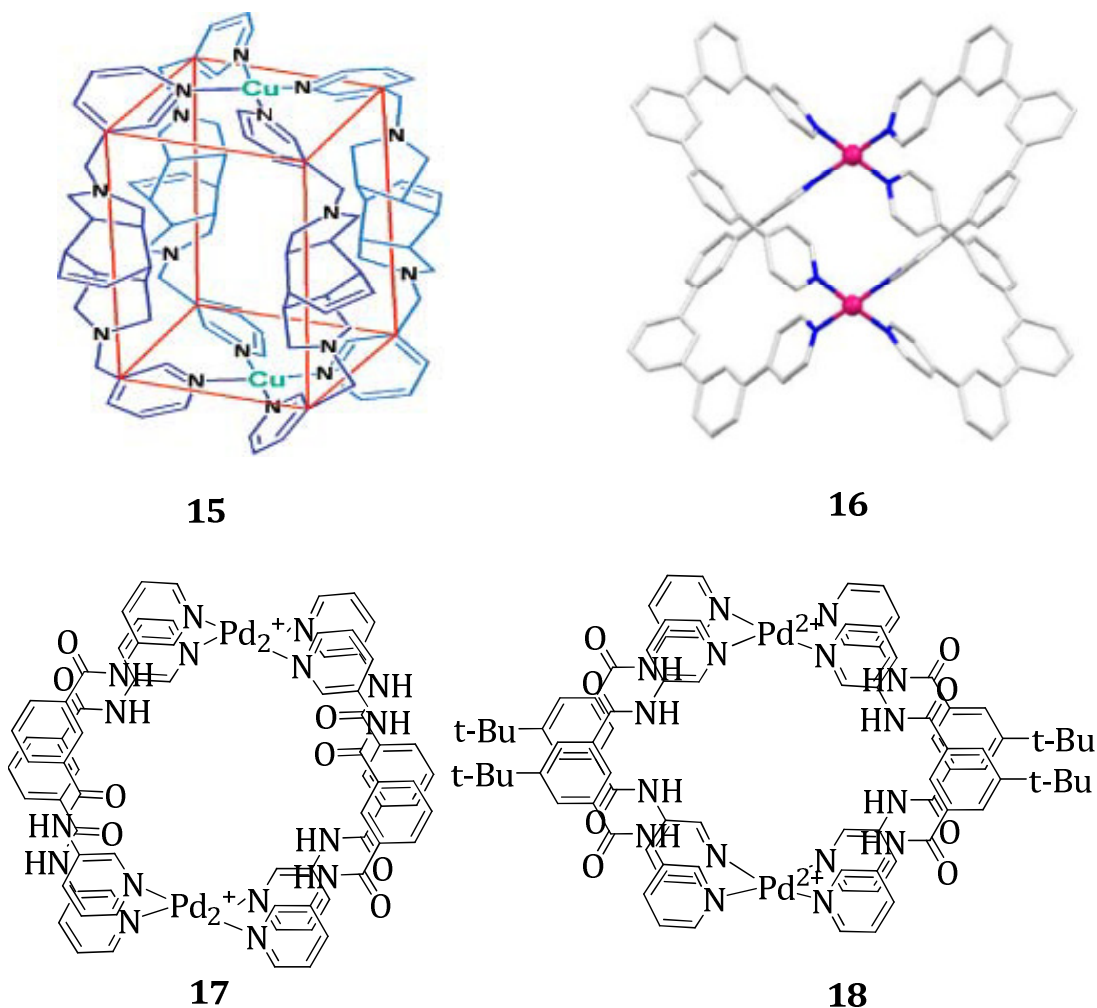


Chart 1.8

a 1:2 ratio to yielded a tetragonal prismatic cage **16**. The X-ray crystal structure of the cage confirmed that a nitrate anion was encapsulated within the central cavity (Chart 1.8).³⁰ Also, Puddephatt and co-workers have reported the formation of the functional tetragonal prismatic cages **17** and **18** (Chart 1.8) by the reaction of pyridin-3-amine based ligands with Pd^{2+} ions.³¹ These complexes exhibited an interesting host-guest

chemistry and have been shown to encapsulate cations, anions and water molecules in their cavity.

1.2.4. Supramolecular Helicates

Helical structures are often found in nature, which include deoxyribonucleic acid (DNA), protein α -helices and collagen. These helical structures may hold their particular shape through conformational restrictions, hydrogen bonding, or metal ion coordination. In 1987, Lehn had used the term, for the first time, helicate to pronounce the supramolecular structures in which one or more covalent organic strands were wrapped about and coordinated to a sequence of metal ions outlining the helical axis. The helicates were formed by self-assembly, therefore the subunits must be pre-designed so that they were complementary in the formation of the helical structure.³² The metal ions were selected based on their coordination number and geometry preferences, which meticulously harmonized to the properties of the ligand. The ligands were designed with two or more binding positions that were accomplished to coordinating to the chosen metal ions. The spacer group among the binding sites was allowed to be flexible enough to permit the ligand to wrap about the

helical axis, but also rigid enough to avert multiple binding sites of that ligand from coordinating to the same metal center.

The helicates can be categorized as homotopic or heterotopic. The homotopic helicates were those in which the coordinated ligand strands contain analogous binding sites along their length, whereas the strands with dissimilar binding sites results in the heterotopic helicates. As shown in Chart 1.9, the heterotopic helicates exist in two isomeric forms.³³

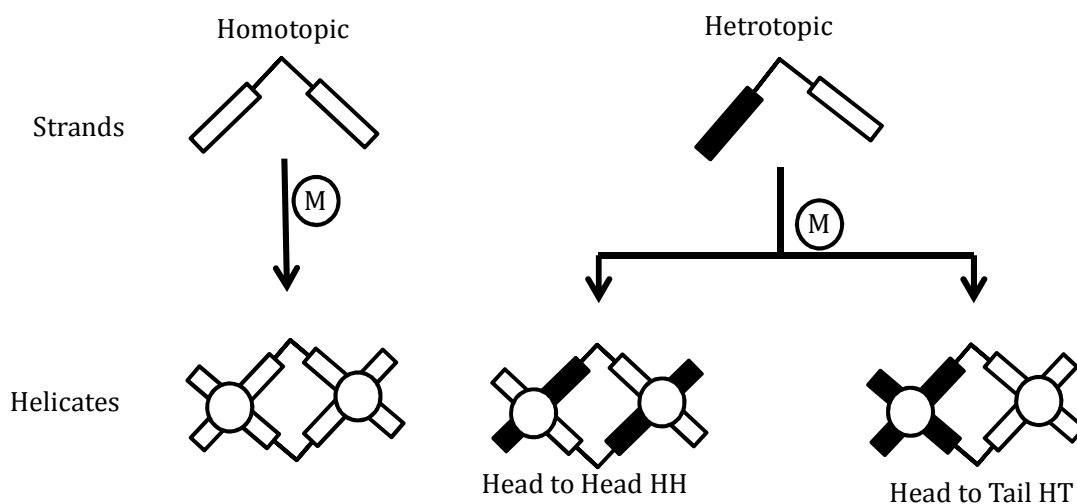


Chart 1.9

The majority of these structures contain one, two, three or four ligand strands and some of these interesting examples of supramolecular helicates are discussed in the following section. Single stranded helicates have been synthesized by efficiently employing a metal ion that was too small to fit the cavity of a multi-dentate ligand. A small

twist was encouraged in the ligand to diminish the steric interactions between the two ends of the strand.

In this context, Constable and co-workers have reported the formation of a single-stranded helicate **19** from the reaction of silver (I) acetate with quinquepyridine. The five nitrogen atoms of the quinquepyridine ligand bound to the metal ions forced the ligand to wrap around it with a slight helical twist (Chart 1.10).³⁴ More recently, Zhang and co-workers have been successful in generating single-stranded Cu^{2+} helicate **20** by intelligently employing a tetradentate ligand (1*S*,2*S*)-*N*¹,*N*²-bis(pyridin-2-ylmethyl)cyclohexane-1,2-diamine (Chart 1.10).³⁵

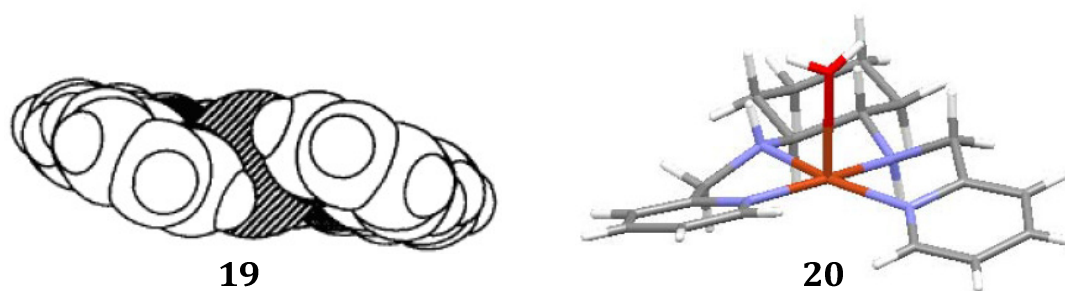


Chart 1.10

Lehn, Sauvage, Ziessel and co-workers have introduced the first strategy for the generation of a dinuclear double-stranded helicate.³⁶ They have prepared the dinuclear double stranded helicate **21** by the

reaction of a sterically hindered and conformationally restricted and preorganized quaterpyridine with the Cu⁺ ions (Chart 1.11).

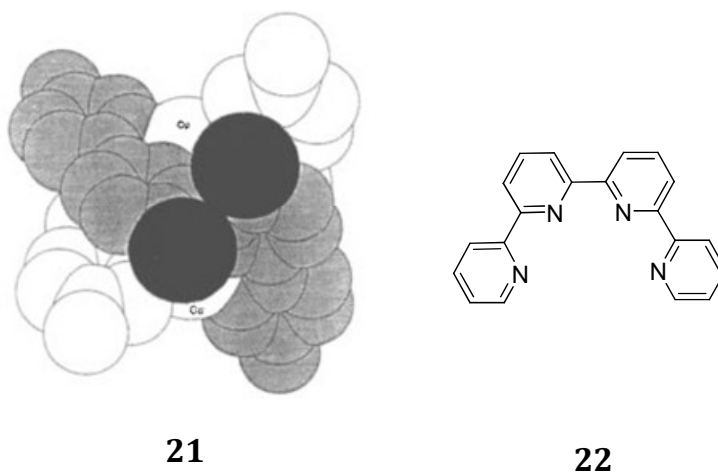


Chart 1.11

The methyl groups bound to the 5' and 3'- positions maintained the two bipyridine subunits in a twisted conformation, which favoured the formation of the dinuclear helical complexes. In 1991, Williams and co-workers have reported for the first time the structurally characterised triple stranded helicate by incorporating a rigid spacer into a tetradentate ligand **22** preventing it from acting as a tetradentate chelator.³⁷ Therefore, the reaction of the ligand with six co-ordinate Co²⁺ resulted in the formation of the triple stranded helicates. During the last two decades, several examples of the helicates have been reported, of which, only a limited number of heteronuclear metallo-helicates were described. Piguet and co-workers have reported the synthesis of the heteronuclear helicates with Ru²⁺ and Eu²⁺ ions, which resulted in the

formation of the heteronuclear helicate.³⁸ This heterotopic ligand consists of bi-dentate and tri-dentate binding sites separated by a rigid spacer unit.

In 1998, Steel and co-workers have reported the formation of a coordinatively saturated, quadruply-stranded helicate. This was achieved by employing a combination of four ligands and two square planar Pd²⁺ centres in a self-assembly process.³⁹ The X-ray crystal structure of the helicate revealed that a hexafluorophosphate ion was encapsulated within the central cavity. The previous section highlights the success of recent advances in supramolecular inorganic chemistry. Our interest in this field stems from the potential of the supramolecular complexes to be used as receptors for nucleosides and nucleotides. In the next section, we have discussed about a few literature reports on the selective recognition of various guest molecules by the metallo-supramolecular architectures.

1.3. Molecular Recognition by Metallocyclic Supramolecular Systems

The metallocyclic supramolecular systems can act as promising hosts for various types of guest molecules since they can be easily

constructed having different cavity size by utilizing a variety of organic ligands and the metal ions. The molecular square **1** reported by Fujita and co-workers showed the unique ability of molecular recognition of the neutral aromatic guests such as benzene, naphthalene and similar aryl systems (Chart 1.12). The central cavity within the square was π -electron deficient and has been shown to bind electron rich benzene derivatives, such as 1,4-dimethoxybenzene and 1,3,5-trimethoxybenzene through hydrophobic and π - π stacking interactions in water (D_2O) to form a 1:1 host-guest complex. In the 1H NMR spectra, chemical shift change of 1.56 ppm for the aromatic protons and 0.59 ppm shift for the methyl protons in D_2O at room temperature were observed. The analysis of the chemical shift changes by the Benesi-Hildebrand and a least squares procedure gave an association constant, $K_a = 750 M^{-1}$ at 25 °C. During the binding process, both the hydrophobic and electrostatic interactions were found to contribute to the formation of the host-guest complexes. Later, the authors have observed that the square **1** showed low binding constants with smaller molecules such as *p*-dimethoxybenzene ($K_a = 330 M^{-1}$), *m*-dimethoxybenzene ($K_a = 580 M^{-1}$) or *o*-dimethoxybenzene ($K_a = 30 M^{-1}$).

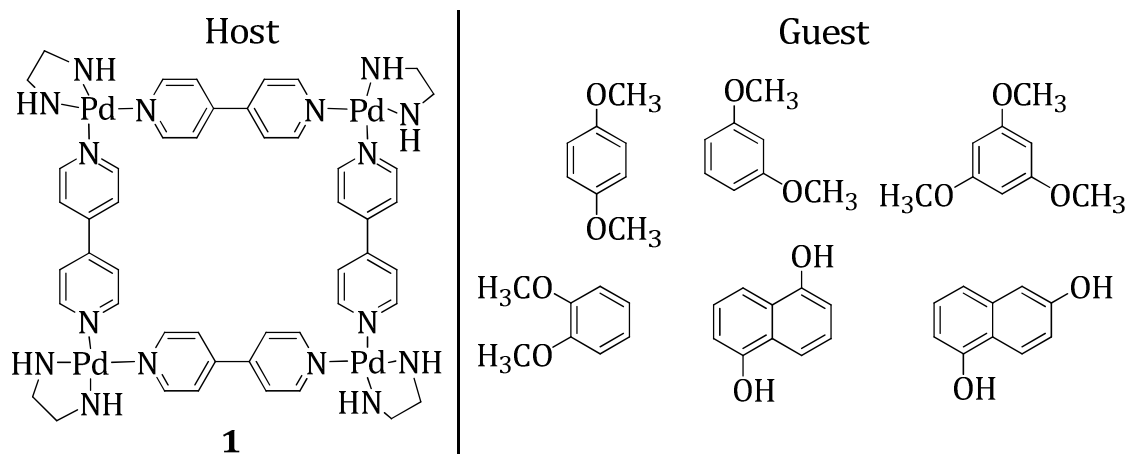


Chart 1.12

The metallocyclophane **2** reported by Fujita and co-workers, on the other hand, showed excellent substrate binding properties with electron rich aromatic moieties. It was observed that the strength of the binding increased as the electron density on the aromatic ring of the substrate increased, suggesting that a donor-acceptor interaction was important for the host-guest recognition. This compound was shown to bind to electron rich aromatic guests in water with strikingly high affinity, which was ascribed to the incorporation of an electron deficient perfluorinated benzene unit (Chart 1.13). It was also capable of binding to 1,3,5-trimethoxybenzene, *p*-dimethoxybenzene, *m*-dimethoxybenzene, and *o*-dimethoxybenzene with association constants of $K_a = 2500, 2680, 1560,$ and 1300 M^{-1} respectively.

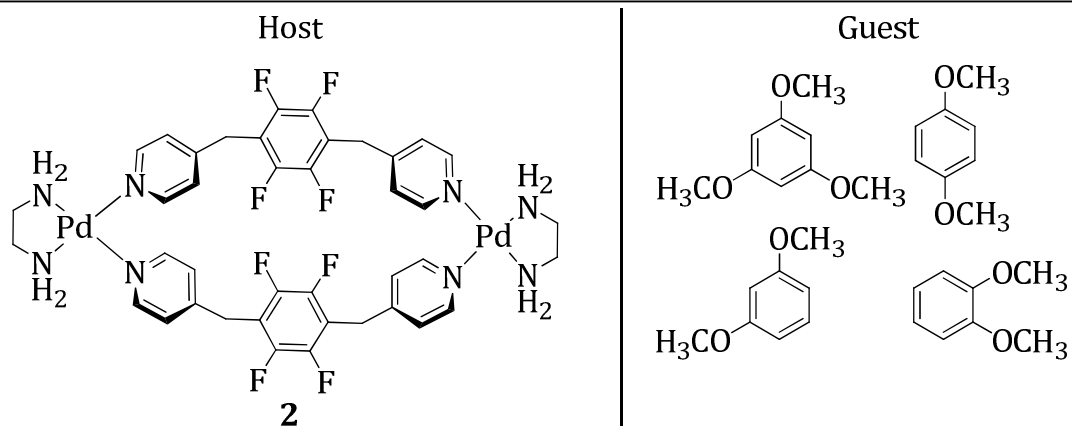
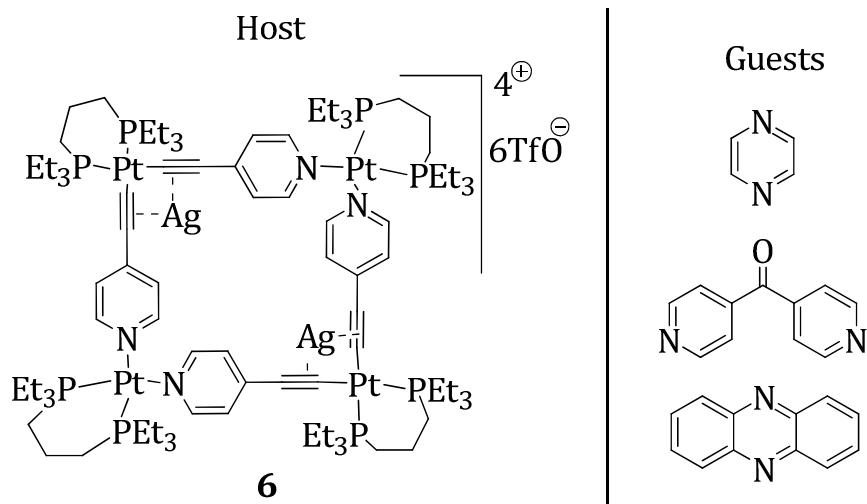


Chart 1.13

For larger guests, such as *N*-(2-naphthyl)-acetamide, only a weak host-guest interaction was observed ($K_a = 15 \text{ M}^{-1}$). Stang and co-workers have designed a few molecular square complexes with Lewis base receptor sites, which showed a variety of metal-binding capability and geometrical predictability. The X-ray crystallography provided new insights into the molecular recognition design of the Lewis acid-base host-guest molecular square **6** (Chart 1.14) with phenazine as the guest unit. It has been observed that the guest phenazine oriented nearly orthogonal to the Pt-Pt²⁺-Pt plane. Further, the metallocyclic square **6**, served as a receptor to bind Lewis basic guests with the appropriate size being achieved through the complexed silver cations.

**Chart 1.14**

The reaction of **6** with equimolar amount of the Lewis bases such as pyrazine, phenazine or 4,4'-bipyridyl ketone in CH_2Cl_2 at room temperature, resulted in the formation of the corresponding ternary complexes (Chart 1.14).

The binuclear Cu^{2+} cyclic derivative **8** reported by Maverick and coworkers have exhibited selectivity as a host for various nitrogen bases such as pyrazine, pyridine, quinuclidine, and diazabicyclo-[2,2,2]octane (DABCO) as well as fullerene (Chart 1.15). The olive green solution of **8** changed to turquoise on addition of the nitrogen bases. The binding constants of the nitrogen bases with **8** were determined spectrophotometrically in chloroform at room temperature. The authors

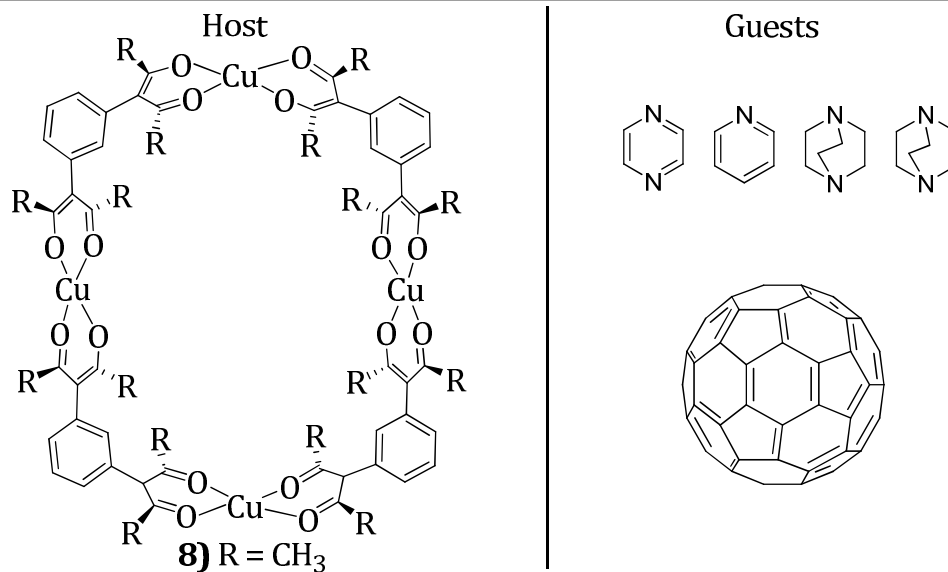


Chart 1.15

have compared the binding constants for **8** with monofunctional and bifunctional Lewis bases such as pyridine ($K_a = 0.5 \text{ M}^{-1}$), quinuclidine ($K_a = 7 \text{ M}^{-1}$), pyrazine ($K_a = 5 \text{ M}^{-1}$) and DABCO ($K_a = 220 \text{ M}^{-1}$) in chloroform solutions showed high association constant and that could be attributed to the internal coordination in the cavity.

Introduction of chromogenic or luminescent properties was especially interesting in metallocyclic supramolecular assemblies since this approach might be used as an alternative to conventional NMR spectroscopy in the detection of guest inclusion. In addition, the photoluminescence allows examination of the excited state behavior of the host-guest complexation. It may be mentioned that the luminescence could be much more sensitive to subtle changes in the

geometry and environment when compared to other techniques. Many luminescent compounds with internal cavities have been demonstrated as having potential applications as probes.⁴⁰ The complementary cavity sizes and the presence of intermolecular forces such as hydrogen bonding, hydrophobic or electrostatic interactions for the receptor can be easily achieved by incorporating fluorescent metal-organic chromophore in the metallocyclic supramolecules. Additionally, the vast literature available on the photophysical and photochemical properties of the metal complexes was an advantageous in designing such metallocyclic supramolecular assemblies. In the next section, a few of similar examples are described as host systems which have been used for the recognition of guest molecules.

Che and co-workers have reported a hexametallic metallocyclic derivative **7** formed from Pt²⁺ and the chelating dicarbene and cyanide ligands. The observed MLCT emission was due to the formation of intramolecular charge transfer transition of the complex (Chart 1.16). The MLCT emission was quenched by the addition of guest molecule such as N,N'-dimethyl-4,4'-bipyridinium hexafluorophosphate because it can block the charge transfer transition within the metal complex.

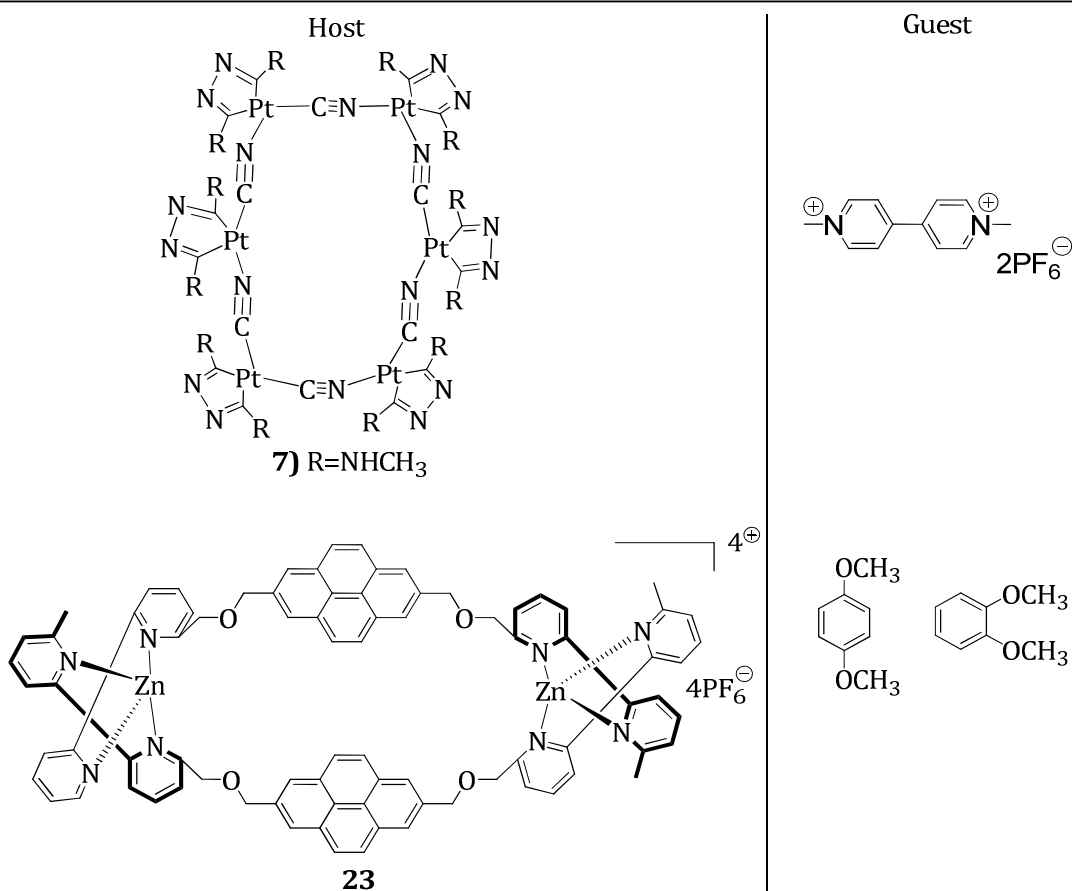


Chart 1.16

Bilyk and Harding have reported the encapsulation of 1,4-dimethoxybenzene and 1,2-dimethoxybenzene into the electron deficient cavity of the dinuclear metallocyclic Zn complex **23** (Chart 1.16). The guest binding was easily monitored by following the photophysical properties of the pyrene moiety. The X-ray structure of the corresponding complexes were determined and which established the inclusion of the guest molecule within the cavity.⁴¹

A luminescent Re^+ based cyclophane has also been reported by Sun and Lees (Chart 1.17). For example, the square structure **24**, was shown to be an effective probe for molecular sensing of an explosive nitro aromatics (e.g. TNT).⁴² A series of nitro-substituted aromatic compounds have been found to effectively quench the thin film luminescence of the molecular square **24**.

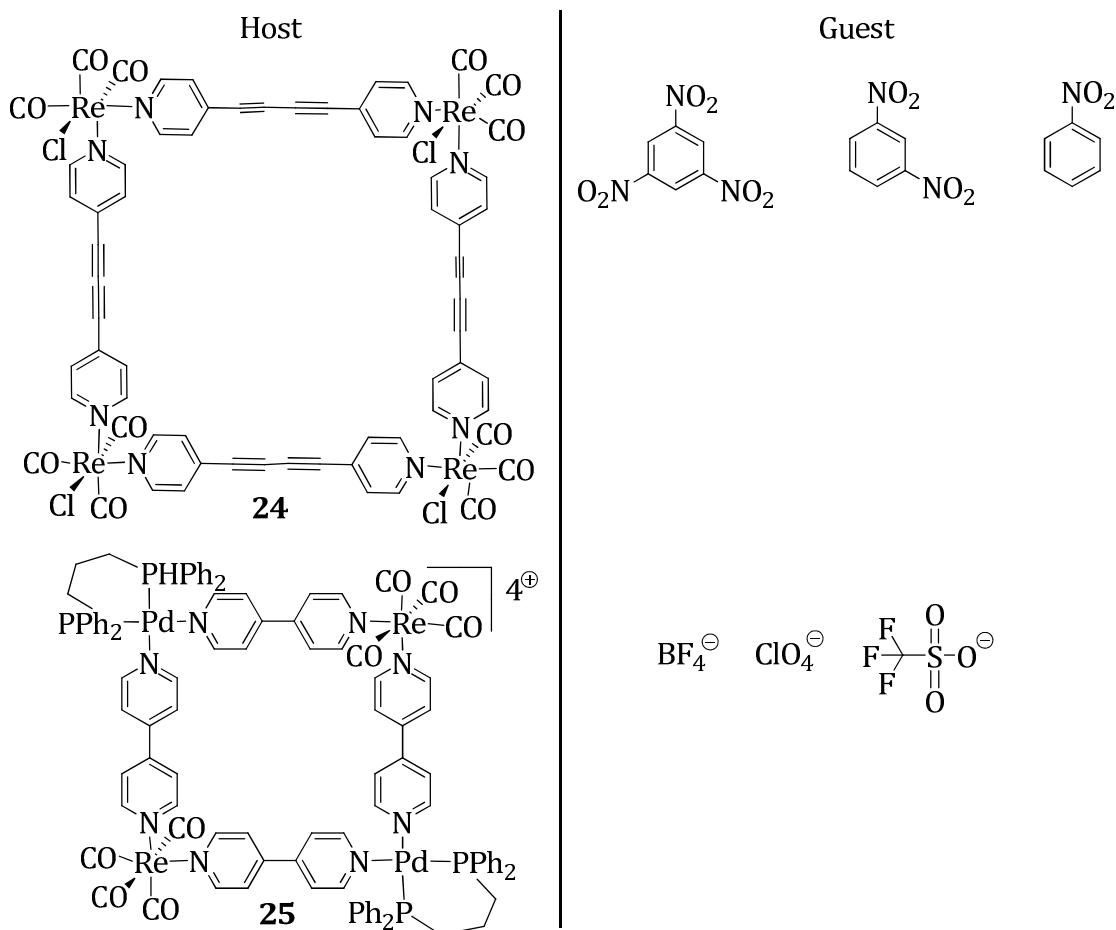
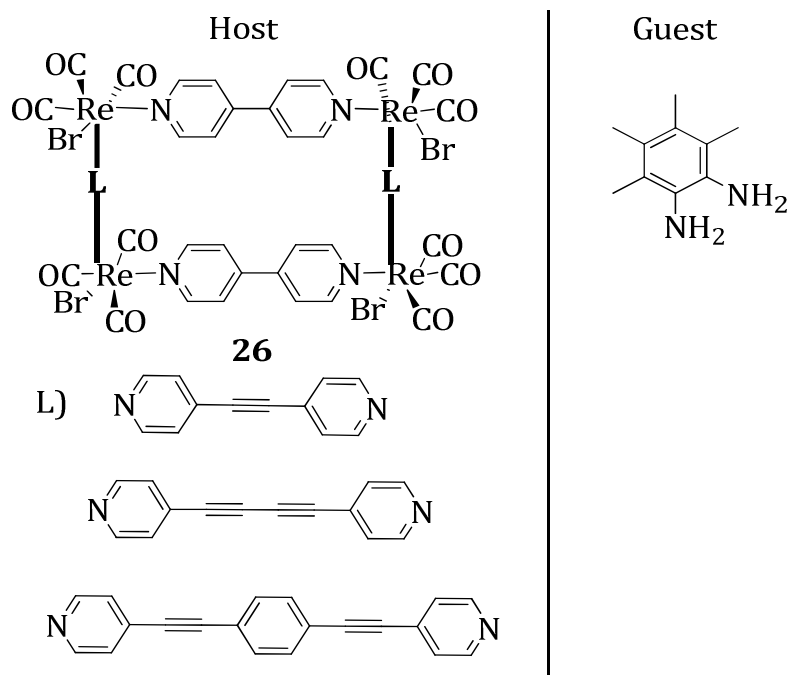


Chart 1.17

The quenching phenomenon was attributed to the porosity that exists in the film of the square **24**, which provides cavities for binding of the quencher molecules. Hupp and co-workers (Chart 1.17) have reported a heterometallic molecular square **25**, with alternating $\text{Re}(\text{CO})_3\text{Cl}$ and $\text{Pd}(\text{dppp})_2$ ($\text{dppp} = 1,3\text{-bis}(\text{diphenylphosphino})\text{propane}$) corners and 4,4'-bipyridine as the bridging unit.⁴³ In acetone solution, the emission from the MLCT state of these complexes was observed at 610 nm. It was expected that these systems would act as a host for various anions because of the cationic nature of the inorganic cyclophane **25**. Addition of ClO_4^- to the solution of **25** increased the luminescence intensity as well as the lifetime of the complex. The enhancement effect was believed to originate from the anion encapsulation-induced inhibition of oxidative quenching by Pd^{2+} sites. On the other hand, the addition of BF_4^- , which binds more strongly than ClO_4^- ($K_a = 6000 \text{ M}^{-1}$ compared to 900 M^{-1}) induced efficient enhancement of the luminescence. In contrast, the addition of trifluoromethanesulphonate, which has a binding constant of intermediate value of 3000 M^{-1} , indicated the enhancement in the luminescence to a degree between that observed for BF_4^- and ClO_4^- .

Lu and co-workers have reported the photoluminescence electron transfer quenching of the MLCT state of Re^+ based rectangle **26** by

**Chart 1.18**

several amine derivatives (Chart 1.18).⁴⁴ The amines with lower oxidation potential showed a higher quenching constant suggesting that it is an electron-transfer process. The association constants of the systems such as *N, N, N', N'*-tetramethylphenylenediamine with the three different rectangles **26** were found to be 2.3×10^4 , 2.6×10^2 and 64 M^{-1} , respectively, which suggest that the rectangle **26** is a better host for amines with larger size. Yip and co-workers have reported a new luminescent Au^+ based rectangle **27** with 9,10-bis-(diphenylphosphino)-anthracene and 4,4'-bipyridine as the bridging ligand as shown in Chart 1.19.⁴⁵ This system exhibited a cavity size of $7.92 \text{ \AA} \times 16.73 \text{ \AA}$. The

emission intensity of the rectangle was quenched in the presence of the aromatic guest molecules. The solvophobic and ion–dipole effects were attributed to the effective formation of the host–guest inclusion complexes between **27** and the aromatic guests.

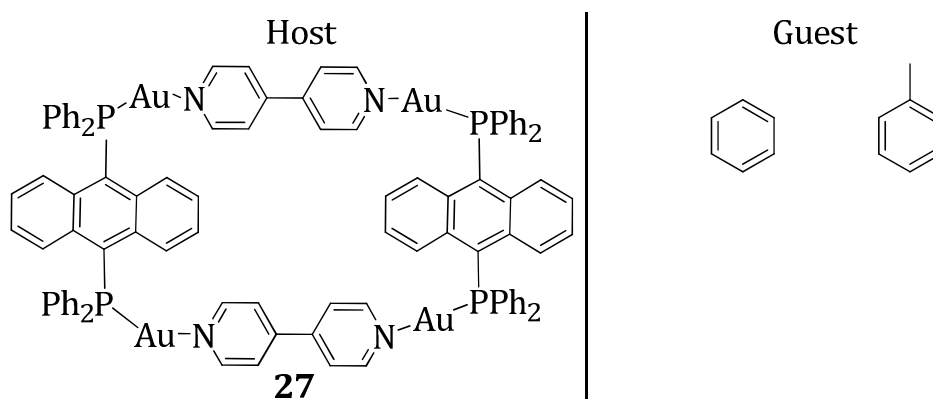


Chart 1.19

The rich photochemistry of the porphyrins has been utilized to construct metallocyclic supramolecules, in which significant changes in absorption as well as luminescent properties were noticed upon guest encapsulation. The zinc(II) metalloporphyrin cycle **28** which was reported by Hunter and Sarson and was created through a Lewis acid–base interaction between the Zn(II)-porphyrin and pyridine.⁴⁶ The intramolecular hydrogen bonding between the central pyridine and amide N–H ensures the approximate right angle in the supramolecular assembly. The porphyrin cycle **28** was able to encapsulate appropriate terephthalamide derivatives with strong hydrogen binding provided by

the amide functionality of the ligand (Chart 1.20). The association constants were determined by ^1H NMR analysis.

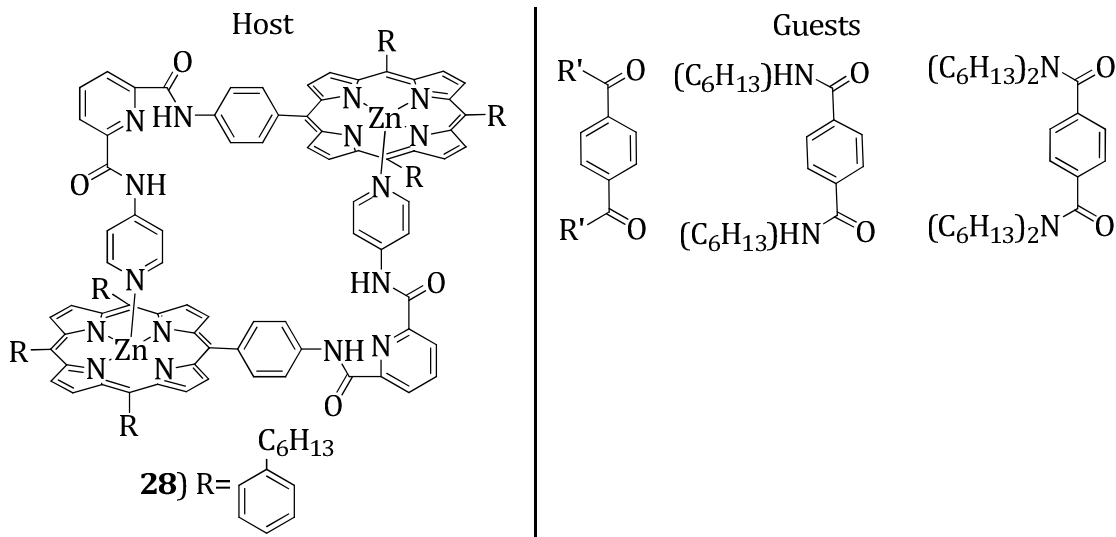


Chart 1.20

The terephthalic ester and bulky groups around the carbonyl moieties showed weak interactions and also similar observations made with isophthalic acid derivatives.

As described above, a few successful applications of the metallo-supramolecular architectures have been achieved through host-guest chemistry. Even though a large number of the metallated assemblies were reported, only a few of them have found the potential in biomolecular recognition, especially for nucleotides and nucleosides. In the following next section, the main focus will be on recent advances

made in the area of metallo-supramolecular assemblies with a particular emphasis on their potential use in the optical recognition of the important biomolecules.

1.4. Metallocyclophanes for Recognition of Nucleosides and Nucleotides

Navarro and co-workers have synthesized a palladium based metallocyclophane **29**, which showed selective interaction with the nucleotide mono-phosphates when compared to the nucleotide di- and tri-phosphates.⁴⁷ The reaction of [(dach)Pd(NO₃)₂] entities (dach = (*R,R*)-1,2-diaminocyclohexane, (*S,S*)-1,2-diaminocyclohexane) and 4,7-phenanthroline (phen) provided, respectively, led to the formation of the two novel positively charged homochiral cyclic trinuclear metallacalix [3] arene species [((*R,R*)-1,2-diaminocyclohexane)-Pd(phen)]₃(NO₃)₆ and [((*S,S*)-1,2-diaminocyclohexane)Pd(phen)]₃(NO₃)₆ **29** having 90° and 120° bond angles. These species have been characterized by ¹H NMR and X-ray structural analysis, which indicated that they possess accessible cavities suited for biomolecular recognition (Chart 1.21). It has also been observed from the ¹H NMR studies that the trinuclear species **29** in aqueous solution exhibited the inclusion of the mononucleotides inside

the cavity. The calculated association constants (K_a) were observed to be in the range from $85 \pm 6 \text{ M}^{-1}$ to $37 \pm 4 \text{ M}^{-1}$ for **29** and adenosine monophosphate and thymidine monophosphate, respectively. The driving force for such recognition of mononucleotides was attributed to be the synergy of electrostatic, anion- π and π - π interactions between nucleotides and **29**.

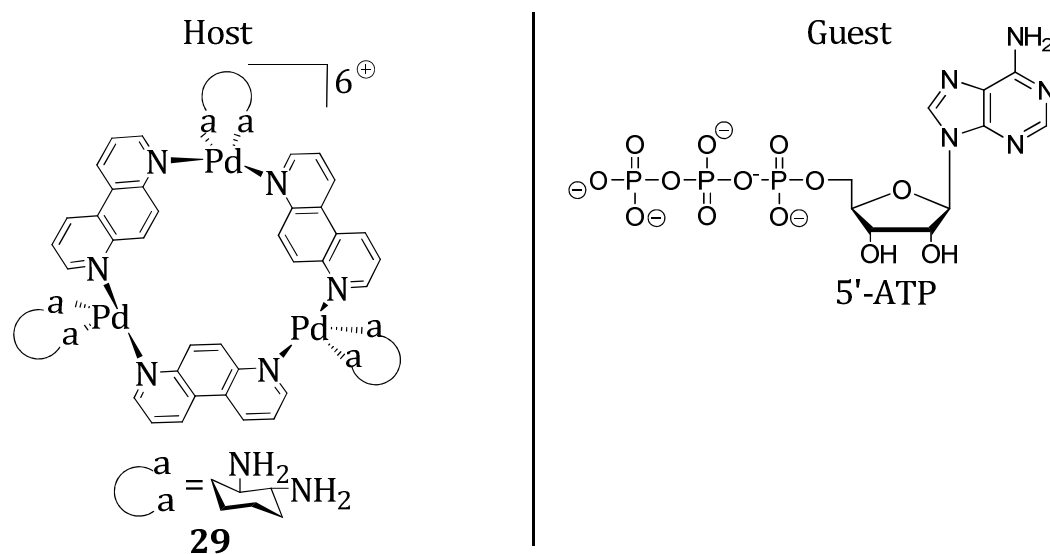


Chart 1.21

The metallohelical triangles based on functionalized amide groups have been reported by Duan and co-workers for the selective detection of 5'-ATP in the DMF-water medium through UV-Vis response (Chart 1.22).⁴⁸ The recognition of 5'-ATP by the host **30** has been due to the contribution of the hydrogen-bonding interactions between the

sulfonamide groups of the host molecule and the adenosine base, which block the photoinduced electron transfer process from the amide groups to the dansyl groups, resulting in the luminescence enhancement.

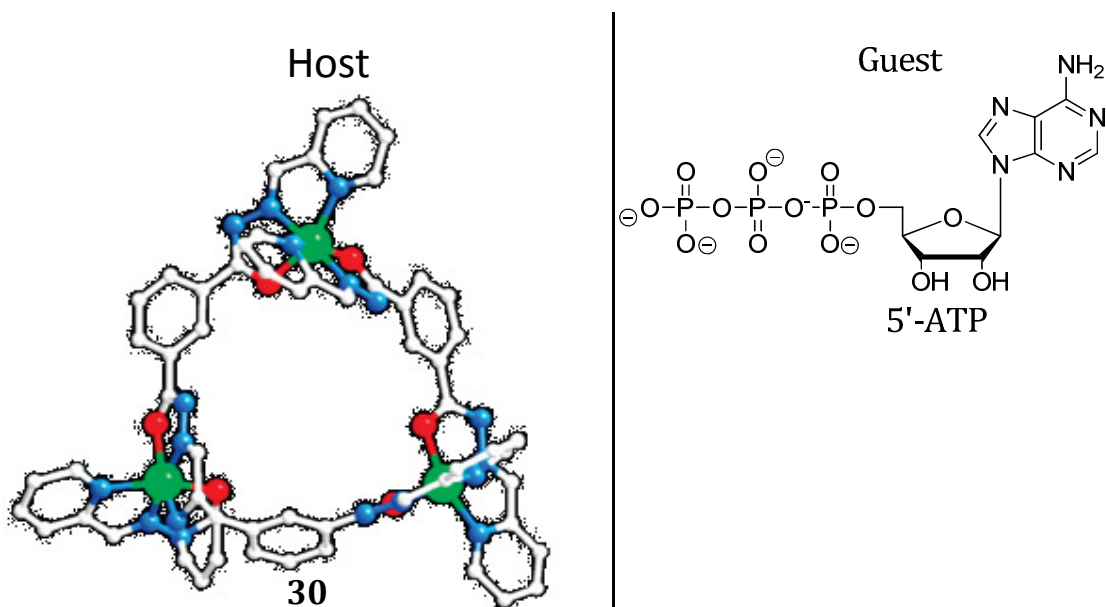


Chart 1.22

Interestingly, the presence of the other ribonucleotide triphosphates, 5'-CTP, 5'-GTP, and 5'-UTP could cause similar luminescence enhancement of the dansyl sulphonamide groups, but the ribonucleotide monophosphates showed negligible changes under the similar experimental conditions. It was also observed that the fluorescence response was size-selective for the nucleotides through hydrogen bonding between the sulfonamide groups and the negatively charged polyphosphate groups. From a mechanistic viewpoint, the amide groups that were fixed at the inflexible backbone of the Werner-

type macrocyclic receptors can respond to 5'-ATP through the hydrogen-bonding patterns between the amide group and the nucleoside. Recently, Fujita and co-workers have reported the selective formation of an anti-Hoogsteen type base pair in the cavity of a Pt²⁺ based metallocyclophane **31**.⁴⁹ The Self-assembled coordination cages formed from the Pt²⁺ ions (Chart 1.23) and the pyrazine pillars provided a flat, hydrophobic

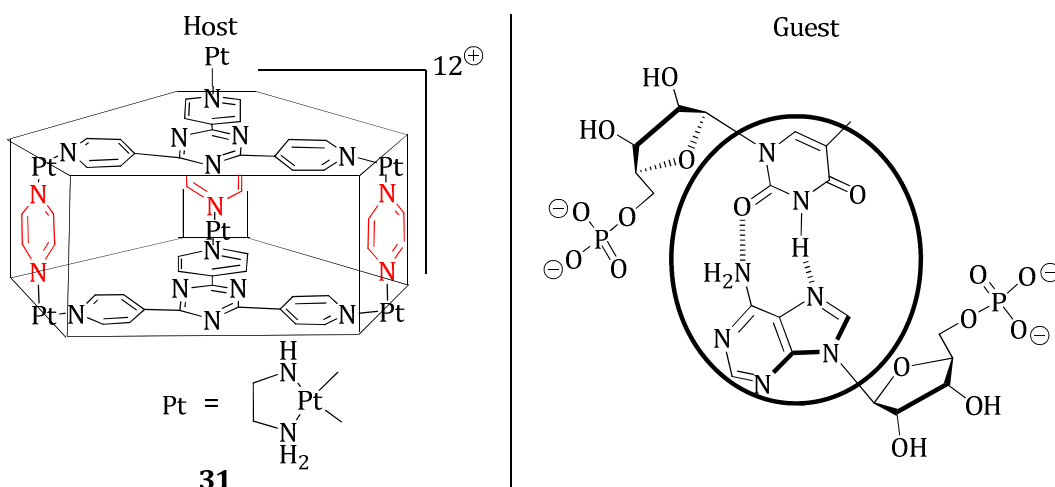


Chart 1.23

microenvironment having an ideal interplanary distance (~6.6 Å) for the binding of single planar aromatic moiety. Expectedly, such a hydrophobic cavity strengthened the hydrogen-bonding interactions and thereby the complementary base pairing in the aqueous solution.

1.5. Objectives of the Present Investigation

The design of selective receptors for a biomolecule of interest is based on the complementarity and preorganization, as well as the involvement of different non-covalent interactions. Since the selectivity of the recognition is decided by the subtle balance between various primary binding forces, the secondary binding interactions between the receptor and the guest molecules would swing the balance in favor of a particular analyte. In spite of the remarkable progress made in the design and development of the functional cyclophanes as probes for the selective optical recognition of various biomolecules, the significant advancements are required in terms of the ease of synthesis, sensitivity and capability of recognition of the receptor under biological conditions.

In this context, it was of our objective to develop functionalized metal ion complexes and or metallocyclophanes as host systems that can selectively bind and recognize nucleosides and nucleotides in the aqueous medium through various non-covalent interactions. It was proposed that such metallocyclophanes would target a large variety of Lewis basic functional groups of the guest molecules and can stabilize the host-guest complexation through employing the supplementary binding interactions such as the coordinative interactions or the cation/anion π -interactions. Yet another objective was to evaluate the

structure-property relationship and importance of the cavity size and the aromatic surface of the receptors in the biomolecular recognition processes.

We have synthesized a few novel anthracene/acridine imidazole conjugates and their corresponding $\text{Cu}^{2+}/\text{Hg}^{2+}$ and Pd^{2+} complexes, respectively, and evaluated their photophysical and biomolecular recognition ability. These systems were found to exhibit solubility in the aqueous medium and favourable photophysical properties. The study of their interactions with various nucleosides and nucleotides indicated that these systems, depending on the cavity size and aromatic nature, exhibited selective interactions with G-based nucleotides and signal the event through visual changes in the fluorescence intensity. These results demonstrate that the metal complexes under investigation are novel and unique in their interactions with nucleosides and nucleotides and hence can have potential use as molecular probes.

1.6. REFERENCES

1. (a) R. Abbel, C. Grenier, M. J. Pouderoijen, J. W. Stouwdam, P. Leclre, R. P. Sijbesma, E. W. Meijer, A. P. H. J. Schenning, *J. Am. Chem. Soc.* **2009**, *131*, 833-843. (b) J. van Herrikhuyzen, A. Syamakumari, A. Schenning, E. W. Meijer, *J. Am. Chem. Soc.* **2004**, *126*, 10021-10027. (c) E. A. Meyer, R. K. Castellano, F. Diederich, *Angew. Chem. Int. Ed.* **2003**, *42*, 1210-1250.
2. (a) S. Leininger, B. Olenyuk, P. J. Stang, *Chem. Rev.* **2000**, *100*, 853-912. (b) A. El-Ghayoury, L. Douce, A. Skoulios, R. Ziessel, *Angew. Chem. Int. Ed.* **1998**, *37*, 2205-2208. (c) J. -M. Lehn, *Supramolecular Chemistry; Concepts and Perspectives*, VCH, Weinheim, **1995**.
3. (a) H. Lodish, A. Berk, L. S. Zipursky, P. Matsudaira, D. Baltimore, J. Darnell, *Molecular Cell Biology*, W. H. Freeman, **2000**. (b) J. Darnell, H. Lodish, B. Baltimore, *Molecular Cell Biology*, Scientific American Books, New York, **1990**.
4. A. Klug, A. C. Bloomer, J. N. Champness, G. Bricogne, R. Staden, *Nature*, **1978**, *276*, 362-368.
5. D. J. Cram and J. M. Cram, *Container Molecules and their Guests*, The Royal Society of Chemistry, Cambridge, **1994**.
6. (a) E. Fischer, *Ber. Dtsch. Chem. Ges.* **1890**, *23*, 2611-2616. (b) E. Fischer, *Ber. Dtsch. Chem. Ges.* **1894**, *27*, 2985-2988. (c) D. E.

- Koshland, *Proc. Natl. Acad. Sci. USA*, **1958**, *44*, 98-105. (d) D. E. Koshland, *Angew. Chem. Int. Ed. Engl.* **1994**, *33*, 2375-2378.
7. (a) D. J. Cram, *Angew. Chem. Int. Ed. Engl.* **1988**, *28*, 1009-1020. (b) C. J. Pedersen, *Angew. Chem. Int. Ed. Engl.* **1988**, *27*, 1021-1027. (c) J.-M. Lehn, *Angew. Chem. Int. Ed. Engl.* **1988**, *27*, 89-112.
8. (a) B. Dietrich, G. Gokel, *Cryptands in Comprehensive Supramolecular Chemistry*, Elsevier, Oxford, **1996**. (b) J. -M. Lehn, J. L. Atwood, J. E. D. Davies, D. D. MacNicol, F. Vogtle, *Comprehensive Supramolecular Chemistry*, Pergamon, Oxford, U.K., **1996**.
9. D. Ramaiah, P. P. Neelakandan, A. K. Nair, R. R. Avirah, *Chem. Soc. Rev.*, **2010**, *39*, 4158-4168.
10. (a) A. Kumar, S. S. Sun, A. J. Lees, *Coord. Chem. Rev.*, **2008**, *252*, 922-939. (b) H. J. Schneider, T. Blatter, P. Zimmermann, *Angew. Chem., Int. Ed. Engl.*, **1990**, *29*, 1161-1162. (c) M. Fujita, J. Yazaki, K. Ogura, *Tetrahedron Lett.*, **1991**, *32*, 5589-5592. (d) M. Albrecht, S. J. Franklin, K. N. Raymond, *Inorg. Chem.*, **1994**, *33*, 5785-5793. (e) M. Fujita, *Chem. Soc. Rev.*, **1998**, *27*, 417-425.
11. E. C. Constable, *J. Chem. Soc., Chem. Commun.*, **1997**, 1073-1076.

12. (a) L. Allouche, A. Marquis, J.-M. Lehn, *Chem. Eur. J.* **2006**, *12*, 7520-7525. (b) Y. Morita, Y. Yakiyama, S. Nakazawa, T. Murata, T. Ise, D. Hashizume, D. Shiomi, K. Sato, M. Kitagawa, K. Nakasuji, T. Takui, *J. Am. Chem. Soc.* **2010**, *132*, 6944-6946. (c) T. N. Parac, M. Scherer, K. N. Raymond, *Angew. Chem. Int. Ed.* **2000**, *39*, 1239-1242. (d) L. N. Dawe, K. V. Shuvaev, L. K. Thompson, *Chem. Soc. Rev.* **2009**, *38*, 2334-2359. (e) K. Suzuki, J. Iida, S. Sato, M. Kawano, M. Fujita, *Angew. Chem. Int. Ed.* **2008**, *47*, 5780-5782.
13. (a) S.-S. Sun, A. J. Lees, *Coord. Chem. Rev.* **2002**, *230*, 171-192. (b) E. J. O'Neil, B. D. Smith, *Coord. Chem. Rev.* **2006**, *250*, 3068-3080.
14. C. R. Rice, *Coord. Chem. Rev.* **2006**, *250*, 3190-3199.
15. M. Fujita, J. Yazaki, K. Ogura, *J. Am. Chem. Soc.*, **1990**, *112*, 5645-5647.
16. M. Fujita, S. Nagao, M. Iida, K. Ogata, K. Ogura, *J. Am. Chem. Soc.* **1993**, *115*, 1574-1576.
17. C. M. Drain, J. M. Lehn, *J. Chem. Soc., Chem. Commun.*, **1994**, 2313-2315.
18. E. C. Constable, E. Schofield, *Chem. Commun.*, **1998**, 403-404.
19. M. J. Hannon, C. L. Painting, W. Errington, *Chem. Commun.*, **1997**, 1805-1807.

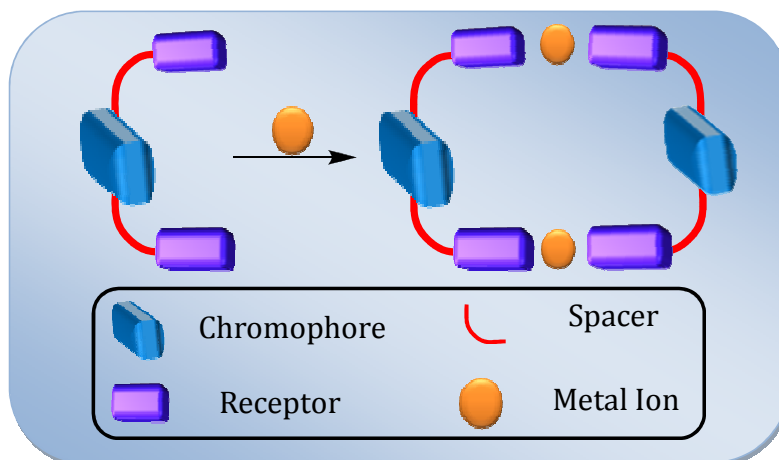
20. P. J. Stang, D. H. Cao, S. Saito, A. M. Arif, *J. Am. Chem. Soc.* **1995**, *117*, 6273-6275.
21. S. -W. Lai, K. -K. Cheung, M. C. -W. Chan, C. -M. Che, *Angew. Chem. Int. Ed.* **1998**, *37*, 182-185.
22. C. Pariya, C. R. Sparrow, C. K. Back, G. Sandi, F. R. Fronczek, A. W. Maverick, *Angew. Chem. Int. Ed.*, **2007**, *46*, 6305-6308.
23. R. D. Schnebeck, E. Freisinger, B. Lippert, *Chem. Commun.*, **1999**, 675-676.
24. S. Ghosh, D. R. Turner, S. R. Batten, P. S. Mukherjee, *Dalton Trans.*, **2007**, 1869-1871.
25. C. Y. Su, Y. P. Cai, C. L. Chen, H. X. Zhang, B. S. Kang, *J. Chem. Soc., Dalton Trans.*, **2001**, 359-361.
26. M. Du, X. J. Zhao, J. H. Guo, *Inorg. Chem. Commun.*, **2005**, *8*, 1-5.
27. L. J. Barbour, G. W. Orr, J. L. Atwood, *Nature*, **1998**, *393*, 671-673.
28. (a) L. J. Barbour, G. W. Orr, J. L. Atwood, *Chem. Commun.*, **2000**, 859-860. (b) Y. B. Xie, J. R. Li, C. Zhang, X. H. Bu, *Crystal Growth Des.*, **2005**, *5*, 1743-1749.
29. Z. M. Liu, Y. Liu, S. R. Zheng, Z. Q. Yu, M. Pan, C. Y. Su, *Inorg. Chem.*, **2007**, *46*, 5814-5816.

30. D. K. Chand, K. Biradha, M. Fujita, *Chem. Commun.*, **2001**, 1652–1653.
31. N. L. S. Yue, D. J. Eisler, M. C. Jennings, R. J. Puddephatt, *Inorg. Chem.*, **2004**, *43*, 7671-7681.
32. J. M. Lehn, A. Rigault, J. Siegel, J. Harrowfield, B. Chevrier, *Proc. Natl. Acad. Sci.*, **1987**, *84*, 2565-2569.
33. C. Piguet, G. Bernardinelli, G. Hopfgartner, *Chem. Rev.*, **1997**, *97*, 2005-2062.
34. E. C. Constable, M. G. B. Drew, G. Forsyth, M. D. Ward, *J. Chem. Soc., Chem. Commun.*, **1988**, *22*, 1450-1451.
35. Y. Zhang, L. Xiang, Q. Wang, X. F. Duan, G. Zi, *Inorg. Chim. Acta.*, **2008**, *361*, 1246–1254.
36. J. M. Lehn, J. -P. Sauvage, J. Simon, R. Ziessel, C. PiccinniLeopardi, G. Germain, J.-P. Declercq, M. Van Meerssche, *Nouv. J. Chim.* **1983**, *7*, 413-417.
37. A. F. Williams, C. Piguet, G. Bernardinelli, *Angew. Chem. Int. Ed.*, **1991**, *30*, 1490-1492.
38. S. Torelli, D. Imbert, M. Cantuel, G. Bernardinelli, S. Delahaye, A. Hauser, J. C. G. Bunzli, C. Piguet, *Chem. Eur. J.*, **2005**, *11*, 3228-3242.
39. D. A. McMorran, P. Steel, *J. Angew. Chem. Int. Ed.*, **1998**, *37*, 3295-3297.

40. R. V. Slone, D. I. Yoon, R. M. Calhoun, J. T. Hupp, *J. Am. Chem. Soc.*, **1995**, *117*, 11813-11814.
41. A. Bilyk, M. M. Harding, P. Turner, T. W. Hambley, *J. Chem. Soc. , Dalton Trans.*, **1994**, 2783-2787.
42. S. S. Sun, A. J. Lees, *J. Am. Chem. Soc.*, **2000**, *122*, 8956-8958
43. R. V. Slone, D. I. Yoon, R. M. Calhoun, J. T. Hupp, *J. Am. Chem. Soc.*, **1995**, *117*, 11813-11815.
44. P. Thanasekaran, R. -T. Liao, B. Manimaran, Y. -H. Liu, P. -T. Chou, S. Rajagopal, K. -L. Lu, *J. Phys. Chem. A*, **2006**, *110*, 10683-10689.
45. R. Lin, J. H. K. Yip, K. Zhang, L. L. Koh, K. -Y. Wong, K. P. Ho, *J. Am. Chem. Soc.* **2004**, *126*, 15852-15854.
46. C. A. Hunter, L. D. Sarson, *Angew. Chem. Int. Ed.* **1994**, *33*, 2313-2316.
47. M. A. Galindo, J. A. R. Navarro, M. A. Romero, M. Quiro' s, *Dalton Trans.*, **2004**, 1563-1566.
48. H. Wu, C. He, Z. Lin, Y. Liu, C. Duan, *Inorg. Chem.*, **2009**, *48*, 408-410.
49. T. Sawada, M. Yoshizawa, S. Sato, M. Fujita, *Nat. Chem.*, **2009**, *1*, 53-56.

CHAPTER 2

SYNTHESIS AND STUDY OF PHOTOPHYSICAL PROPERTIES OF METALLOCYCLOPHANES



2.1. ABSTRACT

With a view to develop efficient metal ion complexes or metallocylophanes as probes for nucleosides and nucleotides, we have synthesized anthracene imidazole based ligands **1** and **3** and their metal complexes $[\mathbf{1}.\text{CuCl}_2]_2$, $[\mathbf{1}.\text{Hg}(\text{ClO}_4)_2]$ and $[(\mathbf{3})_2.\text{CuCl}_2]$ and investigated their photophysical properties. The formation of the metal ion complexes was confirmed by optical spectroscopic techniques. For example, with increasing concentration of $\text{Cu}^{2+}/\text{Hg}^{2+}$ ions, the ligands **1** and **3** showed significant hypochromicity along with a bathochromic shift in their absorption spectra, while their emission spectra showed

quenching in the fluorescence intensity at 421 nm. We have analysed the absorption and emission changes using Job's plot and Benesi-Hildebrand analysis, which gave association constants of $K_{\text{ass}} = 1.75 \pm 0.1 \times 10^5$ and $1.37 \pm 0.1 \times 10^5 \text{ M}^{-1}$ and change in free energy of $\Delta G = -12.1$ and $-11.8 \text{ kJ mol}^{-1}$, respectively, for complexation of the ligand **1** with CuCl_2 and $\text{Hg}(\text{ClO}_4)_2$.

The metal complexation was further confirmed by MALDI-TOF mass spectral analysis, which showed peaks at 944.67 and 737.42, corresponding to a 2:2 and 1:1 stoichiometric complexes formed between the ligand **1** and CuCl_2 and $\text{Hg}(\text{ClO}_4)_2$, respectively. In the ^1H NMR spectrum, we observed regular broadening and complete disappearance of the peaks corresponding to the imidazole protons of the ligand **1** with the addition of CuCl_2 , whereas the peaks corresponding to the anthracene and methylene protons remained unaffected. Based on the MALDI-TOF MS, theoretical calculations and NMR evidence as well as literature reports, we assign a symmetric cyclic structure such as a metallocyclophane for $[\mathbf{1}.\text{CuCl}_2]_2$. This unique arrangement of the metal ions as bridging motifs between the two ligand molecules creates a highly rigid cavity in the metallocyclophane $[\mathbf{1}.\text{CuCl}_2]_2$ making it an ideal choice as a host for biomolecular recognition under physiological conditions.

2.2. INTRODUCTION

Biomolecular recognition processes are often influenced by a number of factors such as hydrogen bonding, electrostatic, π -stacking and hydrophobic interactions.¹ The selective recognition of various biomolecules requires the synergistic interplay of all these non-covalent interactions.² One of the most important concepts to be considered while designing specific receptors is the structural features of the biomolecule that could aid the various non-covalent interactions.³ For example, the aromatic base present in the nucleotides can participate in π -stacking and hydrophobic interactions, while the negatively charged phosphate groups facilitate electrostatic interactions.⁴ Even though non-covalent interactions are weaker than covalent bonds, the cooperative effect of a number of such different non-covalent interactions would stabilize the complexation process. One of the most important challenges in the design of receptors for biomolecules is the feasibility of the recognition in the biologically relevant medium.⁵

Most of the receptors reported for biomolecules rely on hydrogen bonding for the selective recognition process.⁶ However; the recognition by hydrogen bonding interactions becomes limited in the aqueous medium due to the competitive hydrogen bonding by the solvent. In this

point of view, other non-covalent interactions such as electrostatic interactions as well as π - π stacking and solvophobic interactions are preferable in the host system to enhance the capability of selective complexation in water. One of the successful classes of receptors used for the recognition of biomolecules with the aid of various non-covalent interactions are rigid functional cyclophanes.⁷ A number of such cyclophanes have been designed and developed over the years by various research groups with an aim to selectively recognise various guest molecules of interest.⁸ Supplementary modification of these cyclophanes by the incorporation of metal centres opens up a new promises for designing receptors such as the metallocyclophanes and transition metal complexes (Figure 2.1).

The incorporation of additional binding sites such as metal centres in these systems would enable improved binding interactions through coordinative and cation/anion π -interactions. These host systems can target a large variety of Lewis basic functional groups containing guest molecules and can stabilize the host-guest complexation by employing the additional binding interactions such as the coordinative interactions or the cation/anion π -interactions along with the other synergistic interactions.⁹ Albeit a larger number of metallated assemblies are reported, only a few of them have been

investigated for their biomolecular recognition.¹⁰ Therefore, development of novel metal architectures,¹¹⁻¹³ which can selectively recognize nucleosides and nucleotides in the aqueous medium, is an active area of research. In this regard, the ligands that form coordinatively unsaturated complexes with metal ions, and are capable of further binding to Lewis-basic substrates through open coordination sites present in various biomolecules are particularly interesting and are worth exploring for such applications.¹⁴

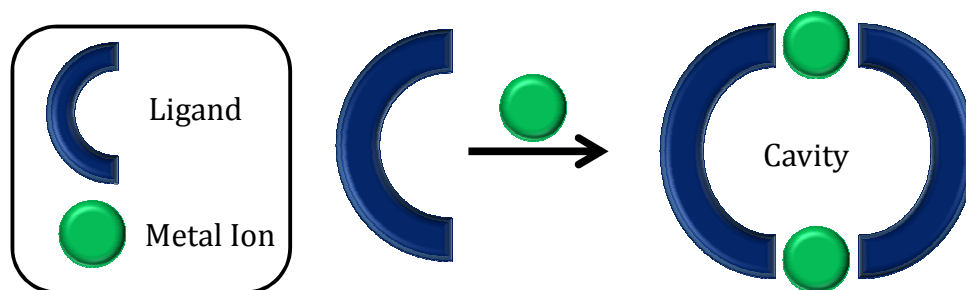


Figure 2.1. Schematic representation of the metallocyclophane formation by the ligands and the metal ions.

With an objective of developing metallocyclophanes as receptors, we have synthesized anthracene-imidazole conjugates **1-3** and have investigated their potential to form complexes with various metal ions (Chart 2.1). Our investigations revealed that these ligands exhibited favourable photophysical properties and undergo selective interactions with Cu^{2+} and Hg^{2+} ions, when compared to other metal ions. Of these

metal complexes, the Cu^{2+} ions induced the formation of novel metallocyclophane with a well-defined cavity for its potential applications as host in the biomolecular recognition.

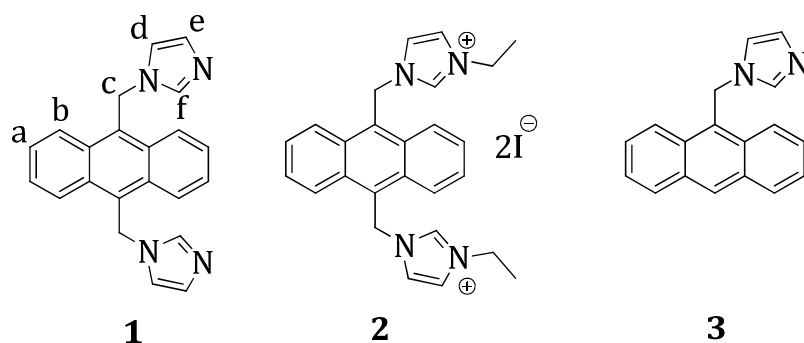


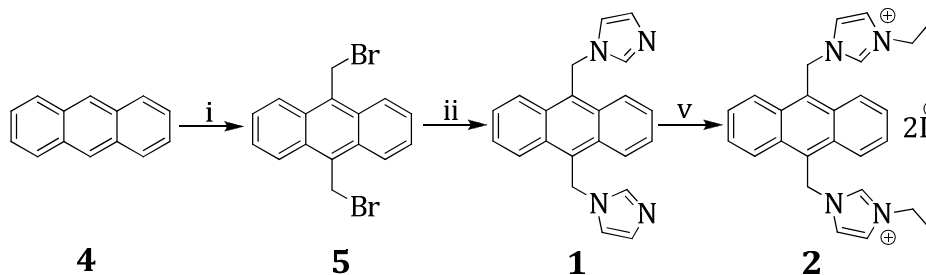
Chart 2.1.

2.3. RESULTS

2.3.1. Synthesis of the Ligands 1, 2 and 3

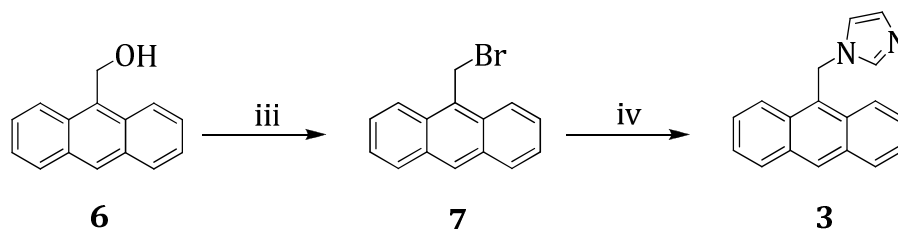
The synthesis of 9,10-bis((1H-imidazol-1-yl)methyl)anthracene (**1**) and 1,1'-(anthracene-9,10-diylbis(ethylene))bis(3-methyl-1H-imidazol-3-ium) iodide (**2**) were achieved in moderate yields by using the modified literature procedures (Scheme 2.1).¹⁵ Bromomethylation of anthracene (**4**) with hydrobromic acid in glacial acetic acid in the presence of paraformaldehyde for 4 h at room temperature gave 9, 10-bis(bromomethyl)anthracene (**5**) in 95% yields. The reaction of **5** with imidazole in the presence of sodium hydride in tetrahydrofuran for 4 h at room temperature resulted in **1** in 78% yields. The synthesis of the

model derivative **2**, on the other hand, was achieved in moderate yields through the reaction of **1** with ethyl iodide in CH₃CN for 24 h at 80 °C. The bromination of anthracen-9-ylmethanol (**6**) using phosphorus tribromide in dichloromethane for 12 h gave **7**, which on reaction with imidazole in presence of sodium hydride in tetrahydrofuran for 4 h at room temperature gave the model derivative **3** (Scheme 2.2).



i) Paraformaldehyde, HBr in glacial acetic acid, 25 °C, 4 h; ii) imidazole, NaH, THF, 25 °C, 4 h; v) CH₃I, CH₃CN, 80 °C, 24 h.

Scheme 2.1



(iii) PBr₃, CH₂Cl₂, 0 °C, 12 h; (vi) imidazole, NaH, THF, 25 °C, 4 h.

Scheme 2.2

These compounds were characterized on the basis of analytical and spectral evidences. For example, the ¹H NMR spectrum of the ligand **1** in DMSO-*d*⁶ showed peaks corresponding to the the imidazole protons

H_d, H_e and H_f at δ 6.7, 6.9 and 7.7, whereas the peaks corresponding to the anthracene (H_a and H_b) protons appeared in the region δ 7.7 - 8.6 and the methylene protons appeared as a singlet at δ 6.3 (H_c). Similarly, the ¹³C NMR spectrum of the ligand **1** showed peaks at δ 109.9, 113.6, 119.1, 124.7, 124.9, 128.3, 129.1, and 130.1, confirming its symmetric structure.

2.3.2. Photophysical Properties of the Ligands 1-3

The photophysical properties of the ligand **1** and the model compounds **2** and **3** have been investigated under different conditions. All these derivatives exhibited characteristic anthracene chromophore absorption having maxima in the region between 365-375 nm in 20% DMSO-water mixture. For example, the ligand **1** showed a structured absorption spectrum with maximum at λ_{max} 373 nm, while the derivative **3** exhibited λ_{max} at 368 nm as shown in Figure 2.2. The absorption spectra of these derivatives in organic solvents such as acetonitrile were found to be similar to that observed in the 20% DMSO-water mixture. The emission spectra of the ligand **1** and the model derivative **3** recorded in 20% DMSO-water mixture, which were also characteristic of the anthracene chromophore. In 20% DMSO-water, all these derivatives exhibited emission maxima in the region between 397

- 430 nm (Figure 2.3). Similarly, the model derivative **2** in the aqueous medium, showed the anthracene chromophore absorption having maxima at 375 and 395 nm as shown in Figure 2.4.

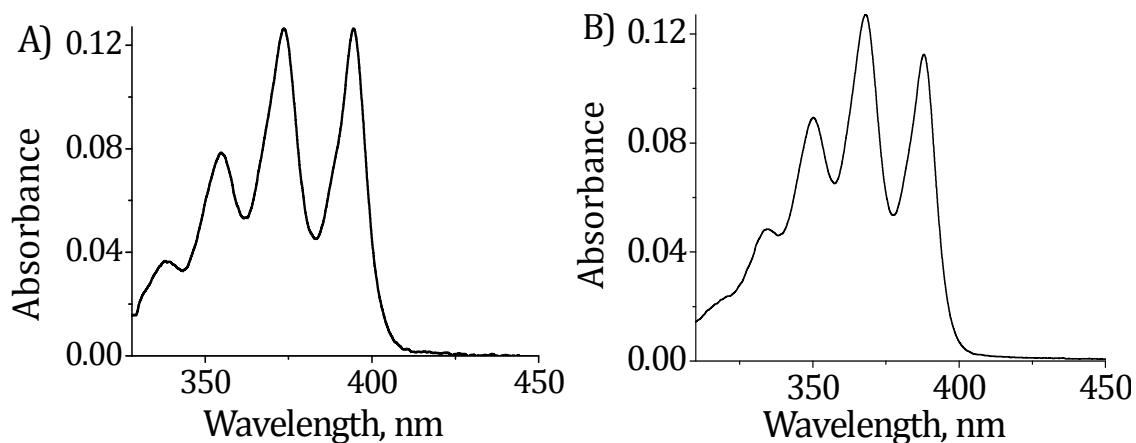


Figure 2.2. Absorption spectra of the ligands A) **1** (20 μM) and B) **3** (36 μM) in 20% DMSO-water mixture.

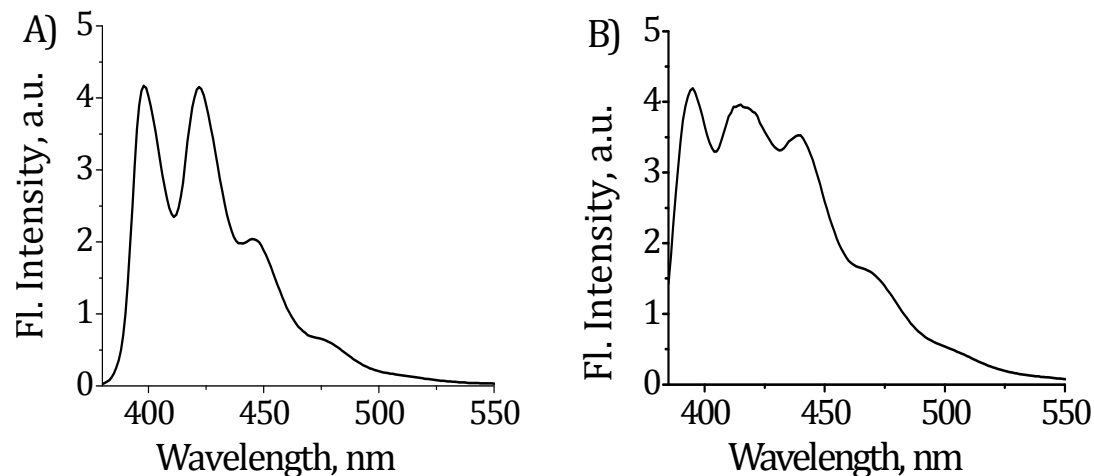


Figure 2.3. Emission spectra of the ligands A) **1** (20 μM) and B) **3** (36 μM) in 20% DMSO-water mixture. λ_{ex} , 375 nm.

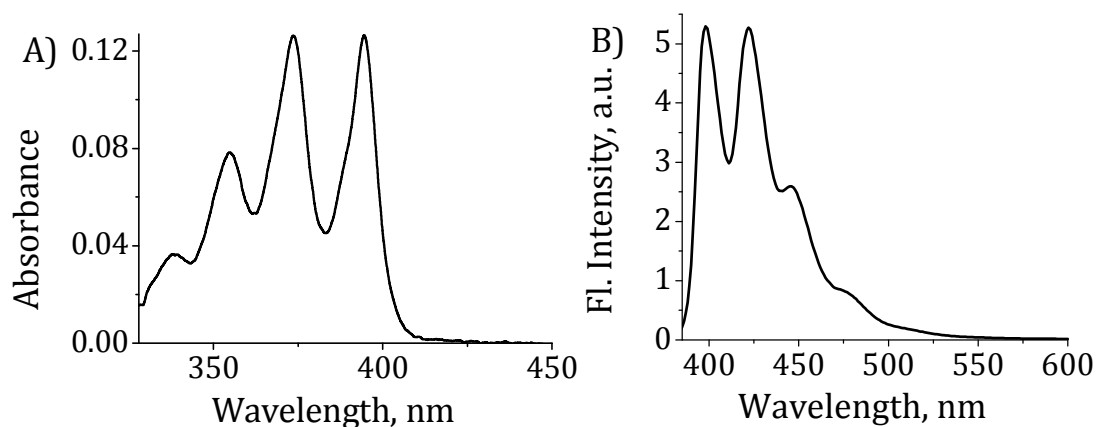


Figure 2.4. A) Absorption and B) emission spectra of the ligand **2** (12 μM) in aqueous solution. λ_{ex} , 375 nm.

We have calculated the fluorescence quantum yields of the ligand **1** and the model derivatives **2** and **3** using quinine sulphate in 0.1 N H_2SO_4 as the standard. The derivatives **1-3** exhibited quantum yield values of $\phi_F = 0.34 \pm 0.01$, 0.54 ± 0.01 and 0.16 ± 0.01 , respectively in 20% DMSO-water mixture. To understand the excited state behavior of the ligands **1-3**, we have carried out their picosecond time-resolved fluorescence analysis.¹⁶ The time-resolved experiments have revealed that these compounds showed mono-exponential fluorescence decay with lifetime values of 6.6 ns, 8.3 ns and 4.2 ns, respectively for **1**, **2**, and **3** in methanol (Figure 2.5).

2.3.3. Study of Interactions with Metal Ions

To understand the potential of the ligands **1-3** as complexing agents, we have monitored their interactions with various mono and

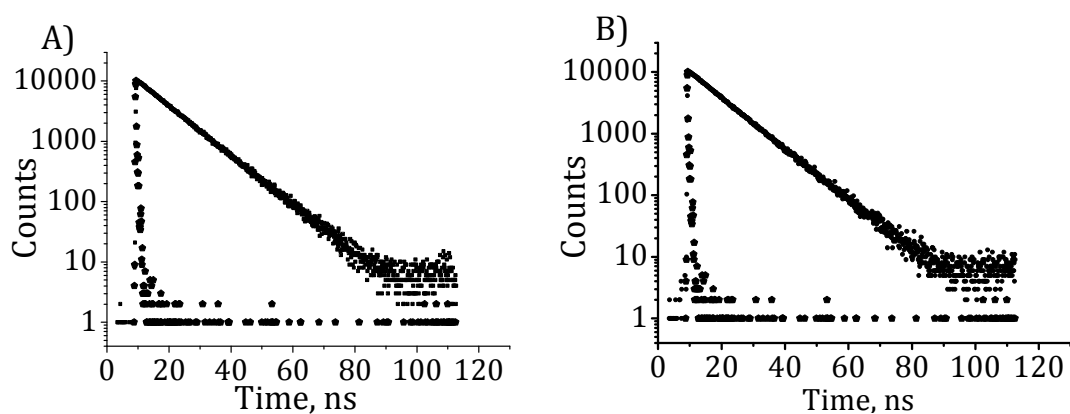


Figure 2.5. Fluorescence decay profiles of the ligands A) **1** (20 μM) and B) **2** (12 μM) in methanol monitored at 418 nm. λ_{ex} , 375 nm.

divalent metal ions such as Na^+ , K^+ , Cu^{2+} , Hg^{2+} , Ca^{2+} , Mg^{2+} , Zn^{2+} , Pb^{2+} , Zn^{2+} and Cd^{2+} ions through optical spectroscopic techniques. For example, Figure 2.6 shows the changes in the absorption spectrum of the ligand **1** upon addition of Cu^{2+} ions. Upon increasing in concentration of Cu^{2+} ions, we observed significant hypochromicity in the absorption spectrum along with a concomitant bathochromic shift. At 156 μM of CuCl_2 , the absorption spectrum of the ligand **1** showed *ca.* 28% hypochromicity along with a bathochromic shift of 2 nm. The corresponding changes in the fluorescence spectra of the ligand **1** with increasing addition of the Cu^{2+} ions are shown in Figure 2.7A. With increasing concentration of Cu^{2+} ions, we observed *ca.* 50% quenching in the fluorescence intensity at 421 nm.

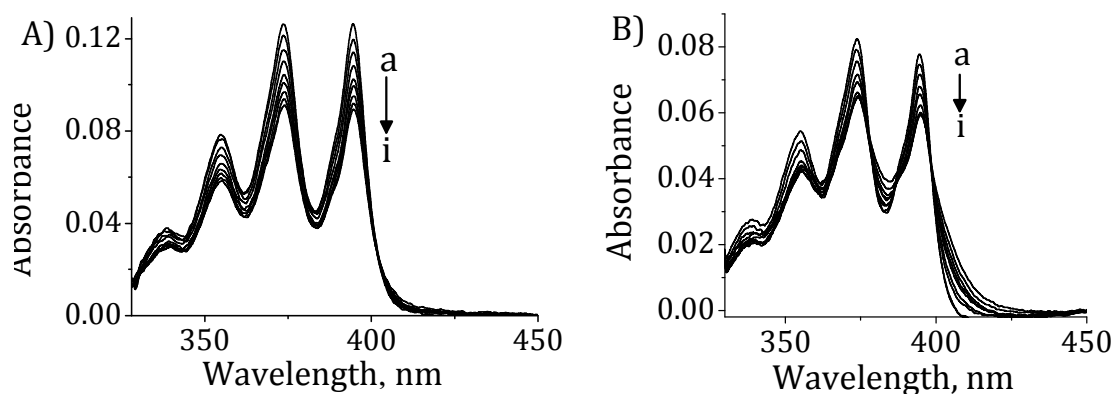


Figure 2.6. Changes in the absorption spectra of **1** (20 μM) with increasing concentration of A) Cu^{2+} and B) Hg^{2+} ions in 20% DMSO-water. [M^{2+}] a) 0 and i) 156 μM . λ_{ex} 375 nm.

Similar experiments were carried out with $\text{Hg}(\text{ClO}_4)_2$ under identical conditions. With increasing concentration of $\text{Hg}(\text{ClO}_4)_2$, the extent of hypochromicity and the quenching in fluorescence intensity was found to be less, when compared to Cu^{2+} ions. With the addition of 156 μM of Hg^{2+} ions, the absorption spectrum of **1** showed *ca.* 22% hypochromicity along with a bathochromic shift of 2 nm as shown in Figure 2.6B, whereas in the emission spectra, we observed *ca.* 40% quenching in the fluorescence intensity (Figure 2.7B). Interestingly, the ligand **1** showed negligible interactions with various other mono and divalent metal ions such as Na^+ , K^+ , Ca^{2+} , Mg^{2+} , Zn^{2+} , Pb^{2+} and Cd^{2+} ions as evidenced through the negligible changes in its absorption and emission spectra.

Figure 2.8 shows the relative changes in the emission intensity observed on titration of the ligand **1** with these metal ions. From the relative plot it is clear that the ligand **1** forms stable complexes with only Cu^{2+} and Hg^{2+} ions. For example, Figure 2.9 shows the changes in the absorption and emission spectra of the ligand **1** ($20\ \mu\text{M}$) with increasing concentration of Zn^{2+} ions in 20% DMSO-water.

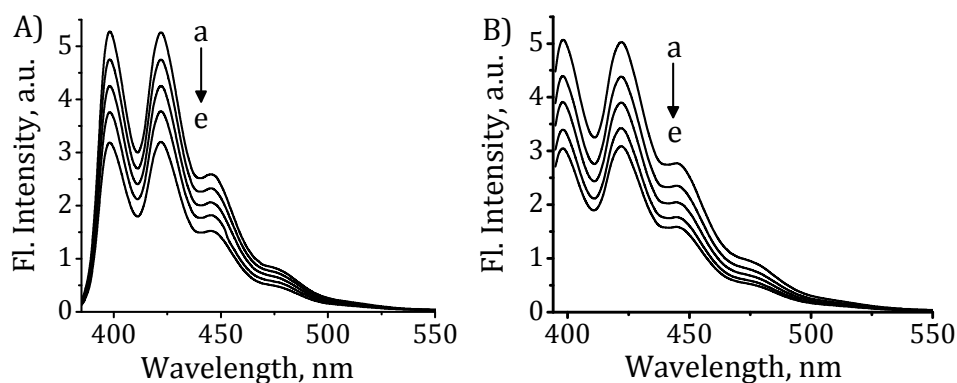


Figure 2.7. Changes in the emission spectra of **1** ($20\ \mu\text{M}$) with the addition of A) Cu^{2+} ions and B) Hg^{2+} ions in 20% DMSO-water. $[\text{M}^{2+}]$ a) 0 and e) $156\ \mu\text{M}$. $\lambda_{\text{ex}} 375\ \text{nm}$.

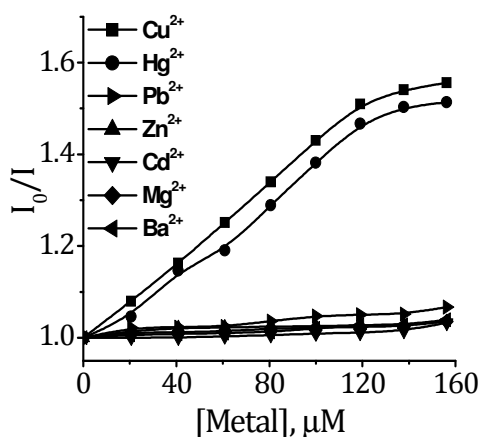


Figure 2.8. Relative changes in fluorescence intensity of the ligand **1** ($20\ \mu\text{M}$) upon interaction with different metal ions.

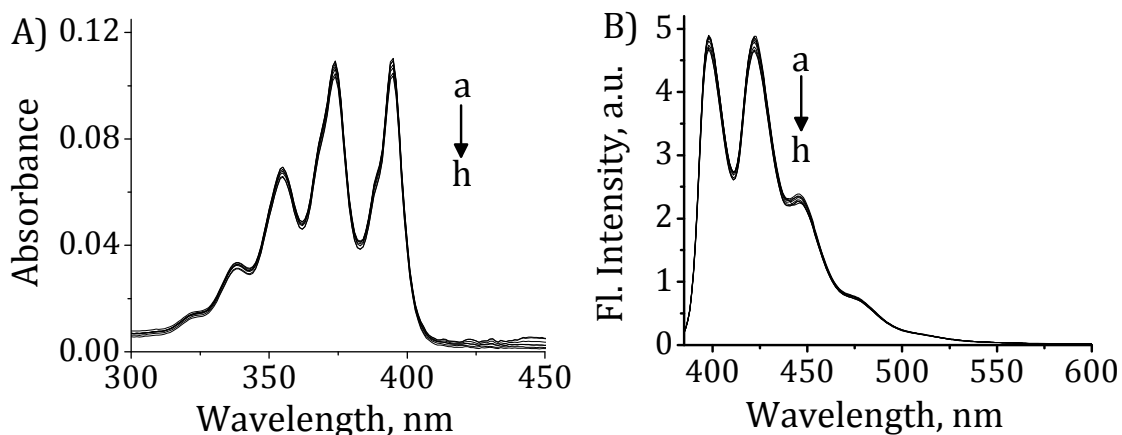


Figure 2.9. Changes in the A) absorption and B) emission spectra of **1** (20 μM) with the addition of Zn^{2+} ions in 20% DMSO-water. $[\text{M}^{2+}]$ a) 0 and h) 156 μM . λ_{ex} 375 nm.

Similarly, we have monitored the binding interactions of the ligands **2** and **3** with various metal ions. We have monitored the absorption and emission properties of the ligand **3** by increasing in concentration of various metal ions. At 156 μM of Cu^{2+} ions, we observed *ca.* 44% quenching in the fluorescence intensity of the ligand **3** in 20% DMSO-water mixture as shown in Figure 2.10A. Figure 2.10B shows the extent of quenching and selectivity of the ligands **1** and **3** for the Cu^{2+} ions. The ligand **2**, on the other hand, exhibited negligible changes in its absorption and emission properties upon interactions with various monovalent and divalent metal ions in the aqueous solution as shown in Figure 2.11.

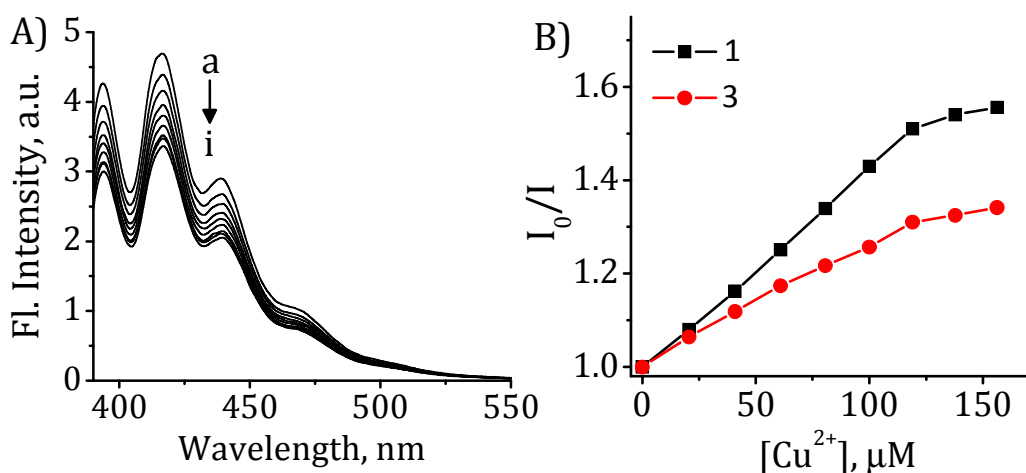


Figure 2.10. Changes in the A) emission spectrum of the model compound **3** (36 μM) with the addition of Cu²⁺ ions in 20% DMSO-water and B) shows the relative changes in the fluorescence intensity of **1** and **3** in the presence of Cu²⁺ ions. [Cu²⁺] a) 0 and i) 156 μM. λ_{ex} , 375 nm.

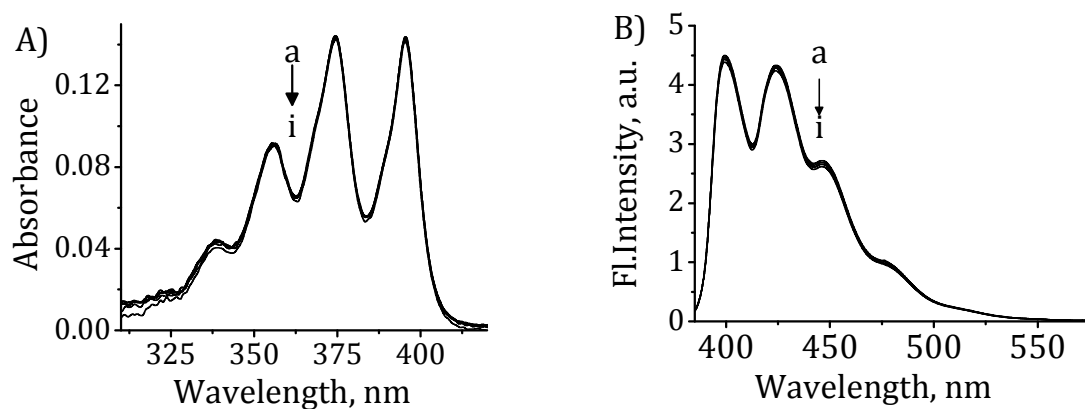


Figure 2.11. Changes in the A) absorption and B) emission spectra of the ligand **2** (12 μM) with the addition of Cu²⁺ ions in 20% DMSO-water. [Cu²⁺] a) 0 and i) 156 μM. λ_{ex} , 375 nm.

To understand the stoichiometry of the complexation of the ligand **1** with CuCl₂ and Hg(ClO₄)₂, we analysed the absorption and emission changes using Job's plot analysis. In this method, the total molar

concentration of the ligand **1** and Cu^{2+} ions and Hg^{2+} ions were held constant, but their mole fractions were varied. The peak area from the emission spectra that was proportional to the complex formation was plotted against the mole fractions of these two components.¹⁷ When the mole fraction of the ligand **1** was reached 0.50, the fluorescence intensity of the ligand **1** in the complex also reached maximum, indicating the formation of a complex with 1:1 ratio between **1** and Cu^{2+} ions and Hg^{2+} ions (Figure 2.12). Further, we have analysed the absorption and fluorescence changes using Benesi-Hildebrand techniques, which indicated a 1:1 stoichiometry for the complexes formed between **1** and $\text{CuCl}_2/\text{Hg}(\text{ClO}_4)_2$ having the association constants of $K_{\text{ass}} = 1.75 \pm 0.1 \times 10^5$

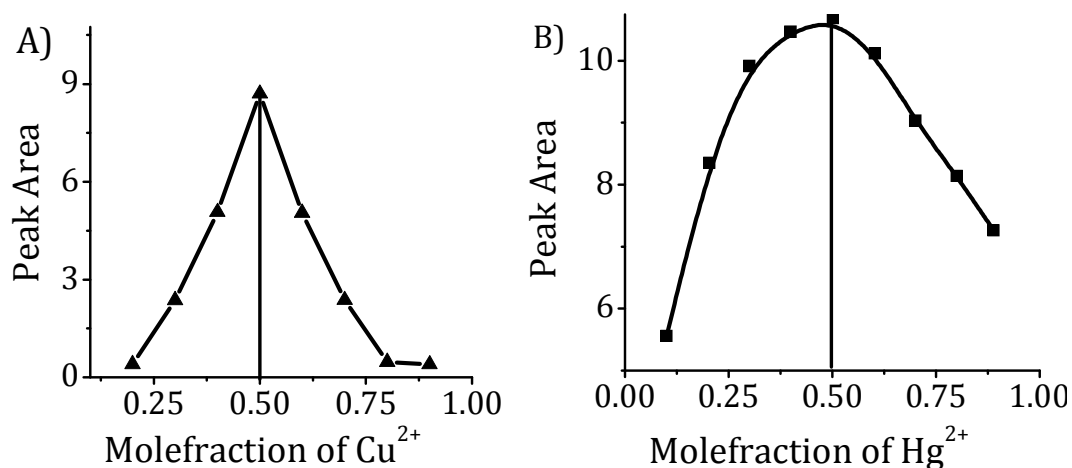


Figure 2.12. Jobs plot analysis of **1** (20 μM) with the addition of A) Cu^{2+} ions and B) Hg^{2+} ions in 20% DMSO-water.

and $1.37 \pm 0.1 \times 10^5 \text{ M}^{-1}$ and change in free energy of $\Delta G = -12.1$ and $-11.8 \text{ kJ mol}^{-1}$, respectively (Figure 2.13).¹⁸

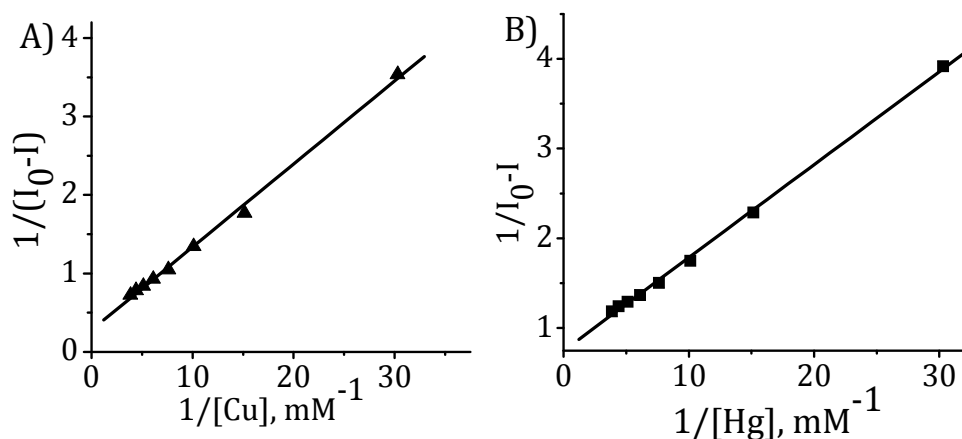
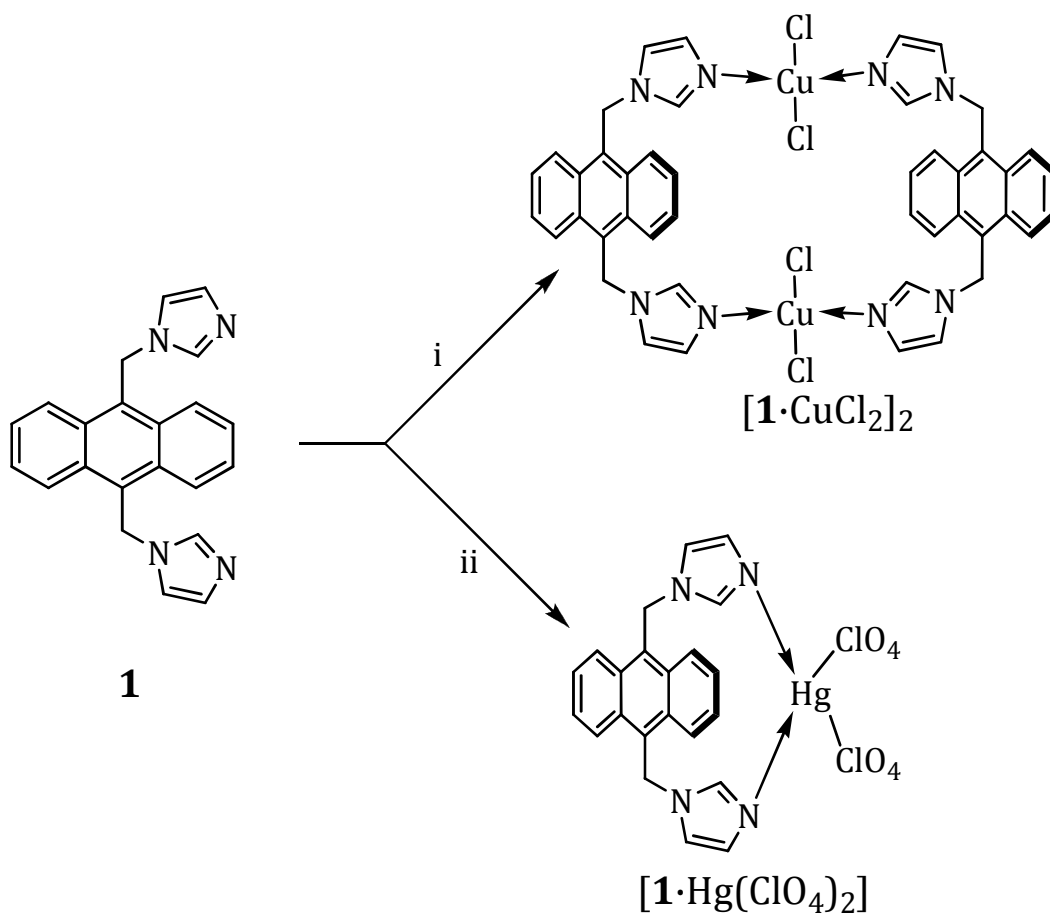


Figure 2.13. The Benesi-Hildebrand fit for fluorescence quenching of the ligand **1** by A) Cu^{2+} and B) Hg^{2+} ions.

2.3.4. Isolation and Characterization of the Metal Complexes

The reaction of the anthracene imidazole conjugate **1** with one equivalent of CuCl_2 in 10% methanol-acetonitrile mixture at room temperature readily gave a complex, which was collected, washed with methanol (Scheme 2.3). The product thus obtained was further purified through recrystallization from acetonitrile. The complex was characterized through matrix assisted laser desorption ionization time of flight (MALDI-TOF) mass spectrometry analysis. We observed a peak at 944.67 in the mass spectrum $[\mathbf{1.CuCl}_2]_2$ formed between the ligand **1** and CuCl_2 . The observed peak in the MALDI-TOF mass spectrum of the



i) CuCl_2 , 10% MeOH- CH_3CN , 25 °C, 1 h; ii) $\text{Hg}(\text{ClO}_4)_2$, CH_3CN , 25 °C, 1 h.

Scheme 2.3

complex **1** with Cu^{2+} ions can be assigned to 2:2 metallosupramolecular complex $[\mathbf{1} \cdot \text{CuCl}_2]_2$. Similarly, the complex obtained after the reaction of the ligand **1** with one equivalent of $\text{Hg}(\text{ClO}_4)_2$ showed a peak at 737.4 in the MALDI-TOF mass spectrum, which corresponds to a 1:1 stoichiometry of the complex $[\mathbf{1} \cdot \text{Hg}(\text{ClO}_4)_2]$. Further, the formation of the metallosupramolecular complex $[\mathbf{1} \cdot \text{CuCl}_2]_2$ by the complexation of the ligand **1** with

CuCl₂ was studied through ¹H NMR spectroscopic techniques. Figure 2.14 shows the changes in the ¹H NMR spectra of the ligand **1** with the addition of Cu²⁺ ions in DMSO-*d*₆. We observed line broadening during NMR titrations because of the paramagnetic nature of the Cu²⁺ ions. To understand the binding interactions, we carried out the NMR titrations at very low concentrations of the Cu(II) (0–11 μM). The gradual addition of Cu²⁺ ions resulted in significant broadening of the peaks corresponding to the imidazole protons H_d, H_e and H_f at δ 6.7, 6.9 and 7.7 ppm, respectively. In addition, as the concentration of Cu²⁺ was gradually increased, the intensity of these peaks decreased drastically and at *ca.* 11 μM, we observed complete disappearance of these peaks. Moreover, no significant changes were observed with the peaks corresponding to the anthracene and methylene in the ¹H NMR titration

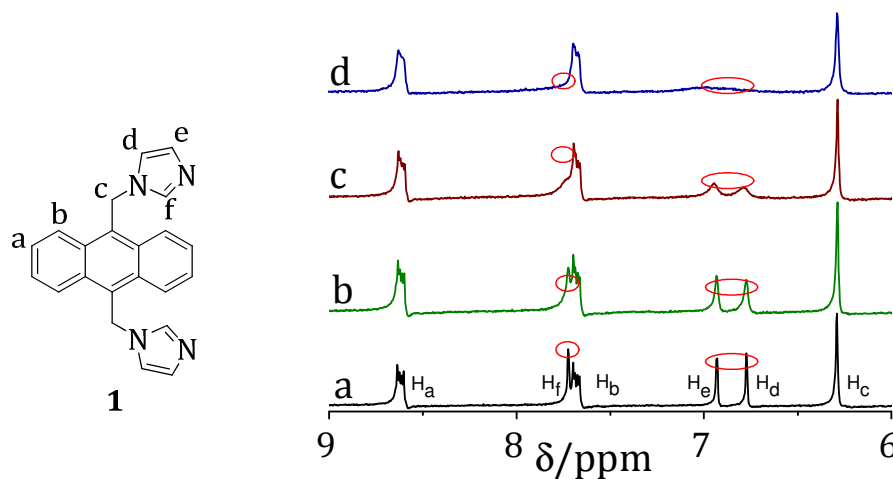


Figure 2.14. Changes in the ¹H NMR spectra of the ligand **1** (4.9 mM) with the addition of CuCl₂ in DMSO-*d*₆. [Cu²⁺] a) 0, b), c) and d) 11 μM.

of the ligand **1** with metal ions. These observations indicate that the anthracene moiety has no significant interactions with the metal ions, whereas the metal complexation is primarily through the imidazole nitrogen atom of the ligand.

To understand the strength and reversibility of the complex, we have investigated the effect of temperature and using a better chelating ligand such as EDTA.¹⁹ Monitoring the emission changes of the anthracene chromophore by the successive additions of EDTA revealed the reversibility of the complex formed by Cu²⁺ ions with the ligand **1**. Due to the strong chelating behavior of EDTA with Cu²⁺ ions, when compared to the ligand **1**, the enhancement in the fluorescence intensity corresponding to anthracene moiety was observed with increasing in concentration of EDTA as shown in Figure 2.15. The quenched fluorescence of the anthracene chromophore in [**1**.CuCl₂]₂ was completely revived by the addition of excess concentration of EDTA. This regenerated ligand **1** by EDTA from the complex [**1**.CuCl₂]₂ showed *ca.* 43% quenching of fluorescent intensity by further addition of Cu²⁺ ions. Similar observations were obtained by increasing the temperature from 25 to 85 °C. At 25 °C, we observed the expected fluorescence emission quenching of the anthracene chromophore in the complex state as shown in Figure 2.15.

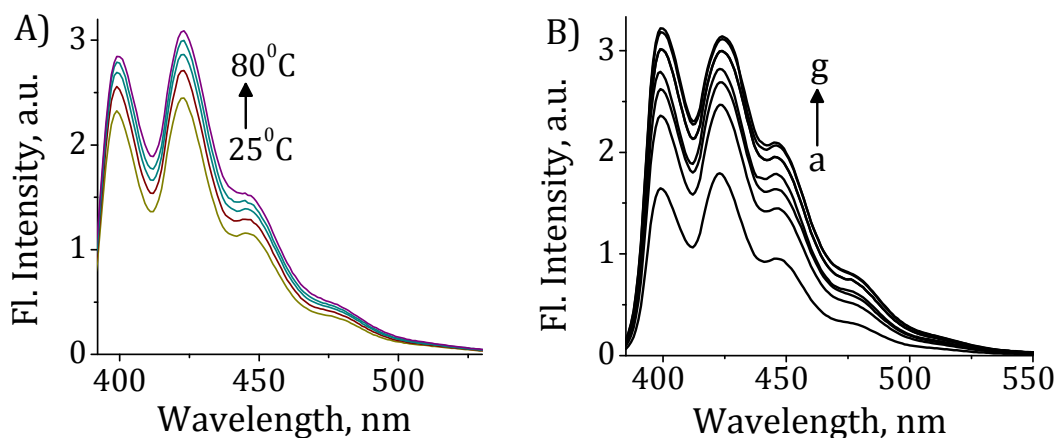


Figure 2.15. Changes in the emission spectrum of $[1.CuCl_2]_2$ ($16 \mu M$) with A) increasing temperature (25-85 °C) and B) addition of EDTA. $[EDTA]$ (a) 0, and (g) $625 \mu M$. λ_{ex} , 375 nm.

However, we observed the enhancement in fluorescent emission corresponding to the anthracene chromophore when the temperature increased from 25 to 85 °C. We have theoretically calculated the minimum energy conformation of the complex using the Universal Force Field (UFF)²⁰ which gave a 2:2 stoichiometric for the metallocyclophane as is shown in Figure 2.16.

2.4. DISCUSSION

We have synthesized the anthracene-imidazole based ligand **1** and the model derivatives **2** and **3** linked together through methylene group as bridging moieties. The ligand **1** and the model derivative **3** exhibited

solubility in the 20% DMSO-water medium, whereas the ligand **2** showed

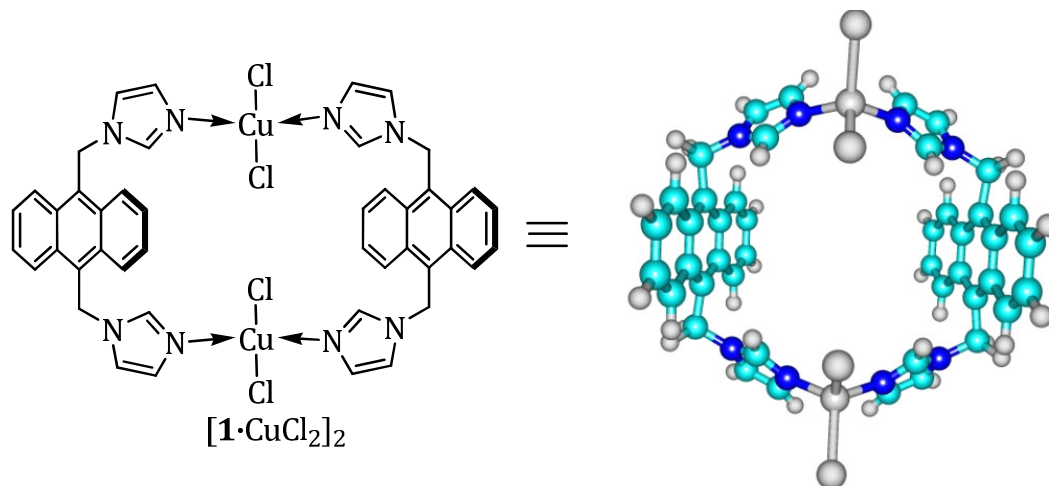


Figure 2.16. Optimized geometry of the metallocyclophane $[1.CuCl_2]_2$.

high solubility in the aqueous medium. These systems showed photophysical properties characteristic of the anthracene chromophore. In this aspect, the anomalous behavior of the metallocyclophane formation of the ligand **1** containing two imidazole moiety bridged together through methylene unit is quite interesting. The extent of the hypochromicity and bathochromic shift observed for the ligands **1** and **3** along with quenching in the fluorescence intensity upon interactions with Cu^{2+} and Hg^{2+} ions can be attributed to the coordinative interactions of the metal ions through imidazole nitrogen.

From the NMR titration experiments, the formation of the metallocyclophane $[1.CuCl_2]_2$ through imidazole nitrogen was confirmed

by the significant broadening of the peaks corresponding to the imidazole protons.²¹ Addition of the Cu²⁺ ions resulted in the selective broadening and disappearance of the imidazole protons, which could be attributed to the inductive effect of paramagnetic nature of the Cu²⁺ ions.²² These results confirm that the Cu²⁺ ions coordinate exclusively with the imidazole moiety through the imidazole nitrogen. The observation of the symmetric nature of the NMR spectrum also supports the formation of a symmetric complex having a 2:2 stoichiometry for [1.CuCl₂]₂.

The observation of the revival of their fluorescence intensity and ¹H NMR signals of the complex upon decomplexation with EDTA clearly explain the existence of reversible coordination interactions between the imidazole nitrogen and the Cu²⁺ ions. The decomplexation of the metallocyclophane by increasing temperature also showed the reversibility of the complex formed by the ligand **1** and CuCl₂. Furthermore, the matrix assisted laser desorption ionization time of flight (MALDI-TOF)²³ mass spectrometry analysis of this complex showed a molecular mass of 946.1, which is in agreement with the formation of a 2:2 stoichiometric complex between the ligand **1** and CuCl₂. In contrast, the model derivative **3** showed selectivity towards Cu²⁺ ions as expected, since it contains one imidazole moiety. As

evidenced from the titration experiments, the extent of the quenching and selectivity of the ligand **3** towards Cu^{2+} ions is not significant because of the fact that the coordination is expected to take place through only one imidazole moiety. The negligible interactions observed with the ligand **2** clearly confirm the fact that the metallocyclophane formation involves the coordination through the imidazole nitrogen. Furthermore, the observed selectivity of the ligand **3** towards Cu^{2+} ions clearly indicated that two imidazole moieties are necessary for the formation of a cyclic structure as in the case of $[\mathbf{1}.\text{CuCl}_2]_2$. The optimized geometry obtained through universal force field modeling showed a cyclic structure for the complex formed between the ligand **1** and CuCl_2 with an interplanar distance of 9.38 Å between the two anthracene moieties.²⁴

2.5. CONCLUSIONS

In conclusion, we have synthesized a few anthracene imidazole based ligands and investigated their binding ability with various metal ions for the formation of metallocyclophanes. These systems were characterized by the presence of the pendant imidazole moiety, due to which these ligands act as mono/bidentate ligands for various metal ions. Among the various metal ions investigated, the ligand **1** displayed

selectivity for Cu²⁺ and Hg²⁺ ions. Our investigation revealed that the ligand **1** with two imidazole pendant moieties forms stable cyclic water soluble metalloctyphane [**1**.CuCl₂]₂ having rigid and well defined cavity. The metalloctyphane formation was characterized by absorption, emission, ¹H NMR, theoretical studies and MALDI TOF MS spectral analysis. The binding of the anthracene imidazole derivatives with Cu²⁺ and Hg²⁺ ions could be visualized through “turn off” fluorescence intensity. The metalloctyphane [**1**.CuCl₂]₂, thus formed showed high solubility in the aqueous medium and exhibited a rigid and well defined cavity. This unique arrangement of the metal ions as bridging motifs between the two ligand molecules creates a highly rigid cavity in the case of the metalloctyphane [**1**.CuCl₂]₂ making it an ideal candidate as a probe for biomolecular recognition in the aqueous medium.

2.6. EXPERIMENTAL SECTION

2.6.1. General Techniques

The equipment and procedures for melting point determination and spectral recordings have been described elsewhere.^{25,26} All melting points were determined on a Mel-Temp 11 melting point apparatus. ¹H and ¹³C NMR spectra were measured on a 300 MHz or 500 MHz Bruker

advanced DPX spectrometer. HRMS were recorded on a JEOL mass spectrometer. MALDI-TOF MS analysis was performed with a Shimadzu Biotech Axima CFRplus instrument equipped with a nitrogen laser in the linear mode using 2, 5-dihydroxybenzoic acid (DHB) as the matrix. The electronic absorption spectra were recorded on a Shimadzu UV-VIS-NIR spectrophotometer. Fluorescence spectra were recorded on a SPEX-Fluorolog Fl₁₂X spectrofluorimeter. The fluorescence quantum yields were determined by using optically matched solutions. Quinine sulphate (*A* = 0.54) in 0.1 N H₂SO₄ was used as the standard.²⁷ The quantum yields of fluorescence were calculated using the equation 2.1,

$$F_u = \frac{A_s F_u n_s^2}{A_u F_s n_u^2} F_s \quad \text{eq. 2.1}$$

wherein, *A_s* and *A_u* are the absorbance of standard and unknown, respectively. *F_u* and *F_s* are the areas of fluorescence peaks of the unknown and standard and *n_s* and *n_u* are the refractive indices of the standard and unknown solvents, respectively. The metal ion binding studies were carried out by the addition of equal aliquots of metal ion stock solution in water to 3 mL of the ligand in 20% DMSO-water medium.

2.6.2. Materials

Anthracene, paraformaldehyde, sodium, diethylmalonate, p-xylene, imidazole, sodium hydride, hydrobromic acid in glacial acetic acid and CuCl_2 were purchased from S. D. Fine and used without further purification. All the solvents used were purified and distilled before use. $\text{Hg}(\text{ClO}_4)_2$, $\text{Pb}(\text{ClO}_4)_2$, $\text{Zn}(\text{ClO}_4)_2$, $\text{Ca}(\text{ClO}_4)_2$, NaClO_4 , KClO_4 , LiClO_4 , $\text{Mg}(\text{ClO}_4)_2$ were purchased from Aldrich and used as such. Petroleum ether used was the fraction with boiling range 60-80 °C.

2.6.3. Synthesis of 9,10-bis((1H-imidazol-1-yl)methyl)anthracene (1)

To a solution of imidazole (500 mg, 7.4 mmol) in dry THF (100 mL) was added NaH (330 mg, 13.8 mmol) at 0 °C. After the reaction mixture was stirred for 30 min at 0 °C, 9,10-bis(bromomethyl)anthracene (500 mg, 1.4 mmol) was added. The reaction mixture was then additionally stirred for 2 h at room temperature; it was poured into 100 mL of water and extracted with dichloromethane. The organic layer was then separated, dried over anhydrous sodium sulphate and evaporation of the solvent under vacuum yielded a residue which was purified by column chromatography over silica gel. Elution of the column with ethyl acetate yielded 370 mg (78%) of the ligand **1**, which was then

recrystallized from a mixture (4:1) of acetonitrile and ethyl acetate; mp 246–247 °C; ^1H NMR (300 MHz, $\text{DMSO-}d_6$, TMS) δ 6.29 (s, 4H), 6.78 (s, 2H), 6.94 (s, 2H), 7.68 – 7.70 (m, 6H), 8.61 – 8.64 (m, 4H); ^{13}C NMR (75 MHz, $\text{DMSO-}d_6$, TMS) δ 109.9, 113.6, 119.1, 124.7, 124.9, 128.3, 129.1, 130.1; HRMS (FAB): m/z Calcd for $\text{C}_{22}\text{H}_{19}\text{N}_4$: 339.4132; Found 338.5208 (M-H) $^+$.

2.6.4. Synthesis of metallocyclophane [**1**.CuCl₂]₂

To a solution of 9,10-bis(imidazolylmethyl) anthracene (**1**, 250 mg, 0.74 mmol) in a mixture of acetonitrile (50 mL) and methanol (5 mL) was added CuCl₂ (100 mg, 0.74 mmol). The reaction of the anthracene-imidazole conjugate **1** with one equivalent of CuCl₂ in methanol-acetonitrile mixture at room temperature readily gave the metallocyclophane in moderate yields. It was further purified through recrystallization from acetonitrile to yield 124 mg (17%) of the metallocyclophane [**1**.CuCl₂]₂; MALDI-TOF MS: m/z Calcd for [$\text{C}_{44}\text{H}_{36}\text{Cl}_4\text{N}_8$]: 945.7; Found 944.67 (M - H) $^+$. The presence of the Cu²⁺ ions was confirmed by atomic absorption spectroscopy (AAS) and also by observation of broadening of the peaks in the ^1H and ^{13}C NMR spectra due to paramagnetic Cu²⁺ ions.

2.6.5. Synthesis of [1.Hg(ClO₄)₂]

To a solution of 9,10-bis(imidazolylmethyl)anthracene (**1**, 250 mg, 0.74 mmol) in a mixture of acetonitrile (50 mL) and methanol (5 mL) was added Hg(ClO₄)₂ (120 mg, 0.74 mmol). As described above, the reaction of the anthracene-imidazole conjugate **1** with one equivalent of Hg(ClO₄)₂ in methanol-acetonitrile mixture at room temperature readily gave the [1.Hg(ClO₄)₂] in moderate yields (15%). It was further purified by re-crystallization from acetonitrile to yield 112 mg of the metallocyclophane [1.Hg(ClO₄)₂]; MALDI-TOF MS: *m/z* Calcd for [C₂₂H₁₈Cl₂HgN₄O₈]: 738.02; Found 737.4 (M – H)⁺. The presence of Hg²⁺ ions was confirmed by AAS.

2.6.6. Synthesis of 1-(anthracen-9-ylmethyl)-1H-imidazole (3)

To a solution of imidazole (250 mg, 3.4 mmol) in dry THF (100 mL) was added NaH (165 mg, 7 mmol) at 0 °C. After the reaction mixture was stirred for 30 min at 0 °C, 9-(bromomethyl)anthracene (500 mg, 1.4 mmol) was added. The reaction mixture was then additionally stirred for 2 h at room temperature; it was poured into 100 mL of water and extracted with dichloromethane. The organic layer was then separated, dried over anhydrous sodium sulphate and evaporation of the solvent under vacuum yielded a residue which was purified by column chromatography over silica gel. Elution of the column with ethyl acetate

yielded 150 mg (63%) of the ligand **3**, which was then recrystallized from a mixture of acetonitrile and ethyl acetate (4:1). mp 218–219 °C; ¹H NMR (300 MHz, DMSO-*d*₆, TMS) δ 5.91 (2H, s), 6.8 (1H, d, J = 3 Hz), 7.16 (1H, s), 7.38 (2H, t, J = 3.5 Hz), 7.39 (2H, t, J = 3 Hz), 7.71 (1H, s), 7.84 (2H, d, J = 3.5 Hz), 8.15 (1H, s); ¹³C NMR (75 MHz, DMSO-*d*₆, TMS) δ 137.8, 128.1, 119.2, 119.2, 130.5, 131.9, 132.2, 124.7, 128.2, 126, 125.3, 49; HRMS (FAB) *m/z* Calcd for C₁₈H₁₄N₂: 259.1332, Found: 258.4495 [M - H]⁺.

2.6.7. Synthesis of 1,1'-(anthracene-9,10-diylbis(methylene))bis(3-methyl-1H-imidazol-3-ium) bromide (**2**)

To a solution of 9,10-bis((1H-imidazol-1-yl)methyl)anthracene (**1**, 0.25 g, 0.74 mmol) in a mixture of acetonitrile (100 mL) and DMF (50 mL) was added ethyl iodide (0.81 g, 0.74 mmol). The reaction mixture was then refluxed for 24 h, cooled to room temperature and the precipitate formed was filtered and washed with 30 mL of dry acetonitrile. It was further purified by recrystallization from acetonitrile to yield 180 mg (40%) of **2**; mp 276-277 °C; ¹H NMR (500 MHz, DMSO-*d*₆, TMS) δ 1.37 (t, 6H, J = 7 Hz), 4.04 (q, 4H, J = 7.5), 6.39 (s, 4H), 7.32 (d, 4H, J = 7 Hz), 7.38 (s, 2H), 7.75 (q, 4H, J = 3.3 Hz), 8.24 (s, 2H), 8.39 (q, 4H, J = 3.5 Hz); ¹³C NMR (125 MHz, DMSO-*d*₆, TMS) δ 14.0, 44.7, 45.3,

122.1, 123.9, 125.9, 127.7, 130.7, 134.6; HRMS (FAB) m/z Calcd for $C_{35}H_{30}Br_2N_4$: 622.5758, Found 621.5753 [M - H]⁺.

2.6.8. Determination of stoichiometry of the complexation

In the Jobs plot method the total molar concentration of the two binding partners (e.g. ligand and metal ion) was held constant, but their mole fractions were varied. The fluorescence intensity (or peak area) that was proportional to complex formation was plotted against the mole fractions of these two components. The fluorescence maximum observed on the plot corresponds to the stoichiometry of the two species if sufficiently high concentrations were used.

2.6.9. Determination of association constants

The binding affinities were calculated using Benesi–Hildebrand equation 2.2,

$$\frac{1}{(I_f - I_{ob})} = \frac{1}{(I_f - I_{fd})} + \frac{1}{K (I_f - I_{fd}) [\text{Metal ion}]} \quad \text{eq. 2.2}$$

wherein, K is the equilibrium constant, I_f is the fluorescence of the ligand, I_{ob} is the observed fluorescence in the presence of various ligands and I_{fc} is the fluorescence at saturation. The linear dependence of $1/(I_f - I_{ob})$ on the reciprocal of the ligand concentration indicates the formation of a 1:1 molecular complex between metal ion and the host.

2.7. REFERENCES

1. (a) *Molecular Recognition - Chemical and Biochemical Problems*, S. M. Roberts (Ed.), Royal Society of Chemistry, Cambridge, **1989**. (b) E. Katchalski-Katzir, In *Design and Synthesis of Organic Molecules Based on Molecular Recognition*, G. Van Binst (Ed.), Springer, New York, **1986**.
2. (a) R. Martinez-Manez, F. Sancenon, *Chem. Rev.* **2003**, *103*, 4419-4476. (b) A. P. de Silva, H. Q. N. Gunaratne, T. Gunnlaugsson, A. J. M. Huxley, C. P. McCoy, J. T. Rademacher, T. E. Rice, *Chem. Rev.* **1997**, *97*, 1515-1566. (c) C. V. Kumar, A. Buranaprapuk, *Angew. Chem. Int. Ed. Engl.* **1997**, *36*, 2085-2087. (d) M. W. Hosseini, A. J. Blacker, J.-M. Lehn, *J. Am. Chem. Soc.* **1990**, *112*, 3896-3904. (e) L. Vial, P. Dumy, *J. Am. Chem. Soc.* **2007**, *129*, 4884-4885. (f) C. Marquez, U. Pischel, W. M. Nau, *Org. Lett.* **2003**, *5*, 3911-3914.
3. (a) B. Alberts, A. Johnson, J. Lewis, M. Raff, K. Roberts, P. Walter, *Molecular Biology of the Cell*, Garland Science, New York, **2002**. (b) G. Li, V. B. G. Segu, M. E. Rabaglia, R. -H. Luo, A. Kowluru, S. A. Metz, *Endocrinology* **1998**, *139*, 3752-3762. (c) C. S. Pinto, R. Seifert, *J. Neurochem.* **2006**, *96*, 454-459.

4. (a) W. N. Lipscomb, N. Strater, *Chem. Rev.* **1996**, *96*, 2375-2433. (b) G. V. Oshovsky, D. N. Reinhoudt, W. Verboom, *Angew. Chem. Int. Ed.* **2007**, *46*, 2366-2393.
5. (a) B. J. Shorthil, C. T. Avetta and T. E. Glass, *J. Am. Chem. Soc.* **2004**, *126*, 12732-12733. (b) E. V. Anslyn, C. L. Hannon, *Bioorganic chemistry frontiers*; Springer, Berlin, **1993**. (c) C. Schmuck, H. Y. Kuchelmeister, *Artificial receptors for chemical sensors*; Wiley-VCH: Weinheim, **2011**.
6. (a) S. M. Biroš, J. Rebek, Jr. *Chem. Soc. Rev.* **2007**, *36*, 93-120. (b) C. Li, M. Numata, M. Takeuchi, S. Shinkai, *Angew. Chem., Int. Ed.* **2005**, *44*, 6371-6375.
7. (a) F. Diederich, *Cyclophanes; Monographs in Supramolecular Chemistry*, The Royal Society of Chemistry, Cambridge, **1991**. (b) E. Weber, *Encyclopedia of Supramolecular Chemistry*, J. L. Atwood, J. Steed, Marcel Dekker, New York, **2003**.
8. (a) N. K. Dalley, X. Kou, R. A. Bartsch, P. J. Kus, *Inclusion Phenom.* **2003**, *45*, 139-145. (b) C. G. Alcantar, A. V. Eliseev, V. Yatsimirsky, *J. Mol. Recogn.* **1996**, *9*, 54-58. (c) N. C. Gianneschi, M. S. Masar III, C. A. Mirkin, *Acc. Chem Res.* **2005**, *38*, 825-845. (d) L. O. Abouderbala, W. J. Belcher, M. G. Boutelle, P. J. Cragg, J. W. Steed, D. R. Turner, K. J. Wallace, *Proc. Natl. Acad. Sci. USA.* **2002**, *99*, 5001-5010.

9. (a) D. A. Dougherty, D. A. Stauffer, *Science*, **1990**, *250*, 1558. (b) C. A. Hunter, *Proc. Natl. Acad. Sci. USA*. **2002**, *99*, 4873-4878. (c) L. Fabbrizzi, A. Poggi, *Chem. Soc. Rev.*, **2013**, *42*, 1681-1699.
10. (a) P. D. Beer, E. J. Hayes, *Coord. Chem. Rev.* **2003**, *240*, 167-192. (b) J. Heo, C. A. Mirkin, *Angew. Chem., Int. Ed.* **2006**, *45*, 941-945.
11. (a) C. G. Oliveri, P. A. Ulmann, M. J. Wiester, C. A. Mirkin, *Acc. Chem. Res.* **2008**, *41*, 1618-1656. (b) S. J. Dalgarno, N. P. Power, J. L. Atwood, *Coord. Chem. Rev.* **2008**, *252*, 825-855. (c) F. Würthner, C. - C. You, C. R. Saha-Möller, *Chem. Soc. Rev.* **2004**, *33*, 133-156. (d) C. M. Niemeyer, *Angew. Chem., Int. Ed.* **2001**, *40*, 4128-4132. (e) S. Leininger, B. Olenyuk, P. J. Stang, *Chem. Rev.* **2000**, *100*, 853-892.
12. (a) K. Kasai, M. Fujita, *Chem. Eur. J.* **2007**, *13*, 3089-3094. (b) S. M. Biroš, R. M. Yeh, K. N. Raymond, *Angew. Chem., Int. Ed.* **2008**, *47*, 6062-6067. (c) K. Hiratani, M. Albrecht, *Chem. Soc. Rev.* **2008**, *37*, 2413-2433.
13. (a) A. Ajayaghosh, P. Chithra, R. Varghese, *Angew. Chem., Int. Ed.* **2006**, *46*, 230-236. (b) C. D. Meyer, C. S. Joiner, J. F. Stoddart, *Chem. Soc. Rev.* **2007**, *36*, 1705-1732. (c) K. Jyothish, M. Hariharan, D. Ramaiah, *Chem. Eur. J.* **2007**, *13*, 5944-5949.
14. B. Linton, A. D. Hamilton, *Chem. Rev.* **1997**, *97*, 1669-1712.

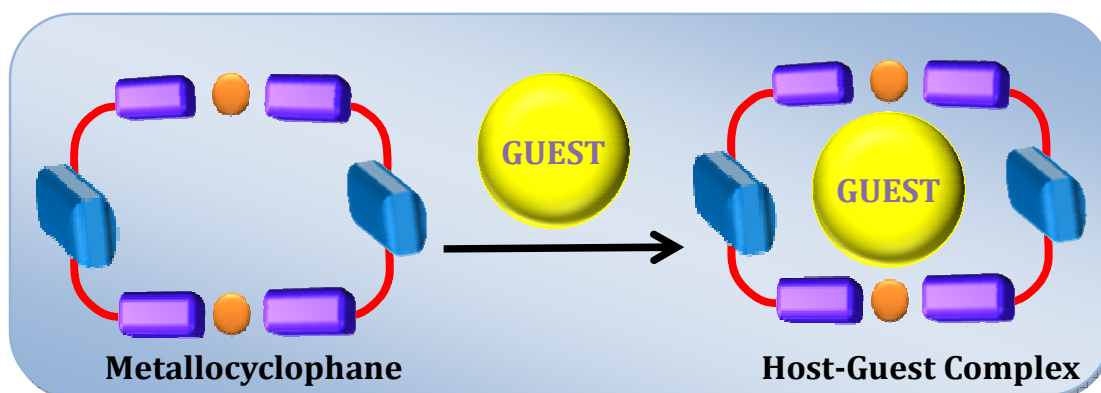
15. P. P. Neelakandan, D. Ramaiah, *Angew. Chem., Int. Ed.* **2008**, *47*, 8407-8411.
16. (a) S. Wang, Y. -T. Chang, *J. Am. Chem. Soc.* **2006**, *128*, 10380-10381.
(b) K. Y. Kwon, N. J. Singh, H. N. Kim, S. K. Kim, K. S. Kim, J. Yoon, *J. Am. Chem. Soc.* **2004**, *126*, 8892-8893. (c) S. K. Kim, B. -S. Moon, J. H. Park, Y. I. Seo, H. S. Koh, Y. J. Yoon, K. D. Lee, J. Yoon, *Tetrahedron Lett.* **2005**, *46*, 6617-6620.
17. P. Job, *Annales de Chimie*, **1928**, *9*, 113-203.
18. (a) V. S. Jisha, K. T. Arun, M. Hariharan, D. Ramaiah, *J. Am. Chem. Soc.* **2006**, *128*, 6024-6025. (b) H. Benesi, J. Hildebrand, *J. Am. Chem. Soc.* **1949**, *71*, 2703-2707.
19. (a) A. Ojida, I. Takashima, T. Kohira, H. Nonaka, I. Hamachi, *J. Am. Chem. Soc.* **2008**, *130*, 12095-12101. (b) F. Zapata, A. Caballero, A. Espinosa, A. Tárraga, P. Molina, *J. Org. Chem.* **2008**, *73*, 4034-4044.
(b) C. Li, M. Numata, M. Takeuchi, S. Shinkai, *Angew. Chem. Int. Ed.* **2005**, *44*, 6371-6374. (c) S. C. McCleskey, M. J. Griffin, S. E. Schneider, J. T. Mcdevitt, E. V. Anslyn, *J. Am. Chem. Soc.* **2003**, *125*, 1114-1115. (d) L. M. Tumir, I. Piantanida, P. Novak, M. Zinic, *J. Phys. Org. Chem.* **2002**, *15*, 599-607.
20. Gaussian 03 (Revision-D.01), M. J. Frisch, G. W. Trucks, H. B. Schlegel, G. E. Scuseria, M. A. Robb, J. R. Cheeseman, J. A.

- Montgomery, Jr., T. Vreven, K. N. Kudin, J. C. Burant, J. M. Millam, S. S. Iyengar, J. Tomasi, V. Barone, B. Mennucci, M. Cossi, G. Scalmani, N. Rega, G. A. Petersson, H. Nakatsuji, M. Hada, M. Ehara, K. Toyota, R. Fukuda, J. Hasegawa, M. Ishida, T. Nakajima, Y. Honda, O. Kitao, H. Nakai, M. Klene, X. Li, J. E. Knox, H. P. Hratchian, J. B. Cross, C. Adamo, J. Jaramillo, R. Gomperts, R. E. Stratmann, O. Yazyev, A. J. Austin, R. Cammi, C. Pomelli, J. W. Ochterski, P. Y. Ayala, K. Morokuma, G. A. Voth, P. Salvador, J. J. Dannenberg, V. G. Zakrzewski, S. Dapprich, A. D. Daniels, M. C. Strain, O. Farkas, D. K. Malick, A. D. Rabuck, K. Raghavachari, J. B. Foresman, J. V. Ortiz, Q. Cui, A. G. Baboul, S. Clifford, J. Cioslowski, B. B. Stefanov, G. Liu, A. Liashenko, P. Piskorz, I. Komaromi, R. L. Martin, D. J. Fox, T. Keith, M. A. Al-Laham, C. Y. Peng, A. Nanayakkara, M. Challacombe, P. M. W. Gill, B. Johnson, W. Chen, M. W. Wong, C. Gonzalez, and J. A. Pople, Gaussian, Inc., Pittsburgh, PA, **2003**.
21. S. Ramadan, T. W. Hambley, B. J. Kennedy, P. A. Lay, *Inorg. Chem.* **2004**, *43*, 2943-2947 (b) L. Dobrzanska, G. O. Lloyd, C. Esterhuysen, L. J. Barbour, *Angew. Chem., Int. Ed.* **2006**, *45*, 5856-5859.
22. D. Abella, V. Blanco, E. Piñ a, M. Chas, C. Platas-Iglesias, C. Peinador, J. M. Quintela, *Chem. Commun.*, **2008**, 2879-2882.

23. I. J. B. Lin, H. M. J. Wang, H. M. *Organometallics* **1998**, *17*, 972-975.
24. (a) J. Rebek, Jr. *Angew. Chem. Int. Ed. Engl.* **1990**, *29*, 245-255. (b) I. Piantanida, V. Tomisic, M. Zinic, *J. Chem. Soc., Perkin Trans. 2*, **2000**, 375-383. (c) J. L. Sessler, V. Kral, T. V. Shishkanova, P. A. Gale, *Proc. Natl. Acad. Sci. USA* **2002**, *99*, 4848-4853.
25. M. Inouye, K. Kim, T. Kitao, *J. Am. Chem. Soc.* **1992**, *114*, 778-780.
26. (a) S. M. Biro, J. Rebek, Jr. *Chem. Soc. Rev.* **2007**, *36*, 93-104. (b) H. Hayashida, N. Ogawa, M. Uchiyama, *J. Am. Chem. Soc.* **2007**, *129*, 13698-13705. (c) V. Dvornikovs, B. E. House, M. Kaetzel, J. R. Dedman, D. B. Smithrud, *J. Am. Chem. Soc.* **2003**, *125*, 8290-8301. (d) J. Yan, Y. Zhou, P. Yu, L. Su, L. Mao, D. Zhang, D. Zhu, *Chem. Commun.* **2008**, 4330-4332.
27. (a) A. H. Flood, Y. Liu, J. F. Stoddart, In *Modern Cyclophane Chemistry*, R. Gleiter, H. Hopf (Eds.) Wiley-VCH, Weinheim, **2004**. (b) F. Diederich, In *Cyclophanes, Monographs in Supramolecular Chemistry*, J. F. Stoddart (Ed.), The Royal Society of Chemistry, London, **1991**.
28. (a) E. A. Meyer, R. K. Castellano, F. Diederich, *Angew. Chem. Int. Ed.* **2003**, *42*, 1210-1250. (b) C. G. Claessens, J. F. Stoddart, *J. Phys. Org. Chem.* **1997**, *10*, 254-272.

CHAPTER 3

STUDY OF INTERACTIONS OF METALLOCYCLOPHANES WITH NUCLOSIDES AND NUCLEOTIDES



3.1. ABSTRACT

With an objective of developing selective probes for nucleosides and nucleotides, we have monitored the interactions of the metal complexes $[1.CuCl_2]_2$, $[1.Hg(ClO_4)_2]$ and $[(3)_2.CuCl_2]$ with nucleosides and nucleotides. The addition of guanosine-5'-monophosphate (5'-GMP) to an aqueous solution of the complex $[1.CuCl_2]_2$, resulted in significant changes in absorption and emission properties. In contrast, negligible changes were observed with the addition of other nucleosides and nucleotides such as 5'-GDP, 5'-GTP, 5'-ATP, 5'-ADP, 5'-AMP, adenosine, guanosine and phosphate ions, indicating thereby that the complex $[1.CuCl_2]_2$ undergoes selective interactions with 5'-GMP. The

complexation between $[\mathbf{1}.\text{CuCl}_2]_2$ and 5'-GMP was evidenced through fluorescence titration experiments. We obtained an association constant of $K_{ass} = 1.2 \pm 0.1 \times 10^4 \text{ M}^{-1}$ through the Benesi–Hildebrand analysis with a change in free energy (ΔG) of -9.4 kJ mol^{-1} . Furthermore, this supramolecular complex was isolated and characterized through MALDI–TOF MS analysis, which showed a peak at 1352.44, corresponding to a calculated mass of 1:1 stoichiometric supramolecular assembly between $[\mathbf{1}.\text{CuCl}_2]_2$ and 5'-GMP.

The selective complexation of $[\mathbf{1}.\text{CuCl}_2]_2$ with 5'-GMP over other nucleotides was confirmed through calorimetric, electrochemical, ^1H and ^{31}P NMR techniques. We observed a significant shift in reduction potential of differential pulse voltammogram of the complex $[\mathbf{1}.\text{CuCl}_2]_2$ by the addition of 5'-GMP, whereas a regular endothermic response was observed by isothermal titration calorimetric (ITC) measurements. With the successive addition of the complex $[\mathbf{1}.\text{CuCl}_2]_2$, the ^1H NMR spectrum of 5'-GMP showed a decrease in the intensity along with a significant broadening of the peak corresponding to H_8 proton of 5'-GMP, whereas the ^{31}P NMR spectrum exhibited a gradual broadening of the peak at δ 3.7 ppm, corresponding to the phosphate group of 5'-GMP. In contrast, other complexes $[\mathbf{1}.\text{Hg}(\text{ClO}_4)_2]$ and $[(\mathbf{3})_2.\text{CuCl}_2]$ showed negligible interactions with 5'-GMP and also with other nucleosides and

nucleotides, thereby indicating the importance of the cavity size in the biomolecular recognition event. The unusual selectivity of the metallocyclophane [**1**.CuCl₂]₂ for 5'-GMP over other nucleotides could be attributed to the synergy of interactions. These include, the electrostatic and coordinative interactions between Cu²⁺ ions of [**1**.CuCl₂]₂ and the phosphate group and N₇ of 5'-GMP as well as π -stacking interactions between the anthracene moieties of [**1**.CuCl₂]₂ and the aromatic unit of 5'-GMP.

3.2. INTRODUCTION

The development of receptors for biologically important anions has received considerable attention in recent years.¹⁻³ Of the various biologically important anions, special attention has been focused on the selective recognition of nucleosides and nucleotides due to their biological implications.^{4,5} For example, guanosine-5'-triphosphate (5'-GTP) is required for many biological activities in the cell such as, synthesis of DNA, RNA, and proteins; nutrient metabolism; and cell signaling,⁶ whereas adenosine-5'-triphosphate (5'-ATP) is well known for its capability to function as the biological currency, chemical energy storage and transfer in the bioenergetics of all living organisms.⁷ Similarly, the recognition of guanosine-5'-monophosphate (5'-GMP) is

vital because 5'-GMP acts as an intermediate in the synthesis of nucleic acids and plays an important role in several metabolic processes. 5'-GMP also displays important extra cellular roles such as trophic effects to neurons and astrocytes, behaves as an antagonist of glutamate receptors and is neuroprotective in hippocampal slices against excitotoxicity or ischemic conditions.⁸

Of all the nucleosides and nucleotides, the biological importance of G-based nucleotides (5'-GMP, 5'-GDP and 5'-GTP) and their versatile roles in different biological process make them attractive targets for their recognition in the aqueous solution (Chart 3.1). In this regard, developments of host systems based on the transition metal complexes are of particular importance in view of their additional non-covalent interactions while considering the rigid functional cyclophanes. For example, the nature exploited the transition metal complexes in carrying out several biological processes in living organisms by

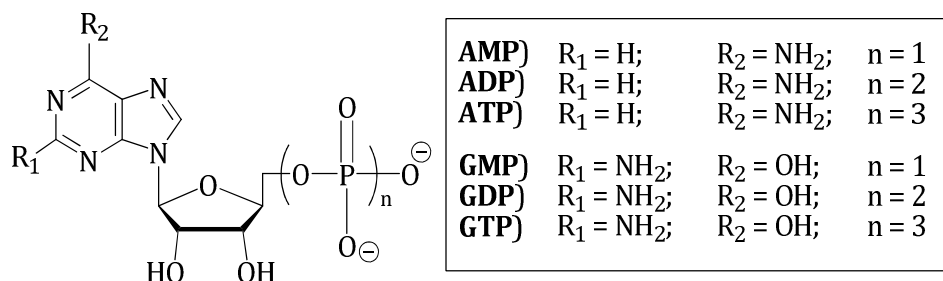


Chart 3.1

associating with various biomolecules in a variety of ways.⁹ The heavy-metal ion interactions with nucleic acids indeed have provided the basis for the successful application of *cis*-platin and its derivatives as anticancer chemotherapeutic agents.¹⁰ In all these endeavours, the nature utilizes the advantage of the coordination chemistry of the transition metal complexes with biomolecules.¹¹

The co-ordination chemistry of the transition metal complexes with most prevalent biomolecule such as nucleosides and nucleotides is quite interesting.¹² As may be evident, each mononucleotide base contains a variety of sites for interactions with the metal ions such as the electrostatic interactions with the anionic phosphate backbone as well as the coordinative interactions between the soft metal ions and nucleophilic positions on the heterocyclic bases. The nucleophilic sites targeted by the soft metal ions with the heterocyclic bases include the N₇ position of adenine, N₃ position on cytosine and the deprotonated N₃ positions of thymine and uracil.¹³ Indeed, it has been reported that the coordination by the metal complexes to one site of the heterocyclic base lowers the *pKa* and increases the metal-binding affinity to the secondary sites.¹⁴ It is noteworthy, however, that in base-paired double-helical DNA, only the N₇ positions on the purines are easily accessible in the major groove of the helix. The nucleic acid base binding at the purine N₇

position is of course, not limited to the soft metal ions such as Pt(II), Pd(II) and Ru(II) but also with first-row transition-metal ions such as Cu(II) and Zn(II) as well.¹⁵ The liability of the complexes formed by the first row transition metal complexes may be an added advantage in the coordination with the heterocyclic bases.¹⁶ Along with this, the transition-metal ions with decreasing softness are capable of coordinating also to the phosphate oxygen atoms. Although the pentose ring in general provides a poor ligand for the metal ions, Osmate esters can form complexes quite easily across the C2'-C3' positions of the ribose rings.¹⁷

In this context, it was of our interest to investigate the potential of the novel metallocyclophanes [**1**.CuCl₂]₂ and [**1**.Hg(ClO₄)₂] and the model compound [(**3**)₂.CuCl₂] reported in Chapter 2 as receptors for nucleosides and nucleotides (Chart 3.2). These systems were associated with a high degree of structural rigidity and well defined cavity and hence these systems can encapsulate and stabilize guest molecules through various non-covalent interactions.¹⁸ We have selected Cu (II) and Hg (II) metallocyclophanes and investigated their interactions with various nucleosides and nucleotides through photophysical, electrochemical, ¹H and ³¹P NMR and calorimetric techniques.

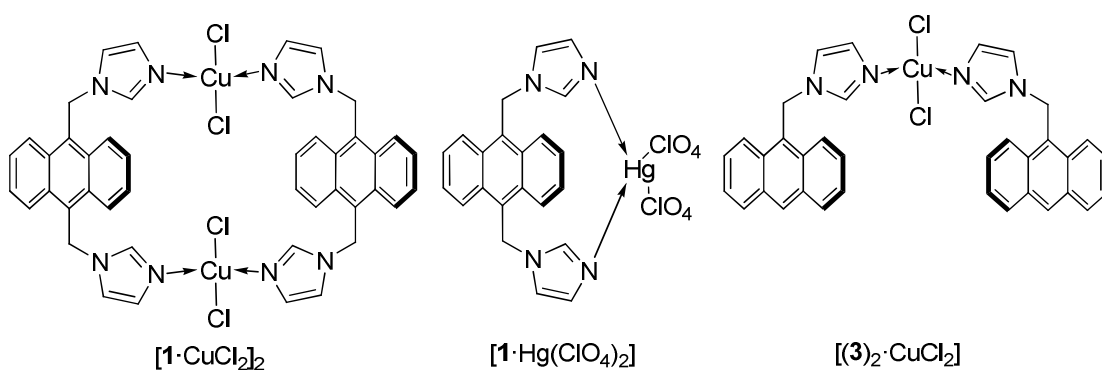


Chart 3.2

Our results indicate that the cavity size, nature of the metal ion and aromatic surface of the metallocyclophane play major roles in their biomolecular recognition process. Of these two systems, the metallocyclophane $[1 \cdot \text{CuCl}_2]_2$ found to undergo selective interactions with 5'-GMP when compared to other nucleosides and nucleotides and signalled the event through changes in fluorescence intensity.

3.3. RESULTS

3.3.1. Interaction of Metallocyclophanes with Nucleosides and Nucleotides

The synthesis of the metallocyclophanes $[1 \cdot \text{CuCl}_2]_2$ and $[1 \cdot \text{Hg}(\text{ClO}_4)_2]$ under investigation as well as the model complex $[(3)_2 \cdot \text{CuCl}_2]$ has been achieved as per the procedures described in Chapter 2 of this thesis. To understand the biomolecular recognition

ability, we have monitored the absorption and fluorescence changes of these metallocyclophanes with the addition of various nucleosides and nucleotides. The gradual addition of 5'-GMP resulted in significant hyperchromicity in the absorption spectrum of the complex $[\mathbf{1}.\text{CuCl}_2]_2$ along with a bathochromic shift of *ca.* 5 nm (Figure 3.1).¹⁹ Under identical conditions, by the addition of 625 μM of 5'-GMP, the emission spectrum showed *ca.* 90% quenching in fluorescence intensity at 425 nm as shown in Figure 3.2A. The Benesi-Hildebrand analysis of the fluorescence changes gave an association constant of $K_{\text{ass}} = 1.2 \pm 0.1 \times 10^4 \text{ M}^{-1}$ for the formation of the supramolecular assembly $[(\mathbf{1}.\text{CuCl}_2)_2] \subset 5'\text{-GMP}$ with a change in free energy of $\Delta G = -9.2 \text{ kJ mol}^{-1}$ (Figure 3.2B).

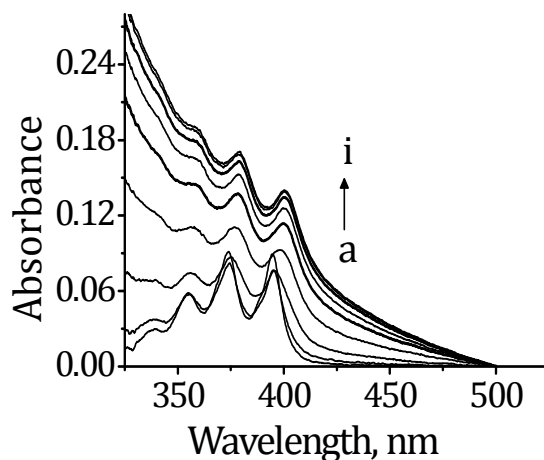


Figure 3.1. Changes in the absorption spectra of the metallocyclophane $[\mathbf{1}.\text{CuCl}_2]_2$ (11 μM) with the successive addition of 5'-GMP in aqueous solution. [5'-GMP], (a) 0 and (i) 625 μM .

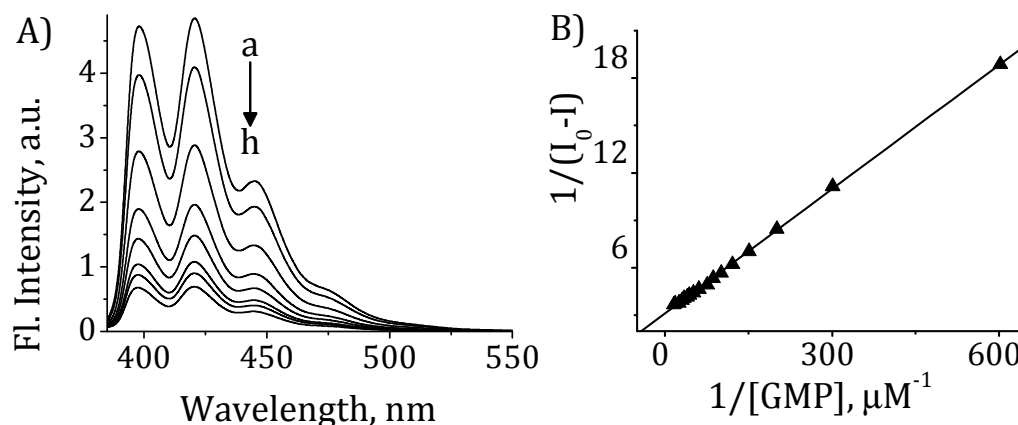


Figure 3.2. Changes in the A) emission spectrum of the metallocyclophane [1.CuCl₂]₂ (11 μM) with the successive addition of 5'-GMP in aqueous medium. [5'-GMP], (a) 0 and (h) 625 μM and B) Benesi-Hildebrand fit for the fluorescence changes of [1.CuCl₂]₂ in presence of 5'-GMP. [5'-GMP], 625 μM. λ_{ex} , 375 nm.

In contrast, negligible changes were observed in the absorption and fluorescence spectra of the metallocyclophane with the addition of other analytes such as adenosine, guanosine, 5'-AMP, 5'-ADP, 5'-GDP, 5'-ATP and 5'-GTP under these conditions (Figure 3.3). Figure 3.4 shows the relative changes in the fluorescence intensity of the metallocyclophane [1.CuCl₂]₂ with the addition of different nucleosides and nucleotides. It is evident from this figure that the metallocyclophane [1.CuCl₂]₂ shows unusually high selectivity towards 5'-GMP as compared to other analytes. The complex [1.CuCl₂]₂⋅5'-GMP was isolated and characterized through MALDI-TOF MS analysis, which showed a peak at

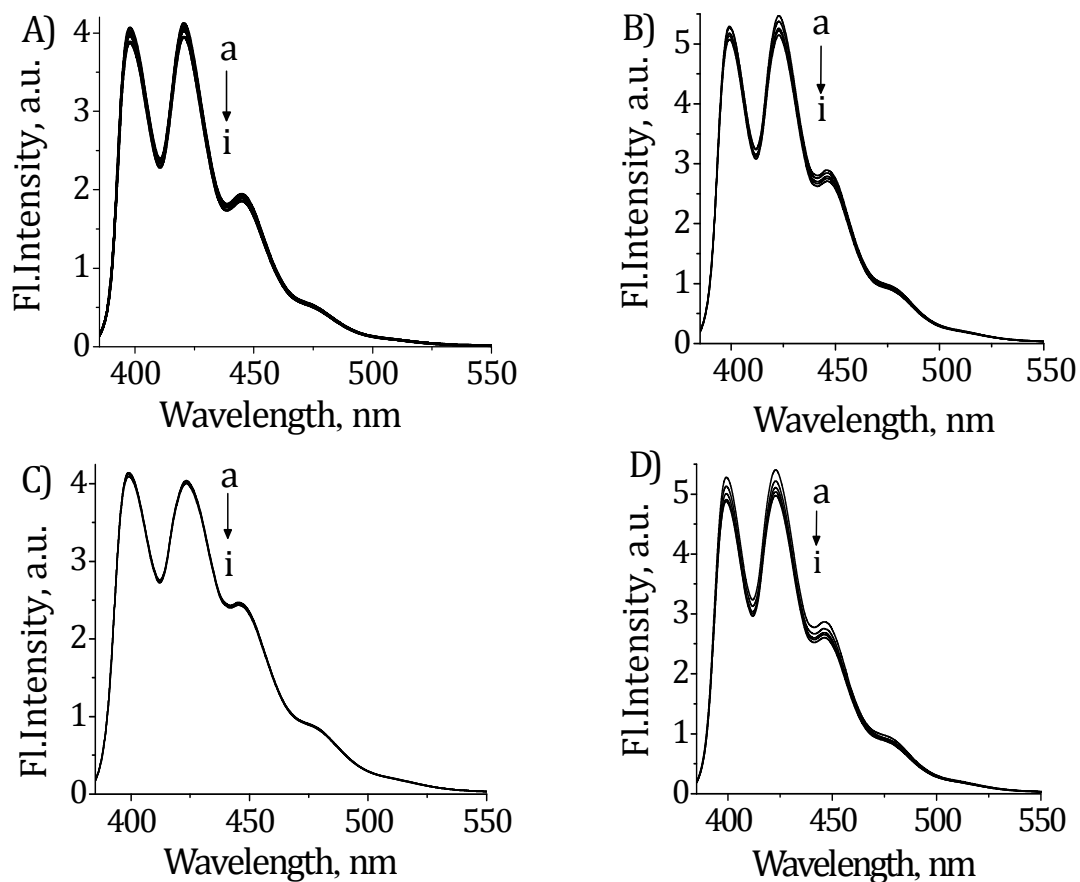


Figure 3.3. Changes in the emission spectra of the metallocyclophane $[1.CuCl_2]_2$ (11 μM) with the successive addition of A) 5'-GDP, B) 5'-GTP, C) 5'-ATP and D) 5'-AMP in the aqueous medium. [Nucleotide], (a) 0 and (i) 625 μM . λ_{ex} , 375 nm.

1352.44, corresponding to a 1:1 stoichiometric assembly between the metallocyclophane $[1.CuCl_2]_2$ and 5'-GMP. In contrast, the absorption and emission spectra of the complex $[1.Hg(ClO_4)_2]$ as well as the model compound $[(3)_2.CuCl_2]$, under identical conditions, showed negligible changes by the addition of 5'-GMP (Figure 3.5).

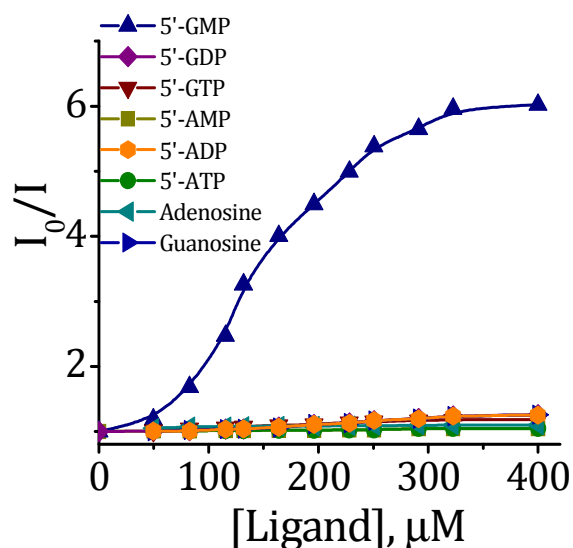


Figure 3.4. Relative changes in the fluorescence intensity of $[1.CuCl_2]_2$ with the addition of 5'-GMP, 5'-GDP, 5'-GTP, 5'-AMP, 5'-ADP, 5'-ATP, adenosine, guanosine.

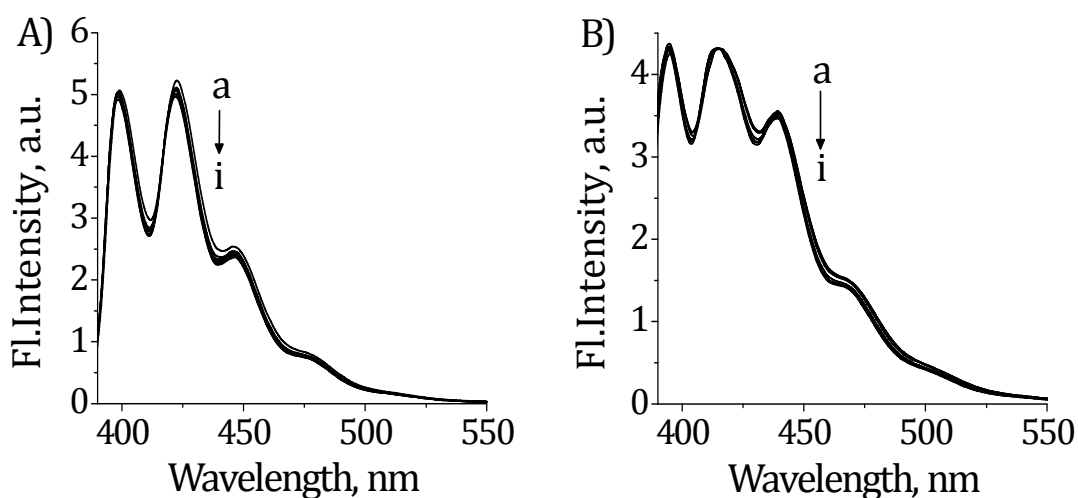


Figure 3.5. Changes in the emission spectra of the metallocyclophanes A) $[1.Hg(ClO_4)_2]$ ($11 \mu M$) and the model complex B) $[(3)_2.CuCl_2]$ ($11 \mu M$) with the successive addition of 5'-GMP in aqueous medium. [5'-GMP], (a) 0 and (i) $625 \mu M$. λ_{ex} , 375 nm.

3.3.2. Characterization of Complexation between $[1.CuCl_2]_2$ and 5'-GMP

To understand the nature of complexation between $[1.CuCl_2]_2$ and 5'-GMP, we have used 1H and ^{31}P NMR, isothermal titration calorimetry and cyclic voltammetric techniques.²⁰ We have followed the 1H NMR spectra of 5'-GMP in DMSO-*d*₆ by the addition of successive amount of the metallocyclophane $[1.CuCl_2]$ (Figure 3.6). The 1H NMR spectrum of

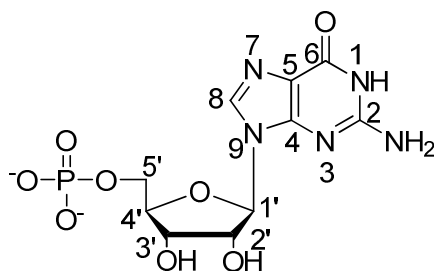


Chart 3.3.

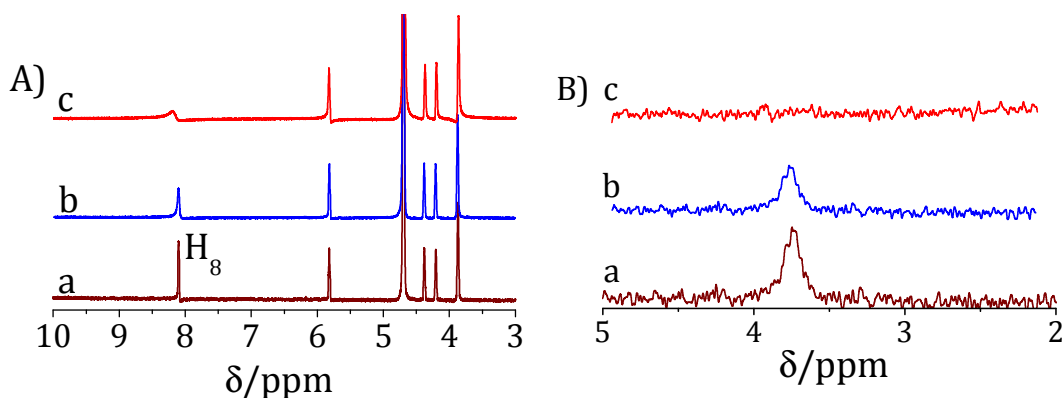


Figure 3.6. Changes in the A) 1H and B) ^{31}P NMR spectra of 5'-GMP (10 mM) with the addition of $[1.CuCl_2]_2$ in DMSO. $[1.CuCl_2]_2$, a) 0, b) 7.4 and c) 15.8 μM .

5'-GMP (10 mM in DMSO-*d*6) exhibited peaks at δ 8.1, 5.8, 4.3, 4.2 and 3.8, corresponding to the protons H₈, H_{1'}, H_{3'}, H_{4'} and H_{5'}, respectively (Chart 3.3). With the successive addition of 15.8 μ M of the complex [1.CuCl₂]₂, we observed a decrease in the intensity along with a significant broadening of H₈ proton alone, whereas other protons remained unaffected. In the ³¹P NMR spectrum of 5'-GMP (Figure 3.7), we observed significant decrease in

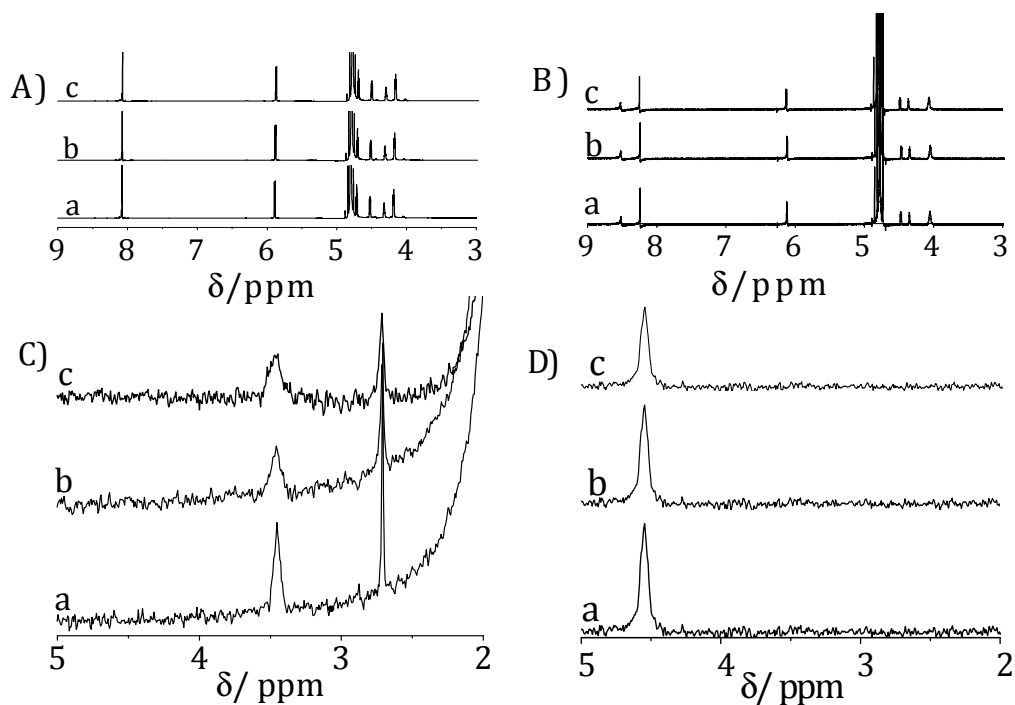


Figure 3.7. Changes in the ¹H NMR spectra of A) 5'-GDP and B) 5'-AMP (10 mM) and ³¹P NMR spectra of C) 5'-GDP and D) 5'-AMP with the addition of [1.CuCl₂]₂ in DMSO. [1.CuCl₂]₂, a) 0, b) 7.4 and c) 15.8 μ M.

intensity and broadening of the peak at δ 3.7 corresponding to the phosphate group, with the gradual addition of the metallocyclophane. At *ca.* 15.8 μ M, we observed the complete disappearance of the phosphate group of 5'-GMP. In contrast, nucleotides such as 5'-AMP, 5'-GDP and 5'-ATP showed negligible changes in both ^1H and ^{31}P and NMR spectra under similar conditions.

Recent technological and methodological advances in the field of calorimetry made it possible to measure the small amount of heat associated with the non-covalent interactions between the components in a binding process.²¹ Measurement of this heat allows for the accurate determination of binding constants (K_b), reaction stoichiometry (n), and a thermodynamic profile of the interaction that includes the observed molar calorimetric enthalpy (ΔH_{obs}), entropy (ΔS_{obs}) and change in free energy.²² We have followed the complexation between [**1**.CuCl₂]₂ with the nucleotides by monitoring the heat change produced during the interaction (Figure 3.8). With the gradual addition of 5'-GMP to a solution of [**1**.CuCl₂]₂ (0.05 mM) at 25 °C, we observed a regular endothermic response in the isothermal titration calorimetric (ITC) measurements. After the addition of 0.07 mM of 5'-GMP, we observed the saturation in the heat changes and on the basis of the ITC data, the

enthalpy change was calculated and is found to be $\Delta H = 1.42 \pm 0.14$ kcal mol⁻¹ with an association constant of $K_a = 3.63 \pm 1.89 \times 10^4$ M⁻¹.

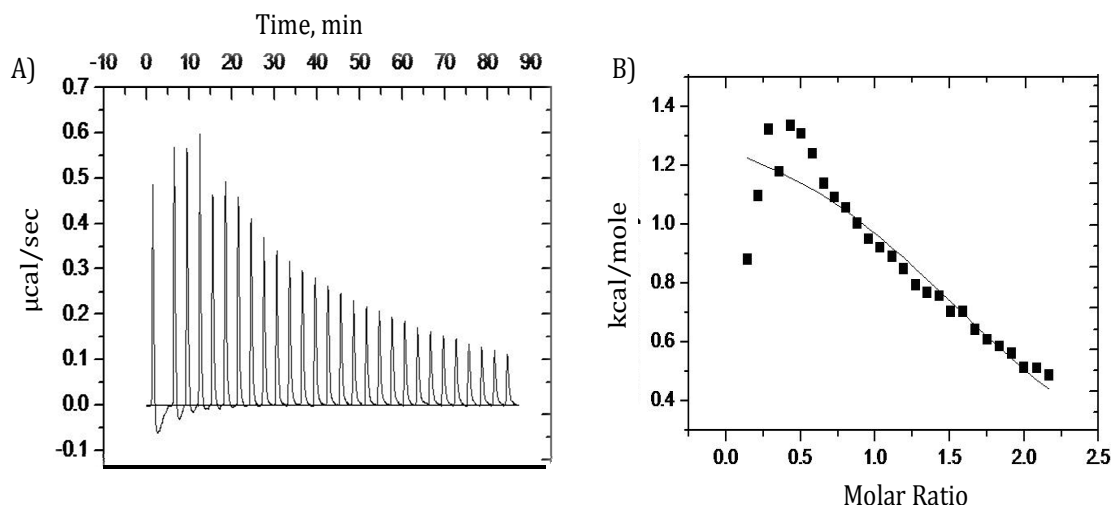


Figure 3.8. Isothermal titration calorimetry data for the addition of 5'-GMP to a solution of metallocyclophane [$1.\text{CuCl}_2$]₂ (0.05 mM) in water at 298 K. [5'-GMP], 0 – 0.07 mM. A) The raw data for the 5 μL sequential addition of 5'-GMP to the metallocyclophane solution and B) the plot of the heat evolved (kcal) per mole of 5'-GMP.

The results obtained from ITC are in agreement with those obtained through fluorescence changes for the complex between the metallocyclophane and 5'-GMP. In contrast, the addition of other nucleotides such as 5'-AMP, 5'-GDP and 5'-GTP under similar conditions showed negligible heat changes in ITC measurements, confirming thereby that only 5'-GMP undergoes selective complexation with the metallocyclophane. For example, Figure 3.9 shows the negligible heat

changes produced by the titrations of 5'-AMP and 5'-GDP with the aqueous solutions of $[\mathbf{1.CuCl}_2]_2$ at 298 K.

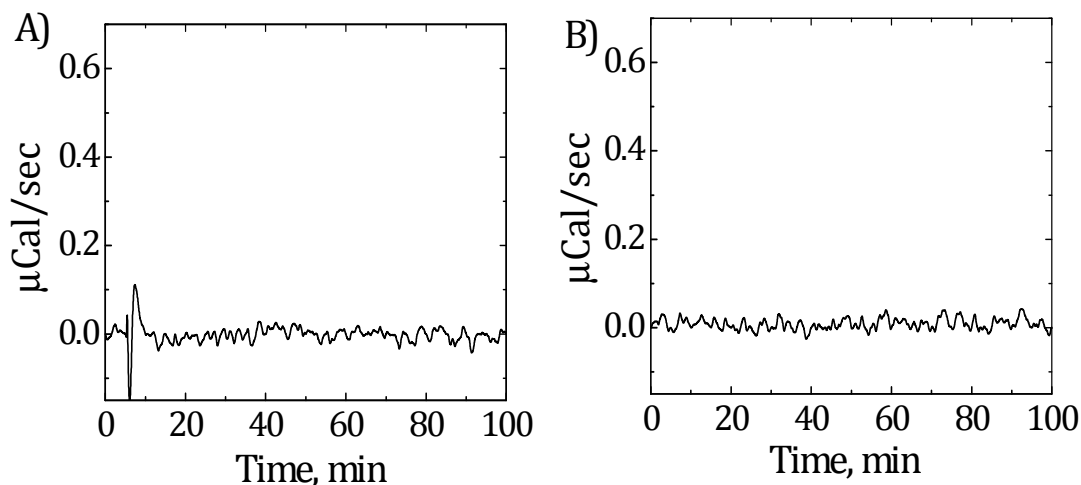


Figure 3.9. Isothermal titration calorimetry raw data for the addition of A) 5'-AMP and B) 5'-GDP to a solution of metallocyclophane $[\mathbf{1.CuCl}_2]_2$ (0.05 mM) in water at 298 K. [5'-AMP/5'-GDP], 0 – 0.07 mM.

We have employed cyclic voltametry, in particular, differential pulse voltammogram (DPV)²³ technique to evaluate the selective interactions of the metallocyclophane $[\mathbf{1.CuCl}_2]_2$ with 5'-GMP. DPV carried out in homogeneous solution showed that the complex $[\mathbf{1.CuCl}_2]_2$ undergoes strong interactions with 5'-GMP, showing the different binding mechanism towards 5'-GMP. As evidenced from the Figure 3.10, the DPV of the metallocyclophane exhibited two peaks at -0.33 and -1.55 V in the aqueous solution. By the addition of 20 mM of 5'-GMP, we observed a significant shift in the reduction potentials by -110

and 40 mV, respectively. On the other hand, the addition of other nucleosides and nucleotides such as guanosine, 5'-AMP, 5'-GDP and 5'-

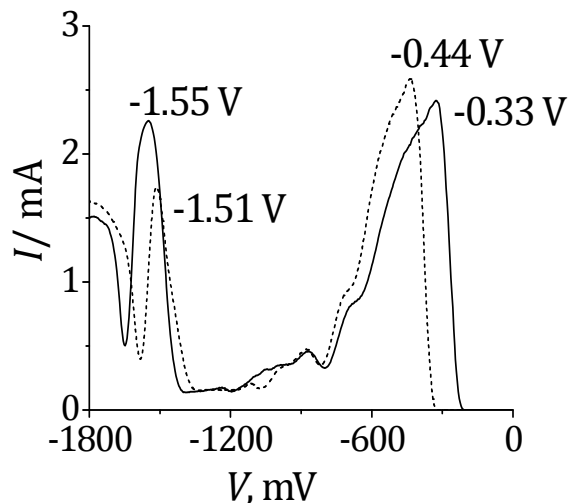


Figure 3.10. Differential pulse voltammogram of the metallocyclophane [1.CuCl₂]₂ (0.98 mM) in the absence (—) and presence (- - -) of 5'-GMP (20 μM) in the aqueous medium.

GTP under similar conditions, showed negligible changes in DPV measurements, confirming thereby that only 5'-GMP undergoes selective complexation with the metallocyclophane.

3.3.3. Selectivity of 5'-GMP Recognition

To understand the effect of cavity size in the biomolecular recognition, we have studied the effect of the metallocyclophane in the supramolecular complexation by monitoring the emission changes of the ligand **1** alone in presence of increasing concentration of various

nucleosides and nucleotides in the absence of Cu(II) ions. Figure 3.11 shows the changes in the fluorescence intensity of the ligand **1** by the sequential addition of 5'-GMP followed by the Cu²⁺ metal ions. The gradual addition of 625 μ M of 5'-GMP to a solution of the ligand **1** led to a negligible quenching (<5%) in its fluorescence intensity. However, when we added Cu²⁺ ions to this solution containing the ligand **1** and 5'-GMP, a significant quenching of the fluorescence intensity (>90%) was observed. These observations confirm the independence of the sequence of addition of the additives and indicate that the metallocyclophane formation is a pre-requisite for the selective recognition of 5'-GMP (Figure 3.11).

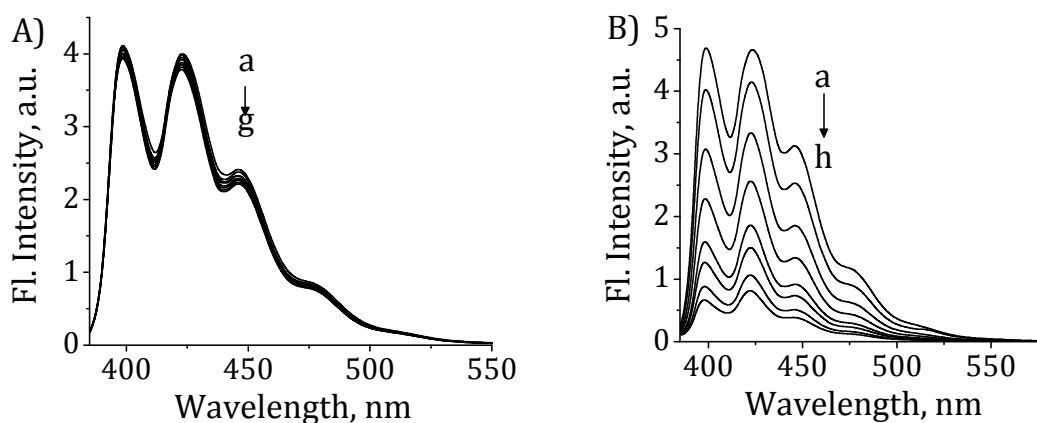


Figure 3.11. Changes in the emission spectrum of ligand **1** (20 μ M) with the sequential addition of A) 5'-GMP (625 μ M) followed by B) Cu²⁺ ions (156 μ M). λ_{ex} , 375 nm.

To understand the reversibility of the complexation in biomolecular recognition, we have studied the interactions between the supramolecular complex and a strong chelating ligand such as EDTA. When EDTA was added to the supramolecular assembly, we observed quantitative revival of fluorescence intensity of the ligand **1**, indicating thereby the dissociation of the supramolecular assembly $[\mathbf{1}.\text{CuCl}_2]_2 \subset 5'$ -GMP under these conditions (Figure 3.12). Similarly, we have studied the effect of temperature on the stability of the supramolecular complex. When we increased the temperature of the supramolecular complex from 25-85 °C, we observed the revival of the fluorescence intensity of the ligand **1** due to the decomplexation of metallocyclophane.

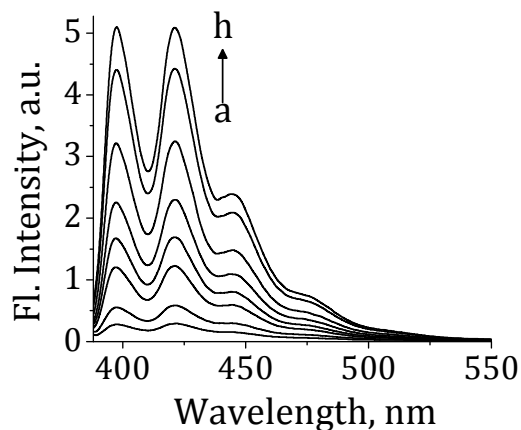


Figure 3.12. Changes in the emission spectra of the complex $[\mathbf{1}.\text{CuCl}_2]_2 \subset 5'$ -GMP (24 μM) upon the addition of EDTA in the aqueous medium. [EDTA], a) 0 and h) 650 μM .

3.4. DISCUSSION

The optimized geometry of $[\mathbf{1.CuCl_2}]_2$ obtained through theoretical calculations utilizing a universal force field showed a 2:2 stoichiometric cyclic structures for the metallocyclophane with an interplanar distance of 9.38 Å between the two anthracene chromophores. This unique arrangement of the metal ions as bridging motifs between the two ligand molecules interestingly creates a highly rigid cavity in the metallocyclophane making it as an ideal choice as a probe for biomolecular recognition in the aqueous medium.²³

The significant changes observed in the photophysical properties of the complex $[\mathbf{1.CuCl_2}]_2$ only in the presence of 5'-GMP indicate that this complex shows unusually high selectivity towards 5'-GMP, when compared to other nucleotides and nucleosides. The high association constant of the supramolecular assembly obtained from the fluorescence changes indicate the high stability for the complex formed between the complex $[\mathbf{1.CuCl_2}]_2$ and 5'-GMP. The observed peak of 1352.44 in the MALDI TOF MS spectra can be attributed to a 1:1 stoichiometric supramolecular assembly between the metallocyclophane $[\mathbf{1.CuCl_2}]_2$ and 5'-GMP. The observed negligible interactions of the metallocyclophane $[\mathbf{1.Hg(ClO_4)}]_2$ towards 5'-GMP clearly establishes the fact that the cavity size plays an importance in the

selective complexation. The limited cavity size and aromatic surface of the metallocyclophane [**1**.Hg(ClO₄)₂] make this complex not useful as a probe in the host-guest complexation process.

Furthermore, the effect of cavity size in host-guest interactions²⁴ again demonstrated by the negligible interactions observed with the complexes formed by ligand **3** with Cu(II) ions. Since the ligand **3** consists of only one imidazole moiety, it was not able to form a rigid cavity after the metal complexation, which makes it inefficient for the host-guest interaction. The high selectivity and stability of the supramolecular assembly formed between the metallocyclophane [**1**.CuCl₂]₂ and 5'-GMP was evidenced through the observation of the endothermic responses and high association constants from fluorescence, ITC and DPV measurements as well as through broadening of peaks in the ¹H and ³¹P NMR spectra.²⁵

The importance of metallocyclophane formation in the selective recognition of 5'-GMP was confirmed by monitoring the interaction of the ligand **1** with 5'-GMP in the presence and absence of Cu²⁺ ions. The negligible quenching observed in the fluorescence intensity of the ligand **1** upon addition of 5'-GMP clearly indicating the less significant interactions between ligand **1** and 5'-GMP. However, when we added Cu²⁺ ions to this solution containing the ligand **1** and 5'-GMP, a

significant quenching of fluorescence intensity was observed. The net fluorescence quenching was comparable to that observed when 5'-GMP was added to the complex $[\mathbf{1.CuCl_2}]_2$ and which demonstrates the independence of the sequence of addition of the additives. Moreover, these results confirm that the metallocyclophane $[\mathbf{1.CuCl_2}]_2$ formation is the first step, which then encapsulates 5'-GMP to form a supramolecular assembly $[\mathbf{1.CuCl_2}]_2 \subset \text{GMP}$. The observed dissociation of the supramolecular assembly at higher temperatures of around 85 °C and also in the presence of a strong chelator such as EDTA demonstrate the reversibility of the supramolecular complex $[\mathbf{1.CuCl_2}]_2 \subset \text{GMP}$ formation.

Figure 3.13 shows the schematic representation for the supramolecular complexation between the metallocyclophane $[\mathbf{1.CuCl_2}]_2$ and 5'-GMP through various non-covalent interactions. The complexation between 5'-GMP and the metallocyclophane is expected to be initiated by the electrostatic interactions, which position the nucleobase subsequently to undergo effective coordinative and π -stacking interactions inside the cavity leading to the formation of a supramolecular assembly $[\mathbf{1.CuCl_2}]_2 \subset 5'\text{-GMP}$.¹⁹ The formation of such a supramolecular assembly results in changes in the fluorescence intensity due to the thermodynamically feasible electron transfer process from the nucleobase to the excited state of the anthracene

chromophore as confirmed through laser flash photolysis studies.²⁶ The evidence for the involvement of the electrostatic interactions was

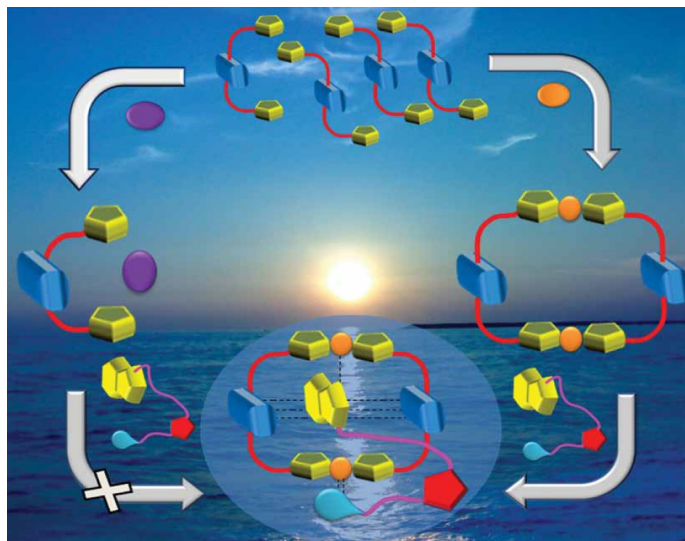


Figure 3.13. Schematic representation for the formation of supramolecular complex $[1.CuCl_2]_2 \subset 5'-GMP$ from the metallocyclophane and 5'-GMP.

obtained from the ^{31}P NMR studies, wherein we observed the disappearance of the phosphate group of 5'-GMP upon complexation as compared to other nucleotides. The coordinative interactions between Cu(II) of the metallocyclophane and N_7 of 5'-GMP were established on the basis of observance of the selective broadening of H_8 proton of 5'-GMP in the 1H NMR spectral analysis. This is in agreement with the literature reports that N_7 of 5'-GMP has a strong binding affinity towards Cu(II) ions and such interactions are the decisive factor in the selectivity observed.^{27,28} The observation of the sigmoidal nature of the relative

fluorescence changes further supports the involvement of these multiple interactions in the selective recognition of 5'-GMP by the metallocyclophane.²⁹

Figure 3.14 shows the visual changes in fluorescence intensity for the formation and reversibility of the metallocyclophane as well as the supramolecular complexation. The ligand **1**, which showed quite intense fluorescence intensity (Figure 3.14A), experienced quenching of its fluorescence intensity (*ca.* 50%) by the addition of Cu²⁺ ions and due to the in situ formation of the metallocyclophane [**1**·CuCl₂]₂ (Figure 3.14B). With the addition of 5'-GMP, the fluorescence of the complex [**1**·CuCl₂]₂ exhibited further quenching in intensity of *ca.* 90% (Figure 3.14C) as a result of formation of the supramolecular assembly [**1**·CuCl₂]₂⊂5'-GMP. The revival in fluorescence intensity of the ligand **1** could be observed

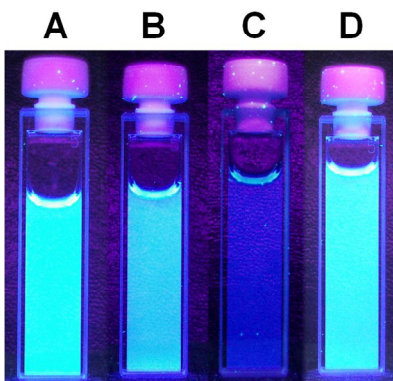


Figure 3.14. Visual observation of fluorescence intensity of A) **1** alone (20 μ M), B) the complex [**1**·CuCl₂]₂, C) [**1**·CuCl₂]₂ in presence of 5'-GMP (625 μ M) and D) in presence of EDTA (625 μ M), respectively.

by the addition of EDTA (Figure 3.14D) which could be attributed to the reversibility of the supramolecular assembly $[\mathbf{1}\cdot\text{CuCl}_2]_2\subset 5'\text{-GMP}$ and destruction of cyclic structure of the metallocyclophane $[\mathbf{1}\cdot\text{CuCl}_2]_2$. Thus, the recognition of 5'-GMP could be achieved selectively through the metallocyclophane $[\mathbf{1}\cdot\text{CuCl}_2]_2$ through changes in fluorescence changes, when compared to other structurally similar nucleotides.

3.5. CONCLUSIONS

In conclusion, we have investigated the interactions of the metal complexes $[\mathbf{1}\cdot\text{CuCl}_2]_2$, $[\mathbf{1}\cdot\text{Hg}(\text{ClO}_4)_2]$ and $[(\mathbf{3})_2\cdot\text{CuCl}_2]$ described in Chapter 2 with nucleosides and nucleotides. The significant changes in the absorption and fluorescence properties of the complex $[\mathbf{1}\cdot\text{CuCl}_2]_2$ by the addition of 5'-GMP when compared to other nucleosides and nucleotides indicated the high selectivity of the complex $[\mathbf{1}\cdot\text{CuCl}_2]_2$ towards 5'-GMP. Furthermore, the selectivity of $[\mathbf{1}\cdot\text{CuCl}_2]_2$ with 5'-GMP over other nucleosides and nucleotides was confirmed through calorimetric, electrochemical, ^1H and ^{31}P NMR techniques. The uniqueness of the metallocyclophane is that it selectively recognizes 5'-GMP over other nucleosides and nucleotides and signals the event through changes in the fluorescence intensity. The unusual selectivity for 5'-GMP over other nucleotides could be attributed to the synergy of

various non-covalent interactions such as electrostatic interactions, coordinative interactions and the π -stacking interactions between the anthracene moieties and the aromatic unit of 5'-GMP and the metal ion present in the cyclophane. These results are important in understanding the role of cavity size, metal ion and aromatic surface in the biomolecular recognition and in the design of efficient receptors based on metallocyclophanes for nucleosides and nucleotides.

3.6. EXPERIMENTAL SECTION

3.6.1. General Techniques

The equipment and procedures for melting point determination and spectral recordings have been described elsewhere. ^1H and ^{13}C NMR spectra were measured on a 500 MHz Bruker advanced DPX spectrometer. ^{31}P NMR spectra were measured on a 500 MHz Bruker advanced DPX spectrometer using *ortho*-phosphoric acid as external standard. MALDI-TOF MS analysis was performed with a Shimadzu Biotech Axima CFR plus instrument equipped with a nitrogen laser in the linear mode using 2, 5-dihydroxybenzoic acid (DHB) as the matrix. Electrochemical measurements were carried out in a Bio analytical Systems Inc., BAS-CV50W cyclic voltammeter. Isothermal titration calorimetry was carried out using a Micorcal ITC 200 instrument. Doubly distilled water was used in all the studies. Ligand binding studies

were carried out by the addition of equal aliquots of nucleosides and nucleotides solution in water to 3 mL of ligand in 20% DMSO-water medium. All experiments were carried out at room temperature (25 ± 1 °C), unless otherwise mentioned.

3.6.2. Materials

Guanosine 5'-monophosphate (GMP), adenosine 5'-monophosphate (AMP), adenosine 5'-triphosphate (ATP), adenosine 5'-diphosphate (ADP), guanosine 5'-diphosphate (GDP), guanosine 5'-triphosphate (GTP), guanosine and adenosine were purchased from Sigma Aldrich and used as received without any further purification. The synthesis of the ligands and the complexes used in the present study was achieved as described in Chapter 2 of the present thesis. All the solvents used were purified and distilled before use. Petroleum ether used was the fraction with boiling range 60-80 °C. The ligands **1-3** and the metal complexes $[\mathbf{1}.\text{CuCl}_2]_2$, $[\mathbf{1}.\text{Hg}(\text{ClO}_4)_2]$ and $[(\mathbf{3})_2.\text{CuCl}_2]$ were synthesized as described in Chapter 2 of this thesis.

3.6.3. Determination of Association Constants

Nucleotidse, nucleosides (Sigma Aldrich) and metallocyclophane $[\mathbf{1}.\text{CuCl}_2]_2$ solutions were prepared in distilled water. The binding affinities were calculated using Benesi-Hildebrand equation 3.1,

$$\frac{1}{(I_f - I_{ob})} = \frac{1}{(I_f - I_{fc})} + \frac{1}{K (I_f - I_{fc}) [\text{Ligand}]} \quad \text{eq. 3.1}$$

wherein, K is the equilibrium constant, I_f is the fluorescence of ligand 1, I_{ob} is the observed fluorescence in the presence of various ligands and I_{fc} is the fluorescence at saturation. The linear dependence of $1/(I_f - I_{ob})$ on the reciprocal of the ligand concentration indicates the formation of a 1:1 molecular complex between ligand and the host.

3.7. REFERENCES

1. (a) D. M. Bailey, A. Hennig, V. D. Uzunova, W. M. Nau, *Chem. Eur. J.* **2008**, *14*, 6069-6073. (b) N. Shao, J. Y. Jin, S. M. Cheung, R. H. Yang, W. H. Chan, T. Mo, *Angew. Chem., Int. Ed.* **2006**, *45*, 4944-4948. (c) M. A. Hortala, L. Fabbrizzi, N. Marcotte, F. Stomeo, A. Taglietti, *J. Am. Chem. Soc.* **2003**, *125*, 20-23. (d) H. Ait-Haddou, S. L. Wiskur, V. M. Lynch, E. V. Anslyn, *J. Am. Chem. Soc.* **2001**, *123*, 11296-11299.
2. (a) D. Choquesillo-Lazarte, M. P. Brandi-Blanco, I. Garcia-Santos, J. M. Gonzalez-Perez, A. Castineiras, J. Niclos-Gutierrez, *Coord. Chem. Rev.* **2008**, *252*, 1241-1283. (b) J. R. Aranzaes, C. Belin, D. Astruc, *Angew. Chem., Int. Ed.* **2006**, *45*, 132-136. (c) S. Aoki, E. Kimura, *Chem. Rev.* **2004**, *104*, 769-848. (d) L. Fabbrizzi, M. Licchelli, F. Mancin, M. Pizzeghello, G. Rabaioli, A. Taglietti, P. Tecilla, U. Tonellato, *Chem. Eur. J.* **2002**, *8*, 94-102.
3. (a) H. Nonaka, S. Tsukiji, A. Ojida, I. Hamachi, *J. Am. Chem. Soc.* **2007**, *129*, 15777-15780 (b) A. Buryak, K. Severin, *Angew. Chem., Int. Ed.* **2004**, *43*, 4771-4374.
4. (a) R. Martinez-Manez, F. Sancenon, *Chem. Rev.* **2003**, *103*, 4419-4476. (b) A. P. de Silva, H. Q. N. Gunaratne, T. Gunnlaugsson, A. J. M. Huxley, C. P. McCoy, J. T. Rademacher, T. E. Rice, *Chem. Rev.* **1997**,

- 97, 1515-1566. (c) C. V. Kumar, A. Buranaprapuk, *Angew. Chem. Int. Ed. Engl.* **1997**, *36*, 2085-2087. (d) M. W. Hosseini, A. J. Blacker, J.-M. Lehn, *J. Am. Chem. Soc.* **1990**, *112*, 3896-3904. (e) L. Vial, P. Dumy, *J. Am. Chem. Soc.* **2007**, *129*, 4884-4885. (f) C. Marquez, U. Pischel, W. M. Nau, *Org. Lett.* **2003**, *5*, 3911-3914.
5. (a) G. Li, V. B. G. Segu, M. E. Rabaglia, R. -H. Luo, A. Kowluru, S. A. Metz, *Endocrinology* **1998**, *139*, 3752-3762. (b) C. S. Pinto, R. Seifert, *J. Neurochem.* **2006**, *96*, 454-459.
6. J. M. Berg, J. L. Tymoczko, L. Stryer, *Biochemistry*, WH Freeman and Company, **2002**. (b) G. Karp, *Cell and Molecular Biology*, Wiley, **2008**. (c) M. S. Vickers, K. S. Martindale, P. D. Beer. *J. Mater. Chem.* **2005**, *15*, 2784-2789. (d) O. Reynes, C. Bucher, J. -C, Moutet, G. Royal, E. S. Aman, *Chem. Commun.* **2004**, 428-432. (e) S. M. Butterfield, M. L. Waters, *J. Am. Chem. Soc.* **2003**, *125*, 9580-9583. (f) M. T. Albelda, J. Aguilar, S. Alves, R. Aucejo, P. Diaz, C. Lodeiro, J. C. Lima, G. E. Espana, F. Pina, C. Soriano, *Helv. Chim. Acta.* **2003**, *86*, 3118-3123.
8. B. Alberts, A. Johnson, J. Lewis, M. Raff, K. Roberts, P. Walter, *Molecular Biology of the Cell*; Garland Science, New York, **2002**.
9. L. Stryer, *Biochemistry*, W. H. Freeman, New York, **1995**.
10. B. Lippert, *Nucleic Acid-Metal Ion Interactions*, RSC, **2009**.

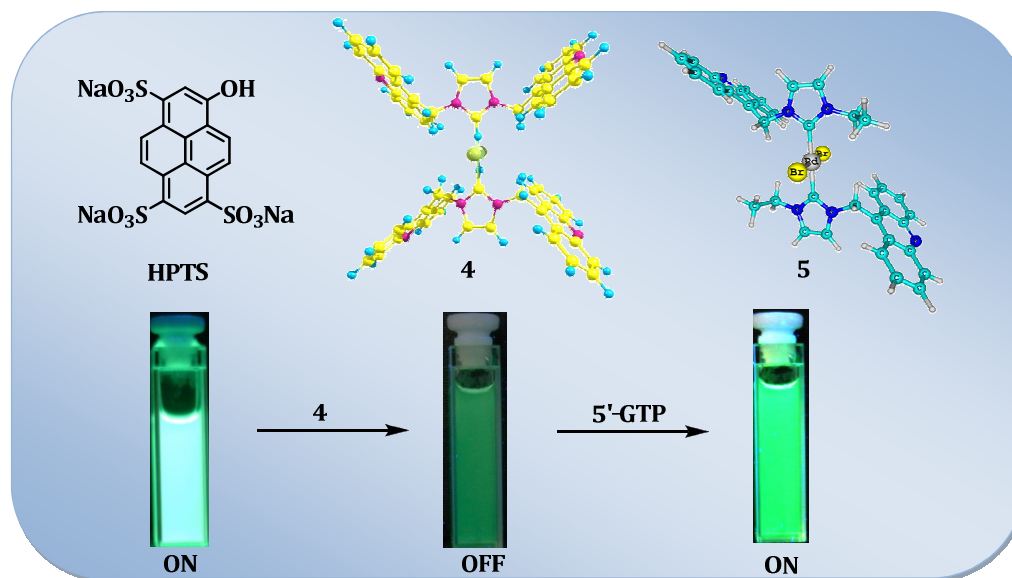
11. (a) J. Miller, A. D. McLachlan, A. Klug, *EMBO J.* **1985**, 4, 1609-1614.
(b) E. A. Berry, M. Guergova-Kuras, L. S. Huang, A. R. Crofts, *Ann. Rev. Biochem.* **2000**, 69, 1005-1075.
12. (a) S. Mansy, G. Y. H. Chu, R. E. Duncan, R. S. Tobias, *J. Am. Chem. Soc.*, **1978**, 100, 607-616. (b) P. De Meester, D. M. L. Goodgame, T. J. Jones, A. C. Skapski, *Biochem. J.* **1974**, 139, 791-792.
13. S. E. Sherman, *Science*, **1985**, 230, 412-419.
14. D. Hodgson, *Prog. Inorg. Chem.* **1977**, 23, 211-218.
15. G. L. Eichhorn, Y. A. Shin, *J. Am. Chem. Soc.* **1968**, 90, 7323-7326.
16. L. G. Marzilli, *Prog. Inorg. Chem.* **1977**, 23, 255-259.
17. (a) C. H. Chang, M. Beer, L. G. Marzilli, *Biochemistry*, **1977**, 16, 33-41.
(b) G. C. Glikin. *Nucleic Acids Res.* **1984**, 12, 1725-1731. (c) I. Bertini, H. B. Gray, S. Lippard, J. Valentine, *Bioinorganic Chemistry*, University Press, **1994**.
18. (a) J. M. Lehn, *Angew Chem Int Ed Engl.* **1990**, 29, 1304-1319. (b) K. Müller-Dethlefs, P. Hobza, *Chem Rev.* **2000**, 100, 143-167.
19. A. K. Nair, P. P. Neelakandan, D. Ramaiah, *Chem. Commun.*, **2009**, 6352-6354.
20. (a) X. Xie, J. H. Reibenspies, T. Hughbanks, *J. Am. Chem. Soc.* **1998**, 120, 11391-11400. (b) J. D. Harris, T. Hughbanks, *J. Am. Chem. Soc.* **1997**, 119, 9449-9459.

21. (a) T. Wiseman, S. Williston, J. F. Brandts, L. Lin, *Anal. Biochem.* **1989**, *179*, 131–137. (b) J. Tellinghuisen, *J. Phys. Chem. B* **2005**, *109*, 20027-20035.
22. J. J. Christensen, R. M. Izatt, L. D. Hansen, *Rev. Sci. Instrum.* **1965**, *36*, 779-793.
23. (a) M. A. Olson, Y. Y. Botros, J. F. Stoddart, *Pure Appl. Chem.*, **2010**, *82*, 1569–1574. (b) H. –J. Schneider, A.K. Yatsimirsky, *Chem. Soc. Rev.*, **2008**, *37*, 263–277. (c) E. A. Meyer, R. K. Castellano, F. Diederich, *Angew. Chem., Int. Ed.*, **2003**, *42*, 1210–1250. (d) B. König, *Top. Curr. Chem.*, **1998**, *196*, 91–136.
24. P. P. Neelakandan, P. C. Nandajan, B. Subymol, D. Ramaiah, *Org. Biomol. Chem.*, **2011**, *9*, 1021–1029.
25. S. Ramadan, T. W. Hambley, B. J. Kennedy, P. A. Lay, *Inorg. Chem.* **2004**, *43*, 2943-2948.
26. (a) M. Hariharan, J. Joseph, D. Ramaiah, *J. Phys. Chem. B* **2006**, *110*, 24678-24686. (b) J. Joseph, N. V. Eldho, D. Ramaiah, *Chem. Eur. J.* **2003**, *9*, 5926-5935.
27. (a) V. Andrushchenko, P. Bouř, *J. Phys. Chem. B* **2009**, *113*, 283-291. (b) M. G. Santangelo, A. Medina–Molner, A. Schweiger, G. Mitrikas, B. J. Spingler, *Biol. Inorg. Chem.* **2007**, *12*, 767-772.

- (c) Y. G. Gao, M. Sriram, A. H. J. Wang, *Nucleic Acids Res.* **1993**, *21*, 4093-4098.
28. M. G. Santangelo, A. Medina-Molner, A. Schweiger, G. Mitrikas, B. Spingler, *J. Biol. Inorg. Chem.* **2007**, *12*, 767-772.
29. (a) B. Linton, A. D. Hamilton, *Chem. Rev.* **1997**, *97*, 1669-1721. (b) H. - J. Schneider, *Angew. Chem., Int. Ed. Engl.*, **1990**, *29*, 1159-1163.

CHAPTER 4

SYNTHESIS AND STUDY OF INTERACTION OF Pd(II)-NHC COMPLEXES WITH NUCLEOSIDES AND NUCLEOTIDES



4.1. ABSTRACT

With the objective of developing fluorescence based probes for biomolecules, we have synthesised Pd-complexes (Pd-NHC) **4** and **5** of the acridine-imidazole conjugates **9** and **10** and have investigated their interactions with nucleosides and nucleotides. The addition of 5'-GMP or 5'-GDP or 5'-GTP or guanosine (G-based) to a solution of the Pd-NHC complex **4** resulted in enhancement in its fluorescence intensity at 500 nm, with an association constant of $K_{ass} = 3.63 \pm 0.12 \times 10^4 \text{ M}^{-1}$, whereas negligible changes were observed with the addition of 5'-AMP, 5'-ADP,

5'-ATP, adenosine and phosphate ions. The Pd-NHC complex **5**, on the other hand, showed negligible selectivity towards these nucleosides and nucleotides. The selectivity of the complex **4** for G-based nucleotides when compared to **5** was confirmed by isothermal titration calorimetry.

To improve the sensitivity of the complex **4**, we developed a fluorescent indicator displacement assay (FID) by making use of the beneficial properties of **4** and a fluorescence indicator, 8-hydroxy-1,3,6-pyrene trisulphonate (HPTS). With increasing in addition of the complex **4**, we observed *ca.* 23% hypochromicity in the absorption spectrum of HPTS along with *ca.* 93% quenching in the fluorescence intensity at 512 nm with an association constant of $4.66 \pm 0.2 \times 10^4 \text{ M}^{-1}$. The successive additions of the G-based nucleotides to a solution of the non-fluorescent complex [4.HPTS] resulted in a regular enhancement in fluorescence intensity corresponding to HPTS at 512 nm, which led to their visual detection through “turn on” fluorescence intensity.

The selectivity of the complex **4** towards the G-based nucleotides has been attributed to the presence of better π -electron cloud to facilitate effective electronic and π -stacking interactions and strong coordinative interactions with N₇ nitrogen of the guanine base and the metal centre. These results demonstrated the importance of the

presence of Lewis acidic center as well as the aromatic surface in the molecular recognition ability of the complex **4** as a probe for the detection of the G-based nucleotides, when compared to the other nucleotides.

4.2. INTRODUCTION

N-Heterocyclic carbenes (NHCs) have been extensively studied and widely accepted as a universal ligands in organometallic chemistry as well as in inorganic coordination chemistry.¹ The NHCs can form stable complexes with various metal ions from the main group to the transition metal ions in different oxidation states with a strong σ bonding and little or no π back bonding.² The metal complexes of the NHCs were first reported in 1968 by Öfele, Wanzlick and Schönherr.³ The transition metal complexes of the NHCs have been actively being investigated because of their wide range of applications such as antibiotics and anticancer drugs (with silver, gold and palladium),^{4,5} building blocks for supramolecular complexes as well as NHC based polymers.⁶ In addition to these, it has been shown that a number of reactions may be catalysed by the transition metal complexes of the NHCs.⁷ A famous example of the successful application of the NHC complex in catalysis is the Grubbs' catalyst. The first generation Grubbs'

catalyst **1** (Chart 4.1).⁸ A ruthenium complex with two phosphane ligands was found to be highly efficient in the metathesis of olefins, whereas the second generation catalyst **2**, in which one of the phosphane ligands was replaced by an NHC ligand, proved to be even more active and stable. In 2005, Robert Grubbs was awarded the Nobel Prize in chemistry for his work on the metathesis reaction. Liu and co-workers have synthesized an alkane-bridged diimidazolium based macrocyclic dinuclear silver (I) NHC complex **3** and exploited its potential as a building block for the formation of the supramolecular complexes.⁹

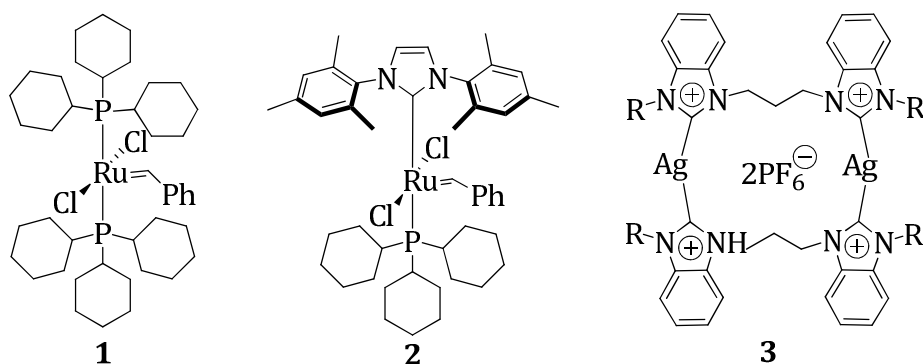


Chart 4.1

The initial achievements in these areas clearly demonstrated that the transition metal complexes bearing the NHC ligands may be promising candidates in the field of host-guest chemistry. The NHC complexes associated with a Lewis acidic metal centre and rich in

aromatic surface can stabilize guest molecules through effective electronic, π -stacking and coordinative interactions.¹⁰ In this context, palladium complexes of the NHCs have attracted much attention because of their easy accessibility and high thermal stability. Particular attention has been devoted to the imidazol(in)-2-ylidene based complexes because they can provide extra stability to the metal centres. Further, it has been reported in literature that the palladium(II)-NHC complexes could be easily prepared from palladium(II) acetate and the corresponding imidazolium salts.¹¹ However, the potential of the transition metal complexes bearing the NHC ligands in the field of host-guest complexation has not been explored till now.

In this context, it was our objective to develop novel Pd-NHC complexes and study of their potential as probes for biomolecular recognition. We have synthesized Pd complexes **4** and **5** of the acridine-imidazole conjugates **9** and **10** (Chart 4.2) and have investigated their interactions with various nucleosides and nucleotides under different conditions through photophysical, calorimetric and ¹H NMR techniques. Of the two systems, the Pd-NHC complex **4** showed selective interactions with G-based nucleotides (5'-GMP, 5'-GDP, 5'-GTP or guanosine) when compared to other analytes and signalled the event through 'turn on' fluorescence mechanism. Our results indicate that the

Lewis acidic metal centre and the aromatic surface of the system play a major role in the biomolecular recognition exhibited by these systems.

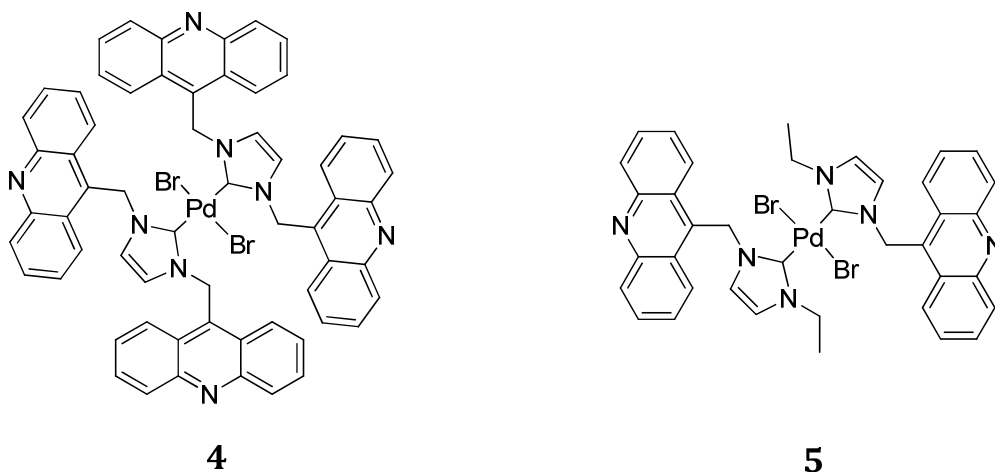
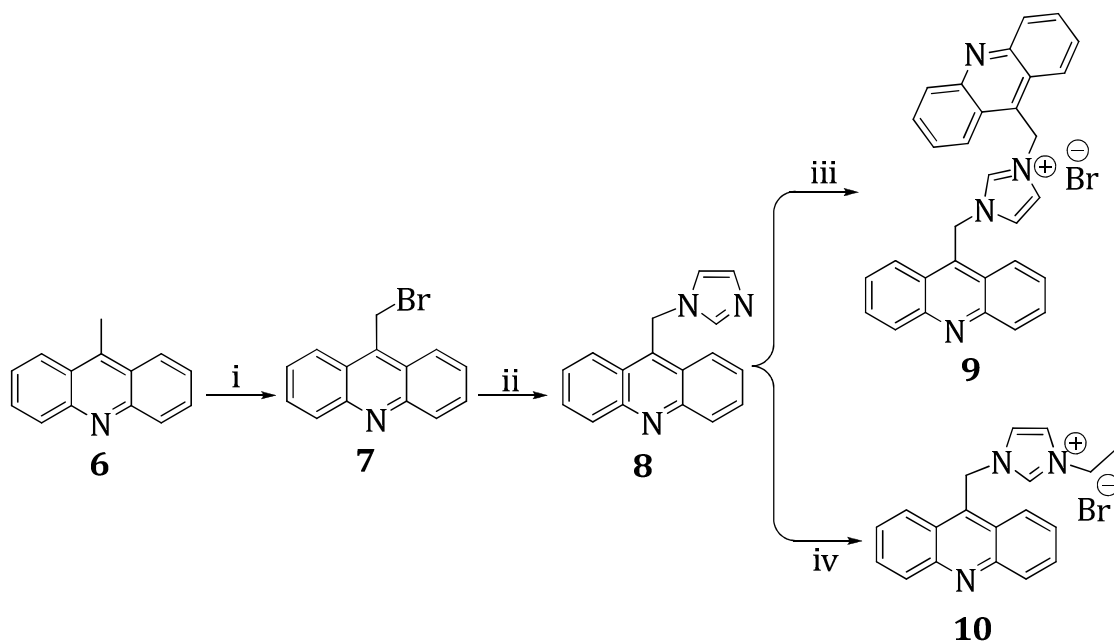


Chart 4.2

4.3. RESULTS

4.3.1. Synthesis and Photophysical Properties of Ligands

The synthesis of the ligands 1,3-bis(acridin-9-ylmethyl)-1H-imidazol-3-ium bromide (**9**) and the 1-(acridin-9-ylmethyl)-3-ethyl-1H-imidazol-3-ium bromide (**10**) was achieved in moderate yields by using the modified procedure (Scheme 4.1).¹² The allylic bromination of 9-methylacridine (**6**) in carbon tetrachloride gave 9-bromomethylacridine (**7**) in *ca.* 75% yield. The reaction of **7** with imidazole in the presence of the aqueous sodium hydroxide and tetra-propyl ammonium hydroxide in benzene yielded *ca.* 68% of 9-Imidazolylmethylacridine (**8**).

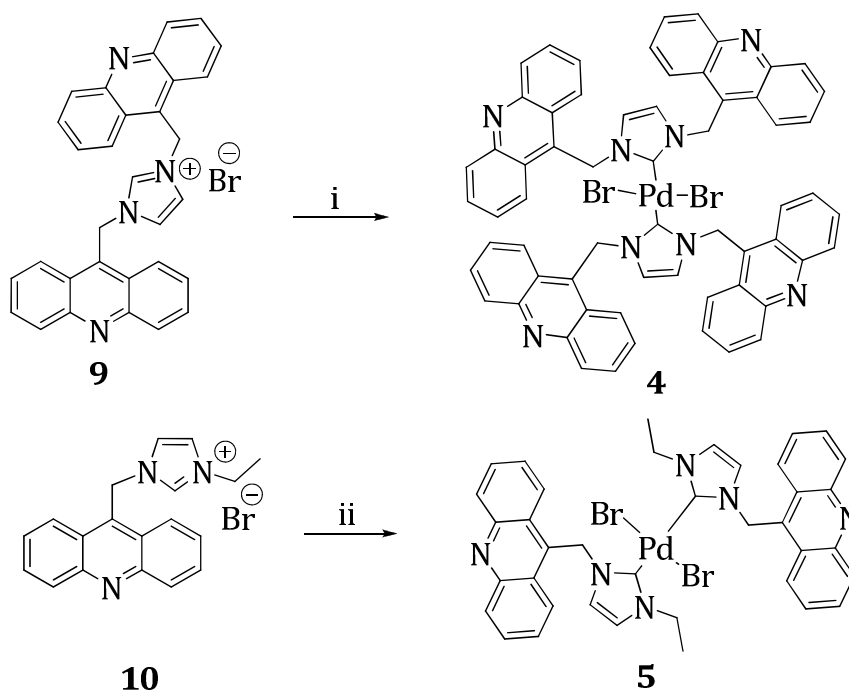


i) NBS, benzoyl peroxide, CCl_4 , $80\text{ }^\circ\text{C}$, 4 h; ii) Imidazole, NaH, THF, $25\text{ }^\circ\text{C}$, 4 h; iii) 9-bromomethylacridine, CH_3CN , $80\text{ }^\circ\text{C}$, 48 h; iv) $\text{C}_2\text{H}_5\text{I}$, CH_3CN , $80\text{ }^\circ\text{C}$, 24 h.

Scheme 4.1

The reaction of **8** with **7** in CH_3CN for 48 h gave **9** in moderate yield. The synthesis of the ligand **10**, on the other hand, was achieved by quaternization of **8** with ethyl iodide in CH_3CN . All these compounds were characterized on the basis of spectral data and analytical results.¹³ For example, the ^1H NMR spectrum of **9** in $\text{DMSO-}d_6$ showed peaks corresponding to the imidazole and acridine protons in the region δ 6.9-7.7, whereas the methylene protons appeared as a singlet at δ 6.3 ppm. The transition metal complexes bearing NHC as ligands are often synthesised *via* reaction of an imidazolium salt with a basic metal salt

(e.g. $\text{Pd}(\text{OAc})_2$) to give a complex of the form $\text{Pd}(\text{carbene})_2\text{X}_2$.¹⁴ The reaction of two equivalents of **9** and/or **10** with one equivalent of $\text{Pd}(\text{OCOCH}_3)_2$ in DMSO at room temperature readily gave the corresponding Pd-NHC complexes **4** and **5** (Scheme 4.2).



i) $\text{Pd}(\text{OCOCH}_3)_2$, CH_3OH - CH_3CN , 25 °C, 2 h; ii) $\text{Pd}(\text{OCOCH}_3)_2$, CH_3OH - CH_3CN , 25 °C, 2 h.

Scheme 4.2

The products thus obtained were purified and were characterized through ^1H and ^{13}C NMR and matrix assisted laser desorption ionization time of flight (MALDI-TOF) mass spectrometry analysis. We observed peaks at 1088.87 and 763.18 in the MALDI-TOF mass spectra for the complexes **4** and **5** formed between Pd^{2+} ions and **9** and **10**, respectively.

The photophysical properties of the ligands **9**, **10** and their Pd complexes **4** and **5** have been investigated under different conditions. All these derivatives exhibited the characteristic acridine chromophore absorption in the region between 365-375 nm in the aqueous medium. For example, the ligand **9** showed a structured absorption band in the region 300-400 nm. Similarly, the fluorescence spectra of the ligands **9** and **10** showed the characteristic of the acridine chromophore emission having maximum in the region between 397-430 nm (Figure 4.1). To understand the excited state behaviour, we have carried out their picosecond time-resolved fluorescence analysis. Figure 4.2 shows the fluorescence decay profiles of **9** and **10** excited at 375 nm, which exhibited monoexponential decay with lifetimes of 10.4 ns and 6.3 ns, respectively, in the aqueous solution.

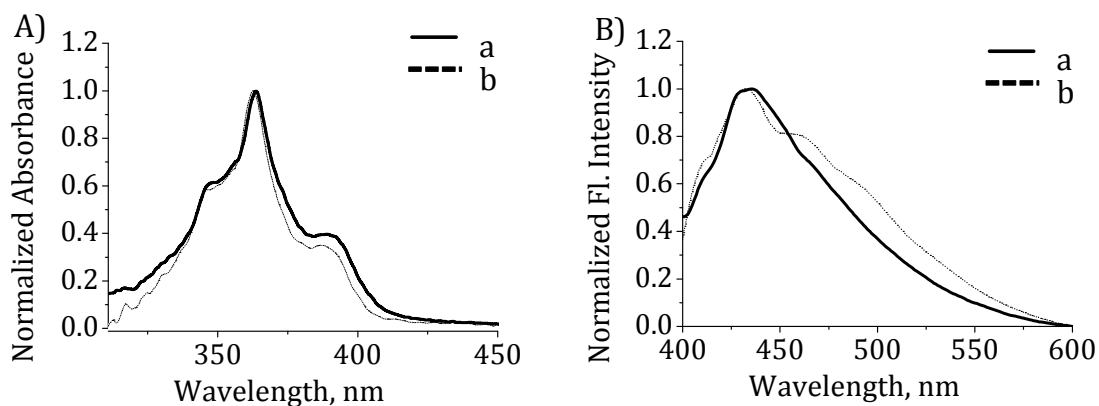


Figure 4.1. A) Absorption and B) emission spectra of the ligands a) **9** (26 μM) and b) **10** (32 μM) in the aqueous medium. λ_{ex} , 375 nm.

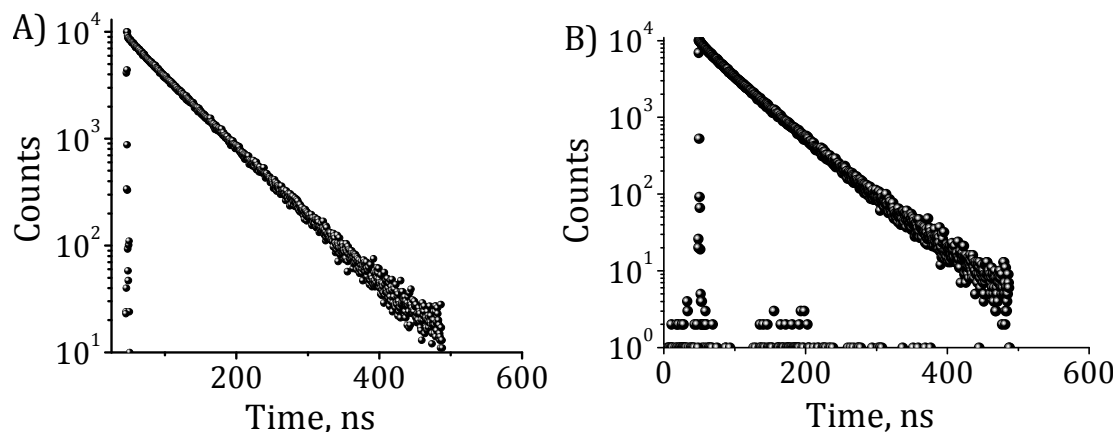


Figure 4.2. Fluorescence decay profiles of the ligands A) **9** (26 μM) and B) **10** (32 μM) in the aqueous solution monitored at 411 nm. λ_{ex} , 375 nm.

4.3.2. Interactions of the Ligands with Mono and Divalent Metal Ions

To understand the formation of the complexes from the ligands **9** and **10** through carbene carbon, we have monitored their interactions with various mono and divalent metal ions such as Na^+ , K^+ , Cu^{2+} , Hg^{2+} , Ca^{2+} , Mg^{2+} , Zn^{2+} , Pb^{2+} , Zn^{2+} , Cd^{2+} and Pd^{2+} ions through optical spectroscopic techniques. For example, Figure 4.3 shows the changes in the absorption and emission spectra of the ligand **9** with the addition of the Pd^{2+} ions. Increasing in concentration of the Pd^{2+} ions to the ligand **9** in water, we observed decrease in the absorbance with a concomitant bathochromic shift. At 17 μM of $\text{Pd}(\text{OAc})_2$, the absorption spectra of the ligand **9** showed *ca.* 8% hyperchromicity along with a bathochromic

shift of 3 nm. The corresponding changes in the fluorescence spectra of the ligand **9** with increasing addition of the Pd²⁺ ions are shown in Figure 4.3. With increasing concentration of Pd²⁺ ions, *ca.* 44% quenching in the fluorescence intensity was observed at 438 nm.

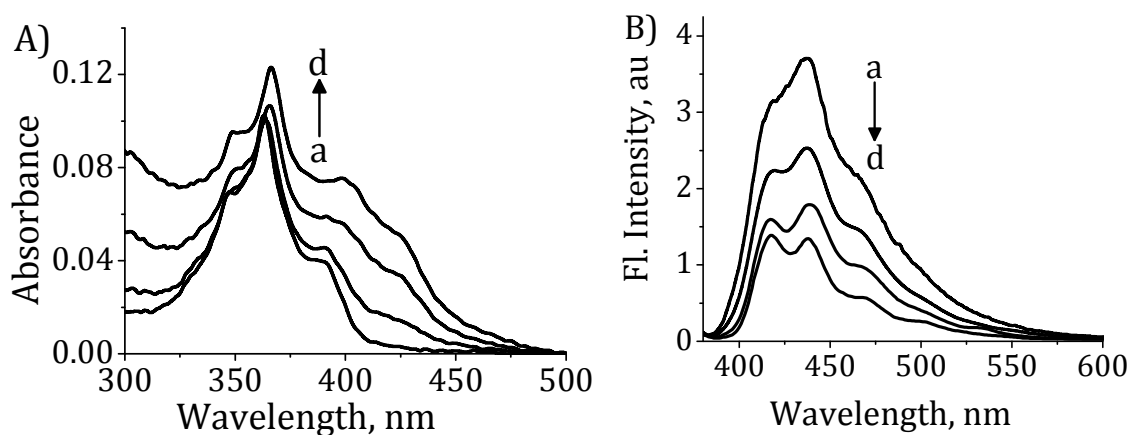


Figure 4.3. Changes in the A) absorption and B) emission spectra of **9** [26 μM] with increasing concentration of Pd²⁺ ions in the aqueous medium. [M²⁺] a) 0 and d) 17 μM. λ_{ex} , 365 nm.

In contrast, the ligand **9** showed negligible interactions in the absorption and emission spectra by the successive additions of various mono and divalent metal ions such as Na⁺, K⁺, Hg²⁺, Cu²⁺, Ca²⁺, Mg²⁺, Zn²⁺, Pb²⁺ and Cd²⁺ ions. For example, Figure 4.4 shows the changes in the emission spectra of the ligand **9** with increasing concentration of Cu²⁺ and Hg²⁺ ions in the aqueous solution. To understand the metal binding properties of the ligand **10**, we have monitored the absorption and emission properties of the ligand **10** by increasing concentration of

various metal ions. At 23 μM of Pd^{2+} ions, we observed *ca.* 23% quenching in fluorescence intensity of **10** in the aqueous solution (Figure 4.5).

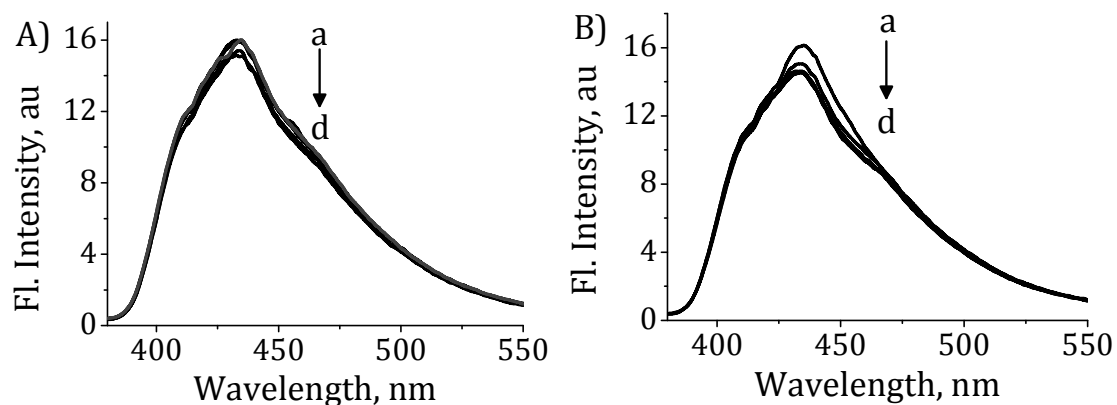


Figure 4.4. Changes in the emission spectra of the ligand **9** (26 μM) with the addition of A) Cu^{2+} and B) Hg^{2+} in aqueous medium. [M^{2+}] a) 0 and d) 17 μM . λ_{ex} , 365 nm.

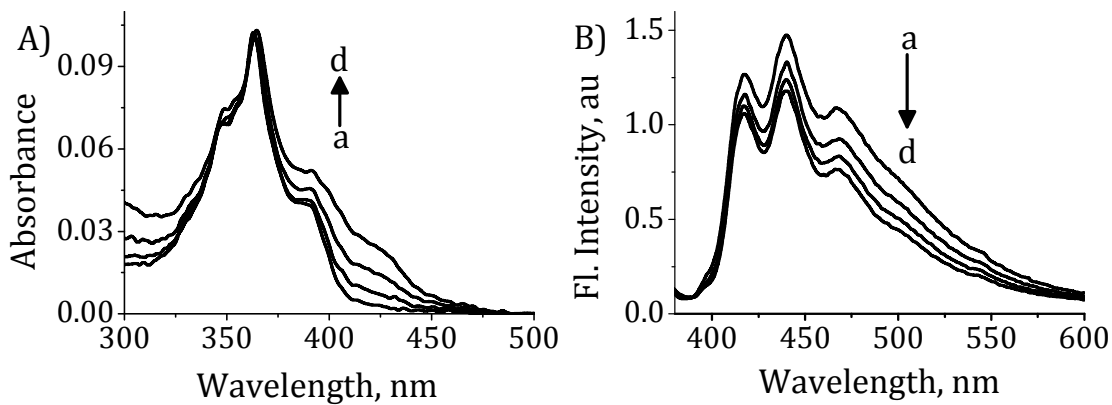


Figure 4.5. Changes in the A) absorption and B) emission spectra of **10** (32 μM) with increasing concentration of Pd^{2+} ions in the aqueous medium. [Pd^{2+}] a) 0 and d) 23 μM . λ_{ex} , 365 nm.

To characterize the metal complexes formed, we carried out the isothermal titration calorimetry.¹⁵ Typical titration curves for Pd²⁺ ions with **9** are shown in Figure 4.6A, in which cumulative heats of the complexation are plotted against the concentration (the reaction was exothermic). With the gradual addition of Pd²⁺ to a solution of **9** (0.2 mM) at 25 °C, we observed a regular exothermic response in the isothermal titration calorimetric (ITC) measurements. After the addition of 1 mM of Pd²⁺, we observed a saturation in the heat changes and on the basis of the ITC data, the enthalpy change was calculated and is found to be $\Delta H = -1.28 \pm 0.14 \text{ kcal mol}^{-1}$ with an association constant of $K_a = 3.35 \pm 1.89 \times 10^4 \text{ M}^{-1}$.

Furthermore, we have carried out single injection method titration of the ligand **9** with Pd²⁺ ions to understand the complexation process as shown in Figure 4.6 B.¹⁶ The results obtained through single injection method analysis were also in agreement with the observations made through the continuous injection ITC measurements. In addition, we have followed the complexation of the ligand **10** and Pd²⁺ ions with ITC by monitoring the heat change produced under the similar conditions. Upon complexation, their interactions exhibited exothermic

responses confirming that Pd²⁺ ions form the stable complex with the ligand **10**.

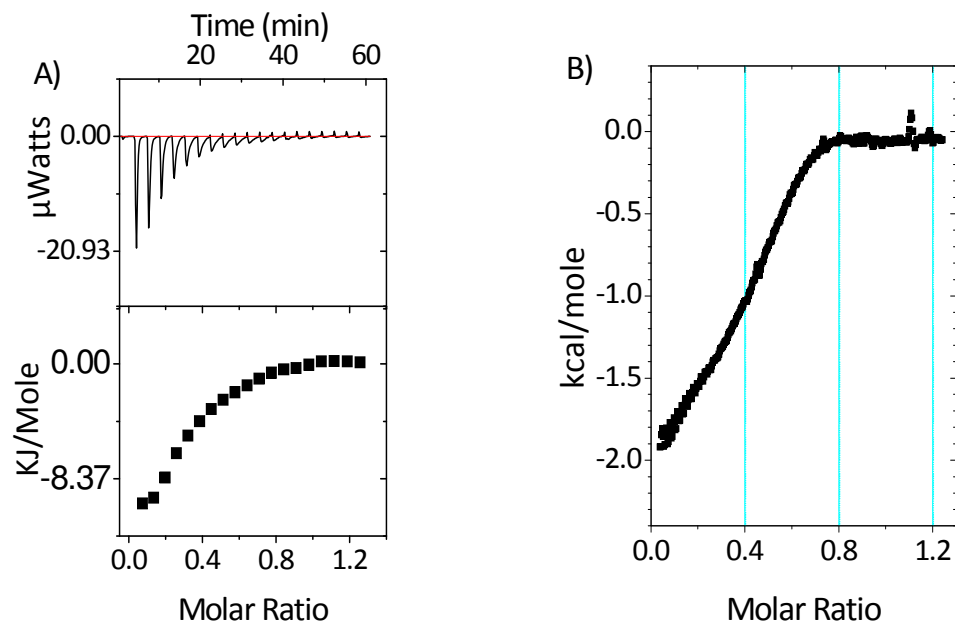


Figure 4.6. Isothermal titration calorimetry data for the addition of Pd²⁺ ions to a solution of the ligand **9** (0.2 mM) in water at 298 K. A) Continuous method and B) single injection method. [Pd²⁺], 1 mM.

Similarly, we have applied the nuclear magnetic resonance technique to characterize the complexation between the ligand **9** with the Pd²⁺ ions. We have monitored the ¹H NMR spectra of the ligand **9** in DMSO by the successive additions of the Pd²⁺ ions (Figure 4.7). At 0.8 mM of Pd²⁺ ions, we observed a decrease in the intensity along with a significant broadening of H₈ proton alone at 9.25 ppm, whereas other protons remained unaffected. Furthermore, the ¹³C NMR spectrum also

showed significant downfield shift in the peak corresponding to the carbene carbon of the ligand **9**.¹⁷

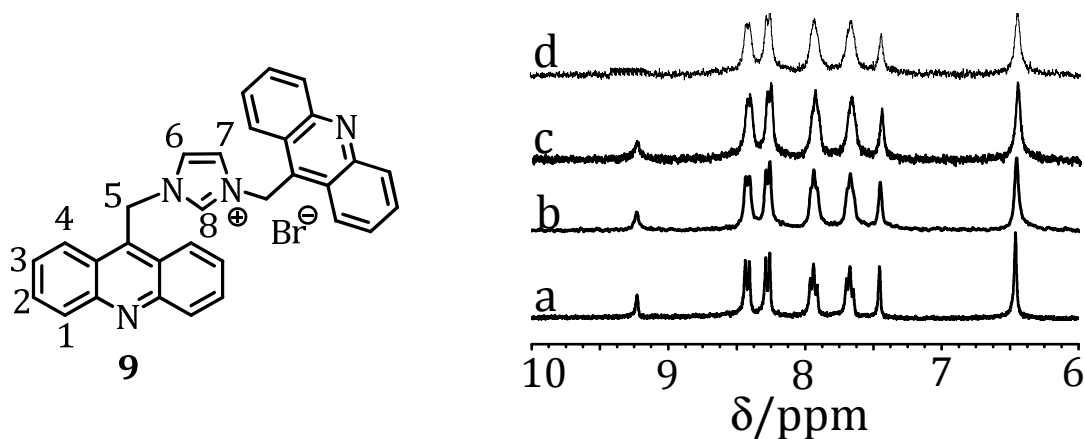


Figure 4.7. Changes in the ^1H NMR spectra of the ligand **9** (1.4 mM) with the addition of Pd^{2+} ions in DMSO. [Pd^{2+}], a) 0, b) 0.2 mM, c) 0.5 mM and d) 0.8 mM.

Figure 4.8 shows the relative changes in the emission intensity of the ligand **9** upon interaction with various metal ions such as Cu^{2+} , Hg^{2+} , Ca^{2+} , Mg^{2+} , Zn^{2+} , Pb^{2+} , and Cd^{2+} ions. It is evident from this figure that the ligand **9** exhibited selectivity towards Pd^{2+} ions, whereas all other metal ions showed negligible changes in emission properties. To understand the strength and reversibility of the complex **4**, we have investigated the effect of temperature and a better chelating ligand EDTA. By monitoring the emission changes in the acridine chromophore upon successive additions of $625\ \mu\text{M}$ of EDTA reveals the irreversibility of the complex

formed by Pd²⁺ ions with the ligand **9**. Figure 4.9A shows negligible changes in the emission intensity corresponding to the acridine moiety

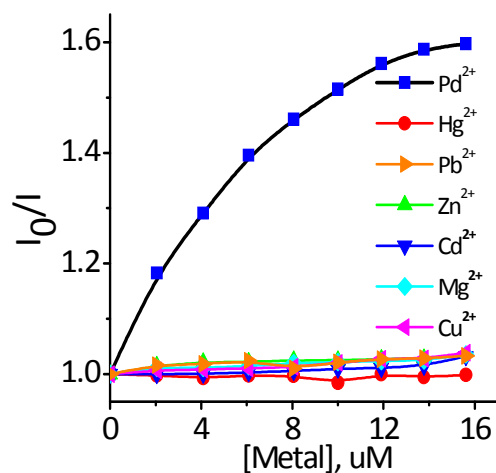


Figure 4.8. Relative changes in the fluorescence intensity of the ligand **9** (26 μM) upon interaction with different metal ions.

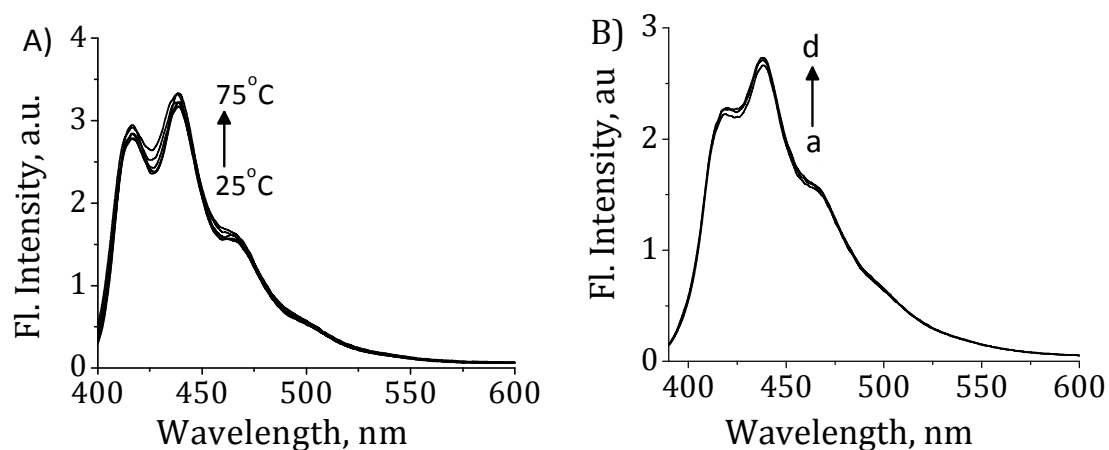


Figure 4.9. Changes in the emission spectra of the complex **4** (16 μM) with A) increasing temperature (25–85 $^{\circ}\text{C}$) and B) addition of EDTA. [EDTA] (a) 0, and (d) 625 μM . λ_{ex} , 365 nm.

with the increasing in concentration of EDTA. Similarly, by increasing the temperature from 25 to 85 °C (Figure 4.9B), we observed negligible revival of the fluorescence intensity of the acridine chromophore. B3LYP level theoretical calculations were also used to support the formation of a 1:2 stoichiometric complexes **4** and **5**.¹⁸ Figure 4.10 shows the energy minimized structures of the complexes **4** and **5** formed between the Pd²⁺ ions and ligand **9** and **10**, respectively.

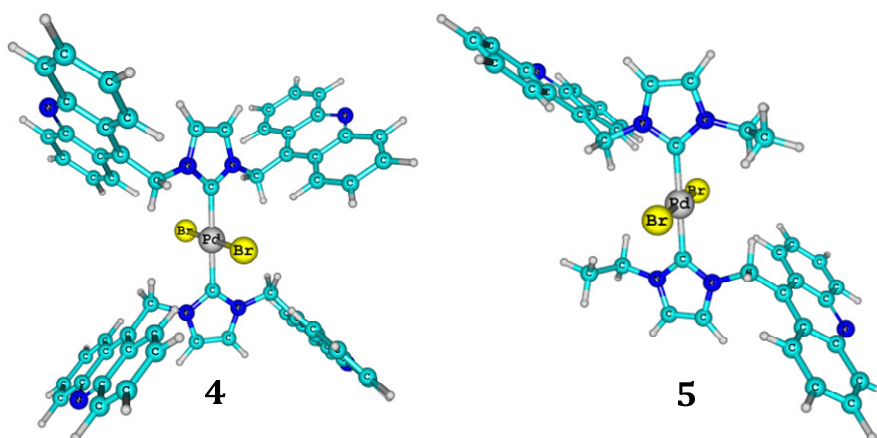


Figure 4.10. Optimized geometry of the Pd-NHC complexes **4** and **5**.

4.3.3. Interaction of Pd(II)-NHC Complexes with Nucleosides and Nucleotides

To investigate the biomolecular recognition ability, we have monitored the changes in the absorption and emission spectra of the Pd-NHC complexes **4** and **5** with the addition of various nucleosides and nucleotides. Addition of 5'-GMP or 5'-GDP or 5'-GTP or guanosine (G-

based) to a solution of the complex **4** showed a significant changes in the absorption and emission spectra corresponding to the acridine chromophore (Figure 4.11). For example, by the successive addition of 5'-GTP, we observed *ca.* 3% hypochromicity in the absorption spectrum of the complex **4**, whereas the emission spectra showed *ca.* 23% enhancement in fluorescence intensity in the long wavelength region around 500 nm. The addition of other guest molecules such as phosphate ion, adenosine 5'-monophosphate (5'-AMP), adenosine 5'-diphosphate (5'-ADP) and adenosine 5'-triphosphate (5'-ATP) resulted in negligible changes in the absorption and emission spectra of **4** (Figure 4.12).

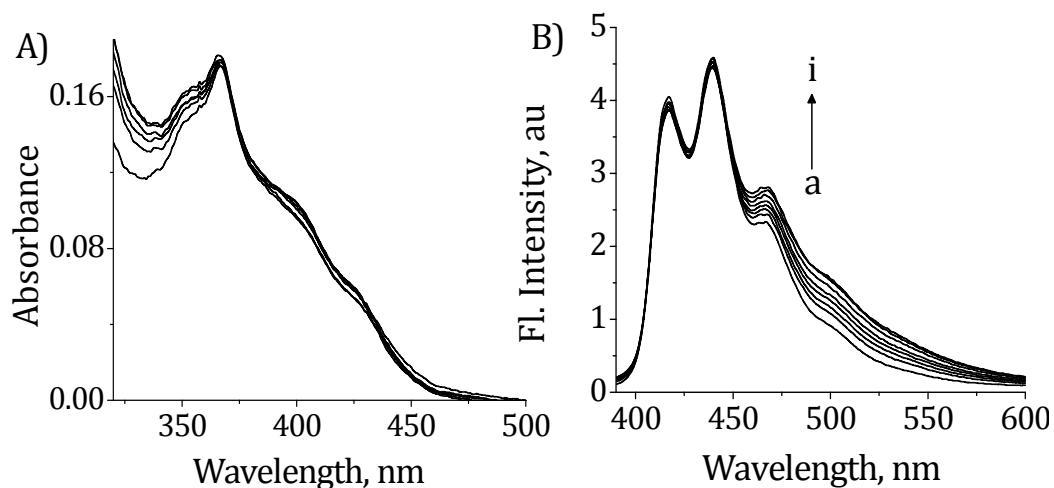


Figure 4.11. Changes in the A) absorption and B) emission spectra of the complex **4** (16 μM) with the successive addition of 5'-GTP. [Ligand], (a) 0 and (i) 500 μM . λ_{ex} , 365.

Similarly, the complex **5** showed *ca.* 2% hypochromicity in the absorption spectra and *ca.* 8% enhancement in fluorescence intensity at 500 nm with the addition of 5'-GTP. In contrast, the Pd-NHC complex **5** displayed significant changes in its absorption and emission spectra by the addition of all the nucleosides and nucleotides as shown in Figure 4.12B, indicating thereby its limitation as a selective receptor.

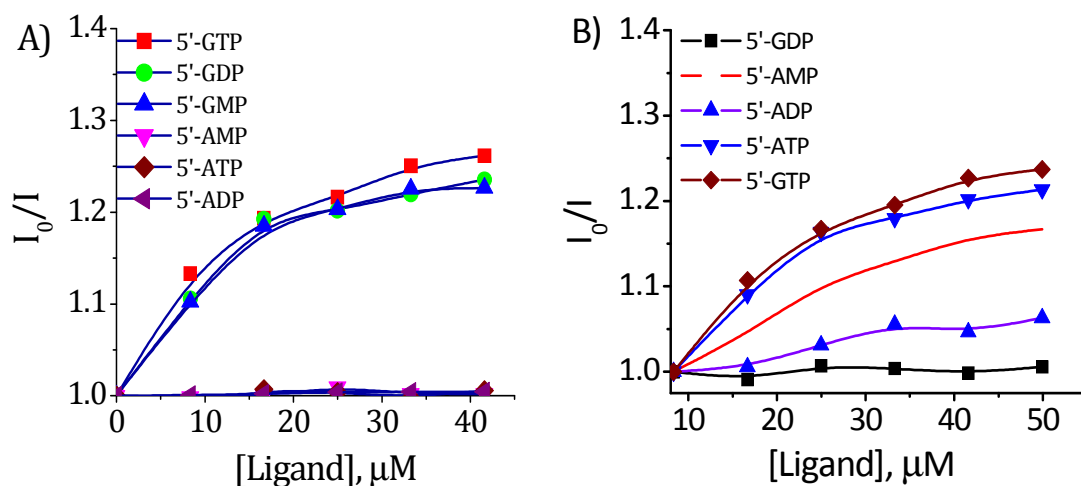


Figure 4.12. Relative changes in the emission of the complexes A) **4** (16 μM) and B) **5** (16 μM) in the presence of various nucleosides and nucleotides.

Further, we have characterized the binding interactions of complex **4** with 5'-GMP or 5'-GDP or 5'-GTP or guanosine using isothermal titration calorimetric (ITC) technique. We have investigated the interactions between the complex **4** and the G-based nucleosides and nucleotides by monitoring the heat change produced as shown in

Figure 4.13. For example, with the gradual addition of 5'-GTP to a solution of **4** (1 mM) at 25 °C, we observed a regular exothermic response in ITC measurements.

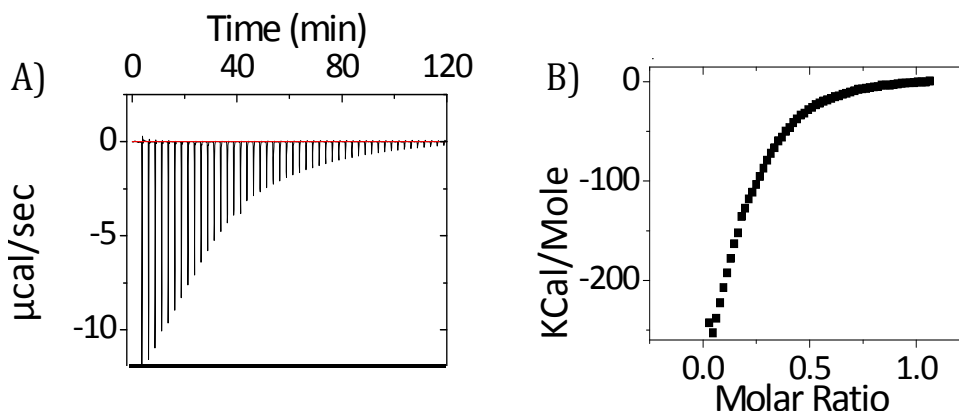


Figure 4.13. Isothermal titration calorimetry data for the addition of 5'-GTP to a solution of the complex **4** (1 mM) in DMSO at 298 K. [Ligand], 12 mM. A) The raw data for the sequential addition of 5'-GTP and B) the plot of the heat evolved (kcal) per mole of 5'-GTP.

After the addition of 12 mM of 5'-GTP, we observed a saturation in the heat changes and on the basis of the ITC data, the enthalpy change was calculated and is found to be $\Delta H = 1.42 \pm 0.14 \text{ kcal mol}^{-1}$ with an association constant of $K_{\text{ass}} = 7.63 \pm 1.89 \times 10^4 \text{ M}^{-1}$. In contrast, the addition of other nucleotides such as 5'-AMP, 5'-ADP and 5'-ATP under similar conditions, showed negligible changes in ITC measurements.

4.3.4. FID Assay: Selectivity of G-Based Nucleosides and Nucleotides Recognition

Even though the Pd-NHC complex **4** showed selectivity towards G-based nucleosides and nucleotides and signalled the event through changes in the fluorescence intensity, its utility as a sensitive probe was limited due to the fact that the recognition is through quenching in fluorescence intensity. By making use of the beneficial non-fluorescent and selective binding properties of the receptor **4**, it was of our interest to exploit its potential as a probe for nucleotides through fluorescent indicator displacement (FID) assay.¹⁹ In this strategy, an indicator is first allowed to bind reversibly to a receptor (Figure 4.14) and such a complexation between the receptor and the indicator results in notable changes in the optical properties of the indicator. Then, a competitive analyte is introduced into the system causing the displacement of the indicator from the host, which in turn modulates an optical signal.

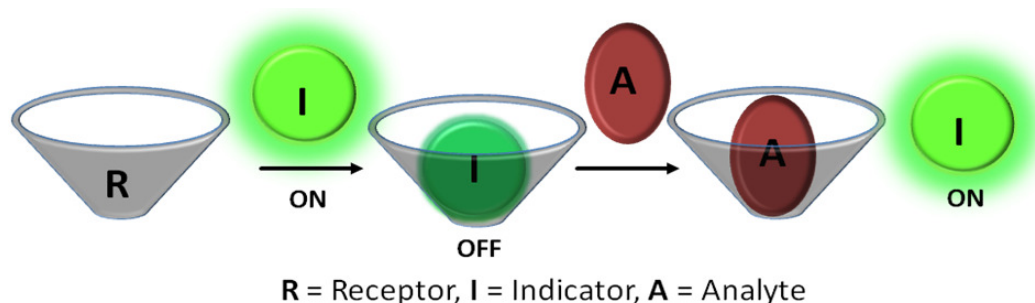


Figure 4.14. Schematic representation of a FID assay.

In this context, we have utilized a highly fluorescent indicator, 8-hydroxy-1,3,6-pyrene trisulphonate (HPTS; $\Phi_F = 0.7$). Based on this principle, the major requirement is that the affinity between the indicator and the receptor be comparable to that between the analyte and the receptor. We first explored the changes in spectral properties of the indicator HPTS upon addition of the complex **4** (Figure 4.15). The successive additions of **4** to a solution of HPTS resulted in a broadening in the absorbance and quenching of the fluorescence intensity of HPTS centred at 512 nm. At ca. 625 μM of **4**, we observed ca. 23% hypochromicity in the absorption spectra of HPTS along with a quantitative quenching in fluorescence intensity (ca. 93%).

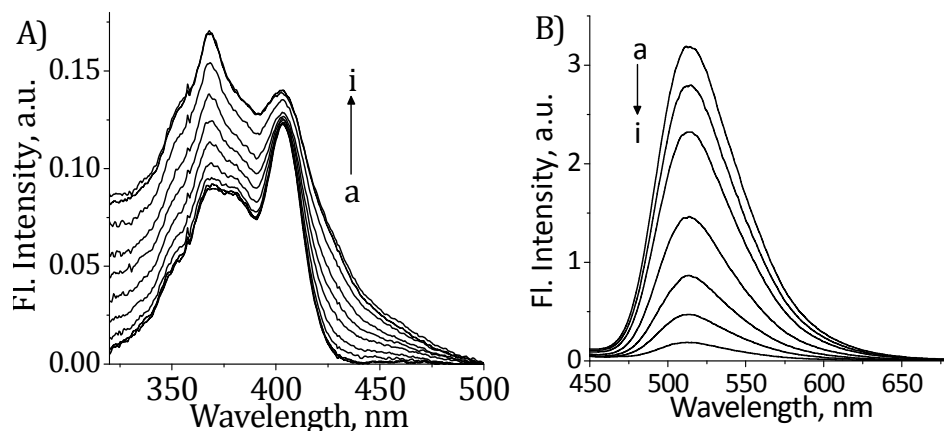


Figure 4.15. Changes in the A) absorption and B) fluorescence spectra of HPTS (7 μM) with the addition of **4** in 20% DMSO-water medium. [**4**], (a) 0 and (i) 625 μM . λ_{ex} , 365 nm.

The changes in the optical properties of HPTS in the presence of **4** are indicative of the formation of a stable complex. The Benesi-Hildebrand

analysis²⁰ of the emission data gave a 1:1 stoichiometry for the complex [4·HPTS], with an association constant (K_a) of $4.66 \pm 0.2 \times 10^4 \text{ M}^{-1}$ and change in free energy of -11 kJ mol^{-1} .

The complexation between the complex **4** and HPTS was further analysed through picosecond time-resolved fluorescence analysis and ITC techniques. HPTS alone exhibited a single exponential fluorescence decay with a lifetime of 5.3 ns (Figure 4.16),²¹ whereas bi-exponential decay with lifetimes of 2.1 ns (70%) and 6.3 ns (30%) was observed in the presence of the complex **4**.

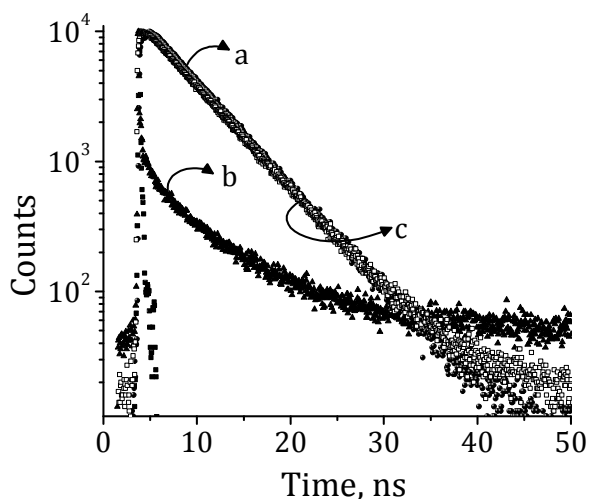


Figure 4.16. Fluorescence decay profiles of (a) HPTS, (b) complex [4·HPTS] and (c) complex [4·HPTS] in the presence of 5'-GTP.

Similarly, with the gradual addition of **4** to a solution of HPTS (1 mM) at 25 °C, we observed a regular exothermic response in the isothermal titration calorimetric (ITC) measurements (Figure 4.17). After the addition of 10 mM of **4**, we observed a saturation in the heat changes

and on the basis of the ITC data, the enthalpy change was calculated and is found to be $\Delta H = 1.42 \pm 0.14$ kcal mol⁻¹ with an association constant of $K_{\text{ass}} = 3.63 \pm 1.89 \times 10^4$ M⁻¹.

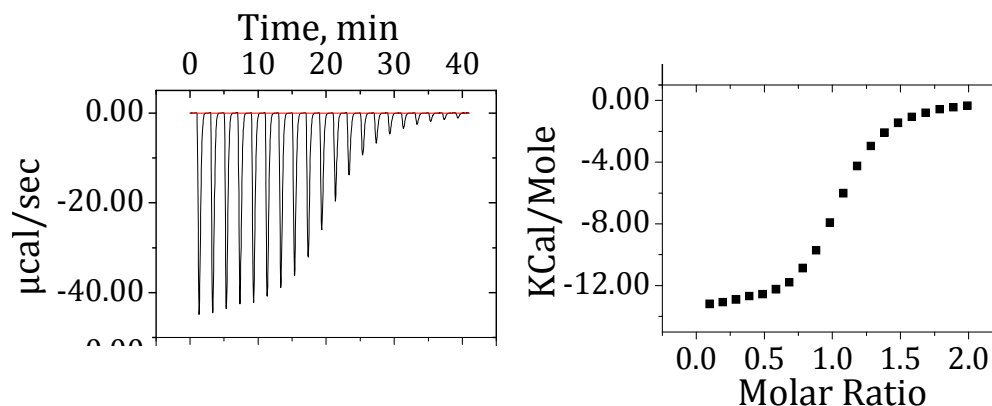


Figure 4.17. Isothermal titration calorimetry data for the addition of HPTS (1 mM) to a solution of complex **4** (10 mM) in DMSO at 298 K.

To understand the nature and strength of the complex formed between the complex **4** and HPTS, we have investigated the effect of temperature (Figure 4.18). For example, when the temperature of the complex [**4**·HPTS] was raised from 293 to 348 K, we observed a regular increase in the emission intensity of HPTS, indicating a gradual dissociation of the complex at these temperatures.

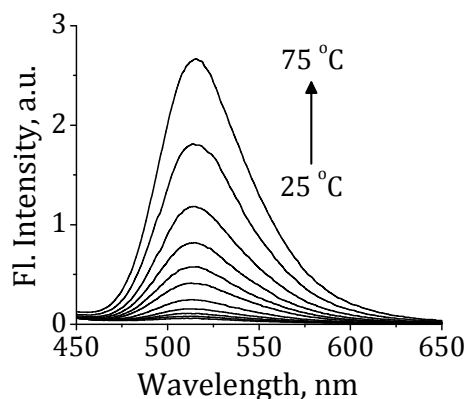


Figure 4.18. Effect of temperature on the emission spectra of complex [4·HPTS]. (a) 293 and (f) 348 K. λ_{ex} , 365 nm.

The beneficial competitiveness of the assay was demonstrated by comparing the efficiency of fluorescence indicator displacement (FID) by various nucleotides and nucleosides. Figure 4.19 shows regular release of HPTS from the complex [4·HPTS] by gradual addition of 5'-GTP. For example, the successive additions of 5'-GTP resulted in a regular enhancement in fluorescence intensity corresponding to HPTS at 512 nm. In 20% DMSO-water, *ca.* 93% enhancement was observed at 1.6 mM of 5'-GTP, which led to the visual detection of 5'-GTP through "turn on" fluorescence intensity. In contrast, the addition of adenosine, 5'-AMP, 5'-ADP, 5'-CTP and 5'-UTP showed negligible changes in the revival of fluorescence intensity of HPTS. To further demonstrate the selectivity of the FID assay, it was tested in the presence of other nucleotides and nucleosides. Even in the presence of

various other nucleosides and nucleotides, the complex [4.HPTS] exhibited selectivity towards only G-based nucleotides (Figure 4.20).

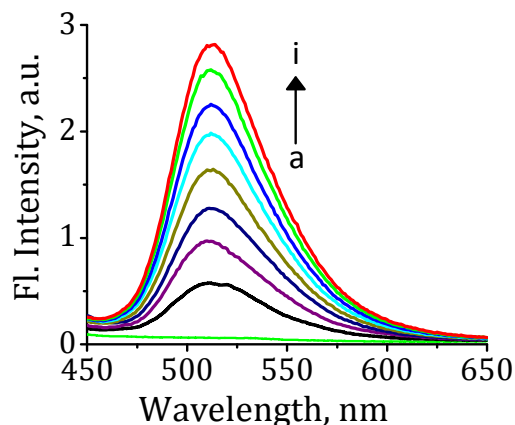


Figure 4.19. Fluorescence indicator displacement (FID) from the complex [4.HPTS] by 5'-GTP. [5'-GTP], (a) 0 and (i) 1.6 mM. λ_{ex} , 365 nm.

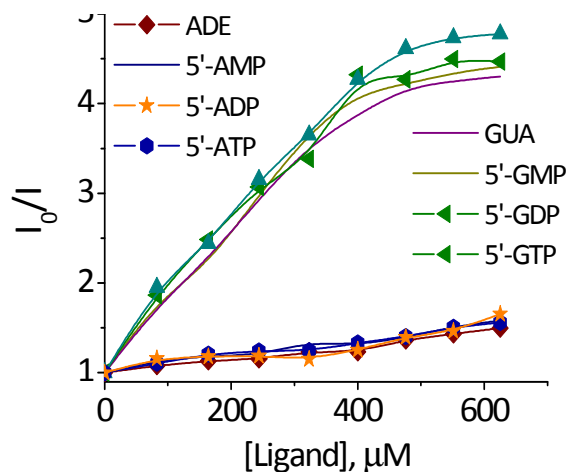


Figure 4.20. Relative concentration dependent FID assay efficiency by [4.HPTS] for various analytes.

The displacement of HPTS from the complex [4.HPTS] was confirmed by time-resolved fluorescence techniques. For example, when 5'-GTP was added to the complex [4.HPTS], we observed a biexponential decay

having lifetimes 5.3 ns (98%) and 8.5 ns (2%) (Figure 4.16). The former lifetime has been attributed to the free HPTS in solution.

4.4. DISCUSSION

The acridine imidazole based ligands **9** and **10** undergo selective complexation with the Pd²⁺ ions resulting in significant hypochromicity and bathochromic shift as well as quenching in the fluorescence intensity. Interestingly, these ligands **9** and **10** showed remarkably high selectivity for the Pd²⁺ ions as compared to other metal ions. The disappearance of the resonances of the imidazolium protons (NCHN) in the ¹H NMR and the significant downfield shift of the carbene carbon in the ¹³C NMR spectra, confirm the coordination of the metal ions through carbene carbon in these complexes. The Pd-NHC complexes **4** and **5** were found to be stable and irreversible as evidenced through the observation of high association constants for the complexation process and their negligible reaction with EDTA and also at higher temperatures.

The increase in the fluorescence intensity of the Pd-NHC complex **4** at the long wavelength region by the addition of 5'-GTP could be attributed to the interaction of the phosphate group of the guanosine base with the acridine nitrogen atom. In comparison to the complex **4**, the replacement of one of the acridine moieties by an ethyl unit as in the case of **5** resulted in a system with lesser aromatic surface. Furthermore,

the presence of hydrophobic space as well as the Lewis acidic metal centre in the complex **4** play major role in its selective recognition of G-based nucleotides as evidenced from the negligible selectivity observed with the complex **5** and also with various other guest molecules. Therefore, the observed selectivity of the Pd-NHC complex **4** towards guanosine based nucleotides can be attributed to the presence of a better π -electron cloud which facilitates effective electronic and π -stacking interactions with the acridine moiety²² and a strong coordinative interaction with N₇ nitrogen of the guanosine base and metal ions present in the centre.²³ These results confirm the importance of the presence of Lewis acidic centre, coordination site and aromatic surface in the molecular recognition ability of the complexes and demonstrate the potential of the complex **4** as a probe for the detection of guanosine based nucleotides.

Interestingly, the fluorescence indicator HPTS undergoes efficient complexation with the Pd-NHC complexes **4** and **5** resulting in complete quenching of its fluorescence intensity. The mechanism of quenching may be attributed to the photoinduced electron transfer process from the excited state of HPTS to the acridine moiety of the complexes. Also, the non-fluorescent [**4**.HPTS] thus formed can be effectively utilized in

the competitive displacement assay as shown in Figure 4.21. The fluorescence indicator, HPTS exhibits *ca.* 72% fluorescence intensity (Figure 4.21a), which on interaction with the Pd-NHC complex **4** showed quantitative quenching in fluorescence intensity resulting the formation of the non-fluorescent complex [**4**·HPTS] (Figure 4.21b). Importantly, the indicator HPTS was successfully displaced from the complex [**4**·HPTS] by G-based nucleotides resulting in the *ca.* 93% enhancement in fluorescence intensity (Figure 4.21c). By virtue of having a better π -electron cloud and low ionization potential,²⁴ the guanosine based nucleotides unusually exhibit better complexing ability with the Pd-NHC complex **4** through synergistic effects of electronic, π -stacking, electrostatic and co-ordinate interactions with four acridine moieties. This was evidenced through the observation of relatively less sensitivity and selectivity with the complex **5** which was substituted with only two acridine moieties. Thus, the Pd-NHC complex **4** can be successfully utilized to discriminate the structurally similar guanine based nucleotides from the adenine nucleotides and recognition can be achieved through 'turn on' fluorescence enhancement.

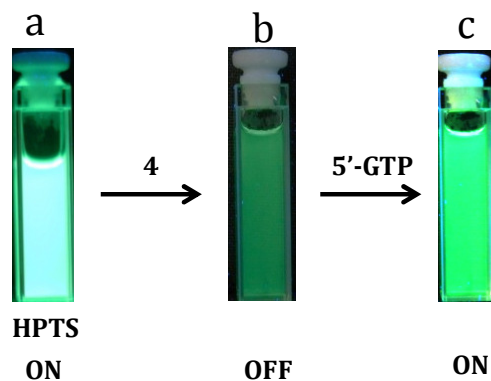


Figure 4.21. Observation of the visual changes in fluorescence intensity of (a) HPTS ($7 \mu\text{M}$) alone, (b) HPTS in presence of the complex **4** ($625 \mu\text{M}$) and (c) the complex [**4**·HPTS] in presence of the analyte, 5'-GTP (1.6 mM).

4.5. CONCLUSIONS

In conclusion, we have synthesised Pd-NHC complexes **4** and **5** of the acridine-imidazole conjugates **9** and **10** and have investigated their interactions with various nucleosides and nucleotides under different conditions through photophysical, calorimetric and ^1H NMR techniques. Of the two complexes, Pd-NHC complex **4** showed selective interactions with the G-based nucleosides and nucleotides and also in presence of other analytes. Subsequently, a sensitive FID assay was developed for the G-based nucleotides through the beneficial properties of the complex **4** and the fluorescence indicator, HPTS. The uniqueness of this assay was that it successfully discriminate G-based nucleotides from

other nucleosides and nucleotides through an “ON-OFF-ON” fluorescence mechanism with a visual change in fluorescence intensity. The selectivity of the complex **4** towards the G-based nucleotides has been attributed to the presence of a better π -electron cloud, which facilitates effective electronic and π -stacking interactions as well as strong coordinative interactions with N₇ nitrogen of the guanine base and the metal ion centre. These results confirm the importance of the presence of Lewis acidic centre and aromatic surface in the molecular recognition ability of the complexes and demonstrate the potential of the complex **4** as a probe for the selective recognition of the G-based nucleotides through visual changes in the fluorescence intensity.

4.6. EXPERIMENTAL SECTION

4.6.1. General Techniques

The equipment and procedures for melting point determination and spectral recordings have been described elsewhere.²⁵ All melting points were determined on a Mel-Temp 4 melting point apparatus. ¹H and ¹³C NMR spectra were measured on a 500 MHz Bruker advanced DPX spectrometer. HRMS were recorded on a JEOL mass spectrometer. The electronic absorption spectra were recorded on a Shimadzu UV-VIS-NIR spectrophotometer. Fluorescence spectra were recorded on a SPEX-

Fluorolog F112X spectrofluorimeter. The fluorescence quantum yields were determined by using optically matched solutions. Quinine sulphate ($A = 0.54$) in 0.1 N H_2SO_4 was used as the standard.²⁶ The quantum yields of fluorescence were calculated using the equation 4.1, wherein, A_s and A_u are the absorbance of standard and unknown, respectively. F_u and F_s are

$$F_u = \frac{A_s F_u n_s^2}{A_u F_s n_u^2} F_s \quad \text{eq 4.1}$$

the areas of fluorescence peaks of the unknown and standard and n_s and n_u are the refractive indices of the standard and unknown solvents, respectively. Φ_s and Φ_u are the fluorescence quantum yields of the standard and unknown. The fluorescence lifetimes were measured using a IBH Picosecond single photon counting system. The fluorescence decay profiles were deconvoluted using IBH data station software V2.1 and minimizing the χ^2 values of the fit to 1 ± 0.1 .itc

4.6.2. Materials

All the nucleosides and nucleotides, $Pd(OAc)_2$, tetrapropyl ammonium hydroxide and the fluorescence indicator, HPTS, were purchased from Sigma-Aldrich and used as received. Doubly distilled water was used for all the experiments. All experiments were carried

out in 20% DMSO-water mixture at room temperature (25 ± 1 °C), unless otherwise mentioned. Petroleum ether used was the fraction with boiling range 60-80 °C.

4.6.3. Preparation of 9-((1H-imidazol-1-yl)methyl)acridine (8)

To a solution of imidazole (500 mg, 7.4 mmol) in dry benzene (100 mL) was added aqueous sodium hydroxide (0.2 M, 25 mL) and tetra propyl ammonium hydroxide as phase transfer catalyst at room temperature with constant stirring. After the reaction mixture was stirred for 30 min, 9-bromomethylacridine (**7**) (500 mg, 1.4 mmol) was added and refluxed for 6 h. The reaction mixture was then additionally stirred for 2 h at room temperature; it was poured into 100 mL of water and extracted with dichloromethane. The organic layer was then separated, dried over anhydrous sodium sulphate and evaporation of the solvent under vacuum yielded a residue which was purified by column chromatography over silica gel. Elution of the column with ethyl acetate yielded 370 mg (48%) of the ligand **8**, which was then recrystallized from a mixture of acetonitrile and ethyl acetate (4:1); mp 226–227 °C; ^1H NMR (300 MHz, DMSO- d_6 , TMS) δ 6.31 (s, 4H), 6.78 (t, 2H), 6.94 (t, 2H), 7.68–7.70 (m, 4H), 7.74 (s, 2H), 8.63–8.65 (m, 4H); ^{13}C NMR (75 MHz, DMSO- d_6 , TMS) δ 43.0, 115.0, 127.8, 128.4, 129.2, 130.3,

131.6, 134.9; HRMS (FAB) m/z Calcd for $C_{17}H_{13}N_3$: 259.3012, Found 258.4208 (M - H)⁺.

4.6.4. Preparation of 1,3-bis(acridin-9-ylmethyl)-1H-imidazol-3-ium bromide (9)

To a solution of **8** (0.25 g, 0.57 mmol) in a mixture (0.5:1) of acetonitrile (100 mL) and DMF (50 mL) was added **7** (0.21 g, 0.57 mmol). The reaction mixture was then warmed and maintained at 80 °C for 24 h. After cooling to room temperature, the precipitated product was filtered and washed with 50 mL dry acetonitrile. It was further purified by recrystallization from a mixture (1:5) of acetonitrile and methanol to yield 0.16 g (35%) of **9**, mp 290 °C; ¹H NMR (300 MHz, DMSO-*d*₆, TMS) δ 6.47 (s, 4H), 7.46-7.47 (d, 4H), 7.66-7.70 (t, 2H), 7.92 - 8.00 (m, 4H), 8.26 - 8.29 (d, 4H, J = 9 Hz), 8.42-8.45 (d, 4H, J = 9 Hz), 9.26 (s, 1H); ¹³C NMR (75 MHz, DMSO-*d*₆, TMS) δ 42.0, 119.0, 124.8, 126.7, 128.2, 129.0, 130.1, 136.9; HRMS (FAB) m/z Calcd for $[C_{31}H_{23}BrN_4]$: 531.4451, Found 530.6703 [M-H]⁺.

4.6.5. Preparation of 1-(acridin-9-ylmethyl)-3-ethyl-1H-imidazol-3-ium bromide (10)

To a solution of **8** (0.25 g, 0.57 mmol) in a mixture (0.5:1) of acetonitrile (100 mL) and DMF (50 mL) was added ethyl iodide (0.21 g, 0.57 mmol). The reaction mixture was then warmed and maintained at

80 °C for 24 h in a seal tube. After cooling to room temperature, the precipitated product was filtered and washed with 50 mL dry acetonitrile. It was further purified by recrystallization from a 1:5 mixture of acetonitrile and methanol to yield 0.16 g (35%) of **10**; mp 278 °C; ¹H NMR (500 MHz, DMSO-*d*₆, TMS) δ 6.53 (s, 4H), 6.98 (t, 2H), 7.24 (t, 2H), 7.58 – 7.62 (m, 4H), 7.76 (s, 2H), 8.32 – 8.34 (m, 4H); ¹³C NMR (125 MHz, DMSO-*d*₆, TMS) δ 44.0, 113.0, 121.8, 124.7, 126.2, 129.0, 132.1, 134.2; HRMS (FAB) *m/z* Calcd for C₁₉H₁₈BrN₃: 368.2703; Found 367.0218 (M - H)⁺.

4.6.6. Synthesis of the Pd-NHC complex **4**

To a solution of **9** in a mixture of acetonitrile (50 mL) and methanol (5 mL) was added Pd(OAc)₂ (100 mg, 0.74 mmol) with constant stirring at 25 °C, readily gave the complex **4**. It was further purified by recrystallization from acetonitrile to yield 124 mg (17%) of the Pd-NHC complex **4**; ¹H NMR (500 MHz, DMSO-*d*₆, TMS) δ 6.47 (s, 4H), 7.46-7.47 (d, 4H), 7.66-7.70 (t, 2H), 7.92 - 8.00 (m, 4H), 8.26 – 8.29 (d, 4H, J = 9 Hz), 8.42-8.45 (d, 4H, J = 9 Hz); ¹³C NMR (125 MHz, DMSO-*d*₆, TMS) δ 46.0, 119.0, 124.8, 126.7, 128.2, 129.0, 130.1, 136.9; MALDI-TOF MS: *m/z* Calcd for [C₆₂H₄₆BrPdN₈]: 1169.3102; Found 1088.87 (M - Br)⁺.

4.6.7. Synthesis of the Pd-NHC complex **5**

To a solution of **10** in a mixture of acetonitrile (50 mL) and methanol (5 mL) was added Pd(OAc)₂ (100 mg, 0.74 mmol) with constant stirring at 25 °C gave the complex **5**. It was further purified by recrystallization from acetonitrile to yield 146 mg (21%) of the Pd-NHC complex **5**; ¹H NMR (500 MHz, DMSO-*d*₆, TMS) δ 6.31 (s, 4H), 6.78 (t, 2H), 6.94 (t, 2H), 7.68–7.70 (m, 4H), 7.74 (s, 2H), 8.63–8.65 (m, 4H); ¹³C NMR (125 MHz, DMSO-*d*₆, TMS) δ 45.7, 119.0, 124.8, 126.7, 128.2, 129.0, 130.1, 136.9. MALDI-TOF MS: *m/z* Calcd for [C₃₈H₃₆BrPdN₈]: 842.94.; Found 763.18 (M – Br)⁺.

4.7. REFERENCES

1. (a) F. E. Hahn, M. C. Jahnke, *Angew. Chem., Int. Ed.*, **2008**, *47*, 3122-3126. (b) W. A. Herrmann, *Angew. Chem., Int. Ed.*, **2002**, *41*, 1290-1294. (c) F. Li, S. Bai, T. S. A. Hor, *Organometallics*, **2008**, *27*, 672-677.
2. (a) S. Liu, T. Hsieh, G. Lee, S. Peng, *Organometallics*, **1998**, *17*, 993-995. (b) D. J. Nielsen, K. J. Cavell, B. W. Skelton, A. H. White, *Inorg. Chim. Acta*, **2003**, *352*, 143-150. (c) H. M. Lee, J. Y. Zeng, C. H. Hu, M. T. Lee, *Inorg. Chem.*, **2004**, *43*, 6822-6829. (d) K. S. Coleman, H. T. Chamberlayne, S. Turberville, M. L. H. Green, A. R. Cowley, *Dalton Trans.*, **2003**, 2917-2922.
3. (a) K. Öfele, *J. Organomet. Chem.*, **1968**, *12*, 42-46. (b) H.-W. Wanzlick, H.-J. Schön herr, *Angew. Chem., Int. Ed. Engl.*, **1968**, *7*, 141-145.
4. (a) M. A. Sharkey , J. P. O'Gara , S. V. Gordon , F. Hackenberg , C. Healy, F. Paradisi , S. Patil , B. Schaible, M. Tacke, *Antibiotics*, **2012**, *1*, 25-28. (b) K. M. Hindi, M. J. Panzner, C. A. Tessier, C. L. Cannon, W. J. Youngs, *Chem. Rev.* **2009**, *109*, 3859-3884.
5. (a) S. Ray, R. Mohan, J. K. Singh, M. K. Samantaray, M. M. Shaikh, D. Panda, P. Ghosh, *J. Am. Chem. Soc.* **2007**, *129*, 15042-15053. (b) M.

- Mascini, G. Bagni, M. L. D. Pietro, M. Ravera, S. Baracco, D. Osella, *Bio. Metals*, **2006**, *19*, 409-418.
6. (a) M. Rubio, M. A. Siegler, A. L. Spek, J. N. H. Reek, *Dalton Trans.*, **2010**, *39*, 5432-5435. (b) A. J. Boydston, K. A. Williams, C. W. Bielawski, *J. Am. Chem. Soc.*, **2005**, *127*, 12496-12497. (c) J. C. Garrison, W. J. Youngs, *Chem. Rev.*, **2005**, *105*, 3978-4008. (d) X. Zhang, Y. Qiu, B. Rao, M. Luo, *Organometallics*, **2009**, *28*, 3093-3099.
7. (a) M. Koželj, B. Orel, *Dalton Trans.*, **2013**, *42*, 9432-9436. (b) S. N. Riduan, Y. Zhang, J. Y. Ying, *Angew. Chem. Int. Ed.* **2009**, *48*, 3322-3325.
8. (a) R. H. Grubbs, *Angew. Chem. Int. Ed.* **2006**, *45*, 3760-3765. (b) T. M. Trnka, R. H. Grubbs, *Acc. Chem. Res.* **2001**, *34*, 18-29. (c) A. Fürstner, *Angew. Chem. Int. Ed.* **2000**, *39*, 3012-3043. (d) A. Fürstner, L. Ackermann, B. Gabor, R. Goddard, C. W. Lehmann, R. Mynott, F. Stelzer, O. R. Thiel, *Chem. Eur. J.* **2001**, *7*, 3236-3253.
9. (a) R. C. Liu, K. Han, *Chem. Mater.* **1999**, *11*, 1237-1241. (b) T. H. T. Hsu, J. J. Naidu, B. -J. Yang, M. -Y. Jang, I. J. B. Lin, *Inorganic Chemistry*, **2012**, *51*, 98-100.

10. (a) C. A. Hunter, J. K. M. Sanders, *J. Am. Chem. Soc.* **1990**, *112*, 5525-5534. (b) L. Fabbrizzi, A. Poggi, *Chem. Soc. Rev.*, **2013**, *42*, 1681-1699.
11. (a) W. A. Herrmann, *Angew. Chem. Int. Ed.* **2002**, *41*, 1290-1309. (b) D. Bourissou, O. Guerret, F. P. Gabbai, G. Bertrand, *Chem. Rev.* **2000**, *100*, 39-92.
12. E. Kuruvilla, D. Ramaiah, *J. Phys. Chem. B* **2007**, *111*, 6549-6556.
13. (a) P. P. Neelakandan, D. Ramaiah, *Angew. Chem. Int. Ed.* **2008**, *47*, 8407-8411. (b) J. Joseph, N. V. Eldho, D. Ramaiah, *Chem. Eur. J.* **2003**, *9*, 5926-5935.
14. A. J. Arduengo, R. L. Harlow, M. Kline, *J. Am. Chem. Soc.* **1991**, *113*, 361-364.
15. (a) D. E. Wilcox, *Inorg. Chim. Acta.*, **2008**, *361*, 857-867. (b) M. L. Doyle, *Curr. Opin. Biotech.*, **1997**, *8*, 31-35.
16. T. Wiseman, S. Williston, J. F. Brandts, L. N. Lin, *Anal. Biochem.*, **1989**, *179*, 131-137.
17. (a) W. Philipsborn, *Pure and Appl. Chem.*, **1986**, *58*, 513-528. (b) F. Li, S. Bai, T. S. A. Hor, *Organometallics*, **2008**, *27*, 672-677.
18. Gaussian 03 (Revision-D.01), M. J. Frisch, G. W. Trucks, H. B. Schlegel, G. E. Scuseria, M. A. Robb, J. R. Cheeseman, J. A.

- Montgomery, Jr., T. Vreven, K. N. Kudin, J. C. Burant, J. M. Millam, S. S. Iyengar, J. Tomasi, V. Barone, B. Mennucci, M. Cossi, G. Scalmani, N. Rega, G. A. Petersson, H. Nakatsuji, M. Hada, M. Ehara, K. Toyota, R. Fukuda, J. Hasegawa, M. Ishida, T. Nakajima, Y. Honda, O. Kitao, H. Nakai, M. Klene, X. Li, J. E. Knox, H. P. Hratchian, J. B. Cross, C. Adamo, J. Jaramillo, R. Gomperts, R. E. Stratmann, O. Yazyev, A. J. Austin, R. Cammi, C. Pomelli, J. W. Ochterski, P. Y. Ayala, K. Morokuma, G. A. Voth, P. Salvador, J. J. Dannenberg, V. G. Zakrzewski, S. Dapprich, A. D. Daniels, M. C. Strain, O. Farkas, D. K. Malick, A. D. Rabuck, K. Raghavachari, J. B. Foresman, J. V. Ortiz, Q. Cui, A. G. Baboul, S. Clifford, J. Cioslowski, B. B. Stefanov, G. Liu, A. Liashenko, P. Piskorz, I. Komaromi, R. L. Martin, D. J. Fox, T. Keith, M. A. Al-Laham, C. Y. Peng, A. Nanayakkara, M. Challacombe, P. M. W. Gill, B. Johnson, W. Chen, M. W. Wong, C. Gonzalez, and J. A. Pople, Gaussian, Inc., Pittsburgh, PA, **2003**.
19. (a) N. Marcotte, A. Taglietti, *Supramol. Chem.*, **2003**, *15*, 617–625.
(b) S. Atilgan, E. U. Akkaya, *Tetrahedron Lett.*, **2004**, *45*, 9269–9271.
20. H. Benesi, J. Hildebrand, *J. Am. Chem. Soc.* **1949**, *71*, 2703–2707.
21. P. P. Neelakandan, M. Hariharan and D. Ramaiah, *J. Am. Chem. Soc.*, **2006**, *128*, 11334–11335.

22. (a) F. Hof, S. L. Craig, C. Nuckolls, J. Rebek, *Angew. Chem., Int. Ed.*, **2002**, *41*, 1488–1508. (b) S. Kubik, *Chem. Soc. Rev.*, **2009**, *38*, 585–605.
23. A. Habtemariam, J. A. Parkinson, N. Margiotta, T. W. Hambley, S. Parsons, P. J. Sadler, *J. Chem. Soc., Dalton Trans.*, **2001**, 362–372
24. (a) M. Hariharan, J. Joseph, D. Ramaiah, *J. Phys. Chem. B* **2006**, *110*, 24678-24686 (b) J. Joseph, N. V. Eldho, D. Ramaiah, *Chem. Eur. J.* **2003**, *9*, 5926-5935.
25. (a) R. R. Avirah, K. Jyothish, D. Ramaiah, *J. Org. Chem.* **2008**, *73*, 274-279. (b) M. Hariharan, P. P. Neelakandan, D. Ramaiah, *J. Phys. Chem. B* **2007**, *111*, 11940-11947. (c) K. Jyothish, M. Hariharan, D. Ramaiah, *Chem. Eur. J.* **2007**, *13*, 5944-5951. (d) E. Kuruvilla, D. Ramaiah, *J. Phys. Chem. B* **2007**, *111*, 6549-6556.
26. A. R. Roshal, J. A. Organero, A. Douhal, *Chem. Phys. Lett.* **2003**, *379*, 53-59.

List of Publications of the Candidate

1. A supramolecular Cu(II) metallocyclophane probe for guanosine 5'-monophosphate, **A. K. Nair**, P. P. Neelakandan and D. Ramaiah, *Chem. Commun.*, **2009**, 6352-6354.
2. Functional cyclophanes: Promising hosts for optical biomolecular recognition, D. Ramaiah, P. P. Neelakandan, **A. K. Nair** and R. R. Avirah, *Chem. Soc. Rev.*, **2010**, 39, 4158-4168.
3. Dye encapsulation and release by a zinc-porphyrin pincer system through morphological transformations, B. Marydasan, **A. K. Nair** and D. Ramaiah, *RSC Adv.*, **2013**, 3, 3815-3818.
4. Optimization of singlet oxygen and triplet quantum yields of porphyrin pincer system through Zinc insertion, B. Marydasan, **A. K. Nair** and D. Ramaiah, *J. Phys. Chem. B*, **2013**, DOI: 10.1021/jp407524w.
5. NHC based turn-on chemodosimeter for selective detection of cyanide in water, M. Viji, **A. K. Nair** and D. Ramaiah, *Inorg. Chem.* **2013** (Submitted).
6. Selective recognition of guanosine based nucleotides by Pd-NHC complex through FID assay, **A. K. Nair**, M. Viji, B. Marydasan and D. Ramaiah, *Chem. Commun.* **2013** (To be communicated).

Posters Presented at conferences

1. "Selective recognition of 5'-GMP by a novel metallocyclophane" **A. K. Nair**, P. P. Neelakandan and D. Ramaiah, a poster presented at 12th CRSI National Symposium in Chemistry held at ICT, Hyderabad, February 3-7, **2010**.
2. A Supramolecular Cu(II) metallocyclophane probe for guanosine 5'-monophosphate, **A. K. Nair**, P. P. Neelakandan and D. Ramaiah, a poster presented at the Vth JNC Research Conference on Chemistry of Materials held at Alappuzha, Kerala, India, September 12-14, **2009**.